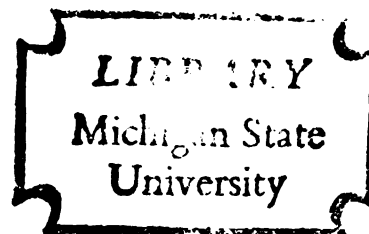


MECHANISMS OF THE EFFECTS OF POTASSIUM  
AND OSMOLALITY ON VASCULAR RESISTANCE  
TO BLOOD FLOW AND ON CELL MEMBRANE  
POTENTIAL

Thesis for the Degree of Ph. D.  
MICHIGAN STATE UNIVERSITY  
ROBERT ALLEN BRACE  
1973



This is to certify that the

thesis entitled

MECHANISMS OF THE EFFECTS OF  
POTASSIUM AND OSMOLALITY ON  
VASCULAR RESISTANCE TO BLOOD FLOW  
AND ON CELL MEMBRANE POTENTIAL

presented by

Robert Allen Brace

has been accepted towards fulfillment  
of the requirements for

Ph.D. degree in Chemical Engr.

A handwritten signature in cursive script, reading "Donald W. McCord", written over a horizontal line.

Major professor

Date May 15, 1973

## ABSTRACT

### MECHANISMS OF THE EFFECTS OF POTASSIUM AND OSMOLALITY ON VASCULAR RESISTANCE TO BLOOD FLOW AND ON CELL MEMBRANE POTENTIAL

by

Robert Allen Brace

When the plasma potassium ion concentration or the plasma osmolality of the blood perfusing a vascular bed is altered, resistance to blood flow in that vascular bed changes. In general, the effects of increasing ion concentrations and osmolality on vascular resistance are established. However the quantitative effects of decreasing the potassium ion concentration or osmolality have not been extensively investigated, probably because of the difficulty involved in producing these changes. Furthermore, the cellular mechanisms which produce the changes in resistance to blood flow have not been elucidated.

In general, changes in resistance are normally associated with changes in the membrane potentials of vascular smooth muscle cells, i.e., depolarization is associated with an increased resistance and hyperpolarization with a reduced resistance.

It has been shown that reductions in plasma  $[K^+]$  increase resistance to blood flow and slight to moderate elevations in plasma  $[K^+]$  decrease resistance. For these changes in  $[K^+]$ , previous equations for calculating membrane potential (Nernst and Goldman equations) predict a hyperpolarization with low  $[K^+]$  and a depolarization with elevated  $[K^+]$ . Thus the experimental changes in resistance are opposite to those predicted.

Studies in isolated tissues have shown that certain nerve cells, Purkinje fibers and intestinal smooth muscle cells depolarize when the extracellular  $[K^+]$  is reduced. These observations are not predictable with either the Nernst or Goldman equation.

It appears that the discrepancies between these experimental and predicted responses are due to the effects of changing the  $[K^+]$  on the electrogenic Na-K pump, an active, energy consuming mechanism which generates an electrical current in the process of transporting more Na ions out of than K ions into a cell.

This hypothesis was examined both experimentally and theoretically. The theoretical effects of varying  $[K^+]$  were investigated with a computer model of a living cell. The model calculates passive diffusional fluxes of  $K^+$ ,  $Na^+$ ,  $Cl^-$ , and water and active fluxes of  $Na^+$  and  $K^+$  (due to the pump) and uses these transmembrane fluxes to calculate transient changes in resting membrane potential, intracellular ion concentrations and cell volume. The model is applicable to any cell type and calculated changes in resting potential



agree with experimental potentials when extracellular  $[K^+]$ ,  $[Na^+]$ ,  $[Cl^-]$  or osmolality is varied. However, experimental changes in potentials can be calculated only when the electrogenic character of the Na-K pump is introduced.

The experimental effects of varying  $[K^+]$  were investigated in the gracilis muscle and coronary vascular beds of the dog. The quantitative and transient effects on vascular resistance of increasing and/or decreasing the plasma  $[K^+]$  were determined before and after administration of ouabain, a well known inhibitor of the Na-K pump.

Desired changes in plasma concentrations were produced by interposing a hemodialyzer in the arterial blood supply of the gracilis muscle or heart. The perfusing blood was then dialyzed against either a normal Ringer's solution, which contained essentially the same ionic makeup as blood plasma, or against a Ringer's solution with a high or low  $[K^+]$ .

In the gracilis muscle, resistance decreased linearly as the plasma  $[K^+]$  was varied from approximately 0.2 to 8.0 mEq/l. In the heart, reducing the plasma  $[K^+]$  in the blood perfusing the coronary artery significantly increased resistance and myocardial contractile force. After ouabain, changing the plasma  $[K^+]$  had little affect on skeletal muscle or coronary vascular resistance or contractile force. In addition, ouabain produced an increase in resistance in both vascular beds which reached a maximum in approximately 5-10 minutes and this was followed by a gradual decline in resistance.

From these studies, it was concluded that the changes in resistance and resting membrane potential produced by altered  $[K^+]$  are opposite to those predicted with the Nernst or Goldman equation because of the effects of  $K^+$  on the electrogenic Na-K pump. Lowering the  $[K^+]$  slows the pump and thus depolarizes the cell membrane and increasing the  $[K^+]$  up to 10-12 mEq/l stimulates the pump and produces hyperpolarization. In addition, the transient effects on resistance of increasing or decreasing the plasma  $[K^+]$  are predictable with the computer model.

The transient effects of ouabain on resistance have also been investigated the the computer model. It appears that the initial increase in resistance is due to a gradual inhibition of the electrogenic pump which depolarizes the vascular smooth muscle cells. The waning of resistance appears to be produced by an increasing intracellular  $[Na^+]$  stimulating the Na-K pump, resulting in a gradual repolarization of the cells.

The studies on osmolality show that resistance increases linearly in skeletal muscle as osmolality is reduced. Furthermore, low osmolality increases coronary vascular resistance and myocardial contractile force. These increases in resistance with low osmolality may be in part the result of active vasoconstriction since calculations indicate that vascular smooth muscle cells depolarize under these conditions.

MECHANISMS OF THE EFFECTS OF  
POTASSIUM AND OSMOLALITY ON  
VASCULAR RESISTANCE TO BLOOD FLOW  
AND ON CELL MEMBRANE POTENTIAL

By

Robert Allen Brace

A THESIS

Submitted to  
Michigan State University  
in partial fulfillment of the requirements  
for the degree of

DOCTOR OF PHILOSOPHY

Department of Chemical Engineering

1973

582-144

To my parents

Richard and Elizabeth Brace

## ACKNOWLEDGMENTS

The author wishes to express his appreciation to Drs. D.K. Anderson, J.B. Scott and F.J. Haddy for their assistance and support during the course of these investigations.

The author also acknowledges the assistance of Mr. Booker Swindall, Mrs. Josephine Johnston and all of the many others who contributed to this work.

## TABLE OF CONTENTS

	Page
INTRODUCTION . . . . .	1
PART I: PREDICTING THE EFFECTS OF IONS ON RESTING MEMBRANE POTENTIAL . . . . .	8
BACKGROUND . . . . .	8
Definition of Membrane Potential . . . . .	8
Forces Which Act Upon Ions . . . . .	9
The Na-K Pump . . . . .	11
Generation and Maintenance of Resting Membrane Potential . . . . .	14
PREDICTING RESTING MEMBRANE POTENTIAL . . . . .	18
Nernst Equation: Electrochemical Equilibrium	19
Derivation . . . . .	19
Applicability . . . . .	20
Nernst-Planck Equation for Ionic Fluxes . . . . .	22
Constant Field Equation . . . . .	24
Derivation . . . . .	24
Applicability . . . . .	27
The Goldman Equation . . . . .	30
Modifications of the Goldman Equation . . . . .	32
General Method of Predicting Changes in Resting Membrane Potential: A Model . . . . .	38
CALCULATED AND EXPERIMENTAL MEMBRANE POTENTIALS . . . . .	44
Effect of Extracellular $K^+$ . . . . .	44
Hyperpolarization After Exposure to Zero $K^+$ . . . . .	49
Effect of $Cl^-$ . . . . .	52
Effect of Deficient $Na^+$ . . . . .	53
Effect of Tonicity . . . . .	56
Effect of Membrane Capacitance . . . . .	58
Na-K Exchange Ratio . . . . .	60
PREDICTED CHANGES IN CELL VOLUME AND INTRACELLULAR ION CONCENTRATIONS . . . . .	62

# Table of Contents.

	Page
DISCUSSION OF THE MODEL FOR PREDICTING RESTING POTENTIALS . . . . .	67
SUMMARY OF CALCULATING RESTING POTENTIALS . . . . .	70
PART II: EFFECTS OF IONS, OSMOLALITY AND OUABAIN ON VASCULAR RESISTANCE TO BLOOD FLOW . . . . .	71
LITERATURE REVIEW . . . . .	73
Potassium . . . . .	73
Magnesium . . . . .	74
Sodium . . . . .	75
Osmolality . . . . .	76
Ouabain . . . . .	76
METHODS . . . . .	78
Gracilis Muscle Preparation . . . . .	78
Heart Preparation . . . . .	80
Forelimb Preparation . . . . .	81
Altering Blood Plasma Ion Concentrations . . . . .	82
Monitoring Resistance . . . . .	85
Hemodialyzers . . . . .	86
Analysis . . . . .	86
EXPERIMENTAL RESULTS . . . . .	89
Potassium . . . . .	89
Gracilis Muscle . . . . .	89
Heart . . . . .	94
Magnesium . . . . .	103
Hypoosmolality . . . . .	103
Gracilis Muscle . . . . .	103
Heart . . . . .	106
Sodium . . . . .	113
Ouabain . . . . .	116
Gracilis Muscle . . . . .	116
Heart . . . . .	118
DISCUSSION OF EXPERIMENTAL RESULTS . . . . .	121
Potassium . . . . .	121
Magnesium . . . . .	123
Hypoosmolality . . . . .	123
Sodium . . . . .	127
Ouabain . . . . .	128

## Table of Contents.

	Page
PART III: MECHANISMS OF THE EFFECTS OF $K^+$ , OUABAIN AND OSMOLALITY ON VASCULAR RESISTANCE TO BLOOD FLOW . . . . .	130
RELATIONSHIP BETWEEN RESTING MEMBRANE POTENTIAL AND VASCULAR RESISTANCE TO BLOOD FLOW . . . . .	131
MECHANISM OF THE EFFECT OF $K^+$ ON VASCULAR RESISTANCE . . . . .	135
MECHANISM OF THE EFFECT OF OUABAIN ON VASCULAR RESISTANCE . . . . .	144
MECHANISM OF THE EFFECT OF OSMOLALITY ON VASCULAR RESISTANCE . . . . .	148
DISCUSSION OF MECHANISMS WHICH ALTER VASCULAR RESISTANCE . . . . .	153
SUMMARY AND CONCLUSIONS. . . . .	157
RECOMMENDATIONS . . . . .	161
BIBLIOGRAPHY . . . . .	163
APPENDIX: TABULATED DATA. . . . .	171



## LIST OF TABLES

Table	Page
1. Representative intracellular and extracellular concentrations of mammalian smooth muscle cells. . . . .	3
2. Permeabilities and intracellular concentrations used in the simulations. . . . .	48
3. A comparison of blood plasma composition and control dialysate composition. . . . .	83
4. Effects of altering plasma $[K^+]$ on gracilis muscle perfusion pressure. . . . .	171
5. Effects of reduced plasma $[K^+]$ on coronary perfusion pressure and heart . . . . .	172
6. Average effects of 5 minute hypokalemic perfusion on coronary artery and heart during constant pressure perfusion. . . . .	173
7. Average effects (n=8) of prolonged hypokalemia on the myocardium and coronary vessels produced while maintaining coronary perfusion pressure constant. . . . .	174
8. Effects of hypoosmolality on gracilis muscle perfusion pressure during constant flow perfusion. . . . .	175
9. Effects of hypoosmotic perfusion of coronary artery on myocardium and coronary resistance. .	176
10. Average effects (n=11) of hypoosmotic perfusion of the coronary artery on myocardium and coronary vessels during constant pressure perfusion. . .	177
11. Effect of isoosmotic replacement of plasma NaCl with mannitol on gracilis artery perfusion pressure. . . . .	178

12.	Effects of hyperosmotic NaCl and glucose (900 mOsm/l) infusions on gracilis muscle vascular resistance. . . . .	179
-----	---	-----

## LIST OF FIGURES

Figure	Page
1. Schematic representation of resting potentials (RP) and action potentials (AP) in selected mammalian cells. . . . .	4
2. Schematic representation of a cell membrane showing distribution of electrical charges. . .	8
3. Effect of sodium and potassium concentration on ouabain sensitive Na-K ATPase activity. . .	15
4. Ion concentrations in a cell membrane as calculated from the constant field equation. .	28
5. Calculated effects of potassium ion on resting potential in skeletal and smooth muscle. . . .	37
6. Algorithm showing sequence of calculations performed by the model. . . . .	43
7. Changes in resting potential of snail neurone in response to a step increase in $[K^+]_e$ and return to the normal $[K^+]_e$ . . . . .	45
8. Changes in ionic fluxes of snail neurone in response to a step increase in $[K^+]_e$ and return to normal. . . . .	46
9. Steady state resting potential of molluscan neurone at various $K^+_e$ concentrations. . . . .	50
10. Resting potential of guinea-pig portal vein during recovery from $Na^+$ loading. . . . .	51
11. Resting potential of snail neurone at various $Cl^-$ concentrations. . . . .	54
12. Calculated transient and steady state effects of sodium deficiency on resting potential of guinea-pig taenia coli. . . . .	55

Figure		Page
13.	Calculated effects of increased tonicity and $[\text{Na}^+]_e$ on resting potential in guinea-pig taenia coli. . . . .	57
14.	Calculated changes in resting potential of guinea-pig taenia coli upon doubling normal tonicity with sucrose. . . . .	59
15.	Effect of membrane capacitance (C) on time course of potential changes simulated in the same cell for the same change in $[\text{K}^+]_e$ . . . . .	61
16.	Calculated changes in red blood cell volume when tonicity is suddenly increased to 1.49 times normal. . . . .	63
17.	Decrease in cell volume and ion content caused by a reduction in $[\text{Na}^+]_e$ . . . . .	65
18.	Effect of potassium ion free bathing fluid on intracellular sodium ion concentration in snail neurone. . . . .	66
19.	Blood and dialysate flow circuits used in the gracilis muscle experiments. . . . .	79
20.	Exploded view of hemodialyzer. . . . .	87
21.	Typical response of gracilis muscle to hypokalemia. . . . .	90
22.	Effects of hyperkalemia on gracilis muscle perfusion pressure. . . . .	91
23.	Effects of altering plasma $[\text{K}^+]$ on gracilis muscle perfusion pressure. . . . .	93
24.	Typical effects of local hypokalemia on left ventricular contractile force, coronary vascular resistance and systemic arterial pressure during perfusion of the coronary vasculature with constant flow. . . . .	95
25.	Changes in coronary perfusion pressure produced by reducing coronary arterial plasma $[\text{K}^+]$ at constant coronary flow. . . . .	96
26.	Changes in left ventricular contractile force produced by reducing coronary arterial plasma $[\text{K}^+]$ at constant coronary flow. . . . .	97

Figure		Page
27.	Effects of hypokalemia on QT interval and myocardial contractility at constant coronary flow. . . . .	99
28.	Average effects of local hypokalemia on the myocardium and coronary vessels produced during constant coronary perfusion pressure. .	101
29.	Average effects (n=8) of prolonged hypokalemia on the myocardium and coronary vessels produced while maintaining coronary perfusion pressure constant. . . . .	102
30.	Effects of low plasma $[Mg^{++}]$ on gracilis muscle perfusion pressure compared to the effects of low plasma $[K^+]$ . . . . .	104
31.	Typical responses of gracilis muscle to hypoosmotic perfusion. . . . .	105
32.	Effects of plasma hypoosmolality on gracilis muscle perfusion pressure. . . . .	107
33.	The effects of local plasma hypoosmolality on coronary perfusion pressure produced during constant coronary flow. . . . .	108
34.	The effects of local plasma hypoosmolality on myocardial contractile force produced during constant coronary flow. . . . .	110
35.	Simultaneous changes in QT interval and contractile force produced by hypoosmotic perfusion of coronary artery at constant flow..	111
36.	Effects of local hypoosmolality on myocardium and coronary vessels produced during constant pressure perfusion of coronary artery. . . . .	112
37.	Effect of hyponatremia on gracilis muscle perfusion pressure. . . . .	114
38.	Effects of hyponatremia on gracilis perfusion pressure. . . . .	115
39.	Average effects of a continuous ouabain infusion on gracilis perfusion pressure. . . .	117
40.	Effect of flow rate on time of maximum response during ouabain infusion. . . . .	119

Figure		Page
41.	Average effects (n=6) of ouabain administration on myocardial contractile force, coronary perfusion pressure, and systemic arterial pressure during perfusion of the coronary bed at constant flow. . . . .	120
42.	Changes in smooth muscle tension as a function of membrane potential. . . . .	132
43.	Changes in resting membrane potential as a function of tension. . . . .	133
44.	Average effects (n=12) of ouabain on skeletal muscle vascular response to hypokalemia. . . .	137
45.	Average effects (n=12) of ouabain on skeletal muscle vascular response to hyperkalemia. . . .	138
46.	Predicted and experimental changes in resistance produced by altered plasma potassium ion concentration. . . . .	140
47.	Calculated transient changes in resting potential with increased and decreased potassium ion concentration. . . . .	141
48.	Transient changes in forelimb perfusion pressure produced by hypo- and hyperkalemic perfusion during constant flow. . . . .	143
49.	Calculated and experimental effects of ouabain on coronary vascular resistance during constant flow perfusion of left common coronary artery..	145
50.	Calculated effects of osmolality on vascular smooth muscle resting membrane potential. . . .	150

## NOMENCLATURE

<u>SYMBOL</u>	<u>DEFINITION</u>
a	activity of Na-K pump; chemical activity
A	cell surface area; reference activity of Na-K pump
b	partition coefficient
C	membrane capacitance; concentration
Ca	calcium
Cl	chloride
d	membrane thickness
D	diffusivity; diameter
E	electrical potential
F	Faraday
H	hydrogen
j	molar flux
J	current flux
K	potassium
L	length
M	molar flux; concentration within membrane
Mg	magnesium
n	ion species n
N	integration constant
P	permeability; pressure

## Nomenclature

Q	electrical charge; flow rate
r	Na to K exchange ratio of pump
R	gas constant; resistance
t	time
T	absolute temperature
u	ion mobility; viscosity
U	chemical potential
V	cell volume
z	ion valence

## Subscripts

act	active
d	membrane thickness
dif	diffusion
e	extracellular
el	electrical
i	intracellular
m	membrane
met	metabolic
n	ion species n
o	standard state or reference condition
p	pump
pas	passive



## INTRODUCTION

The electrical potential differences which exist across biological membranes (referred to as membrane potentials) are of tremendous importance in many processes that maintain life. Examples include the following:

1) Changes in membrane potential of the cells in the blood vessels of an organ cause vessel diameters to change, thereby altering blood flow rate and thus nutritional supply to the organ. 2) The heart beat is initiated by changes in membrane potential of the pacemaker cells. 3) Muscle contraction results from changes in membrane potential of the muscle cells. 4) Nervous function is entirely dependent upon changes in membrane potential of the nerve cells. Consequently, a knowledge of the processes which produce and alter membrane potentials in living cells will help toward an understanding of life and may increase our knowledge of many diseases and even aid in their cure.

Living cells can be characterized by the concentration gradients and electrical potentials maintained across their membranes. On an elementary level, a cell can be considered to be a small volume of a dilute water solution separated by a thin membrane (approximately  $75 \text{ \AA}$  thick) from the dilute water solution which bathes it. The solutes are

almost entirely ions as can be seen from the representative intracellular and extracellular concentrations given in Table 1. Ion concentrations and cell membrane permeabilities to these ions are directly responsible for the membrane potential.

In general, membrane potentials can be considered to be either resting potentials or action potentials, depending upon their rate of change. A membrane potential is a resting potential if it is changing either slowly or not at all. Typical values of resting membrane potentials vary from -100 mvolts to -40 mvolts, depending upon cell type. (resting potentials are negative by convention since the inside of the cell membrane is negatively charged with respect to the outside.) On the other hand, when an action potential occurs, membrane potential rapidly increases from its resting value, often to a positive potential (+10 to +40 mvolts), and returns to its resting value within a few milliseconds (msec.). (An exception occurs in the heart where the duration of action potentials is from 200 to 300 msec.) Examples of resting and action potentials are shown in Figure 1.

Varying the concentrations of the ions in the fluid bathing a cell leads to changes in resting potential. In some cells, there are also changes in frequency, duration and shape of the action potentials, while in other cells (referred to as "quiet" cells), even though the resting potential changes, no action potentials occur.

Table 1. Representative intracellular and extracellular concentrations of mammalian smooth muscle cells.

Substance	Concentrations (mEq/l)		Nernst Equilibrium Potential
	Intracellular	Extracellular	
K <sup>+</sup>	145	4	-96
Na <sup>+</sup>	10 <sup>*</sup>	150	+72
Cl <sup>-</sup>	17	110	-50
HCO <sub>3</sub> <sup>-</sup>	8	27	-32
H <sup>+</sup> (pH)	1.25x10 <sup>-4</sup> (6.9)	4x10 <sup>-5</sup> (7.4)	-31
Mg <sup>++</sup>	1 <sup>*</sup>	2	+19
Ca <sup>++</sup>	10 <sup>-4</sup> *	5	+289
glucose	-	5	-
proteins anions	140	3	-
TOTAL (mOsm/kg)	300	300	E <sub>m</sub> = -50

\* approximate free ionic concentration

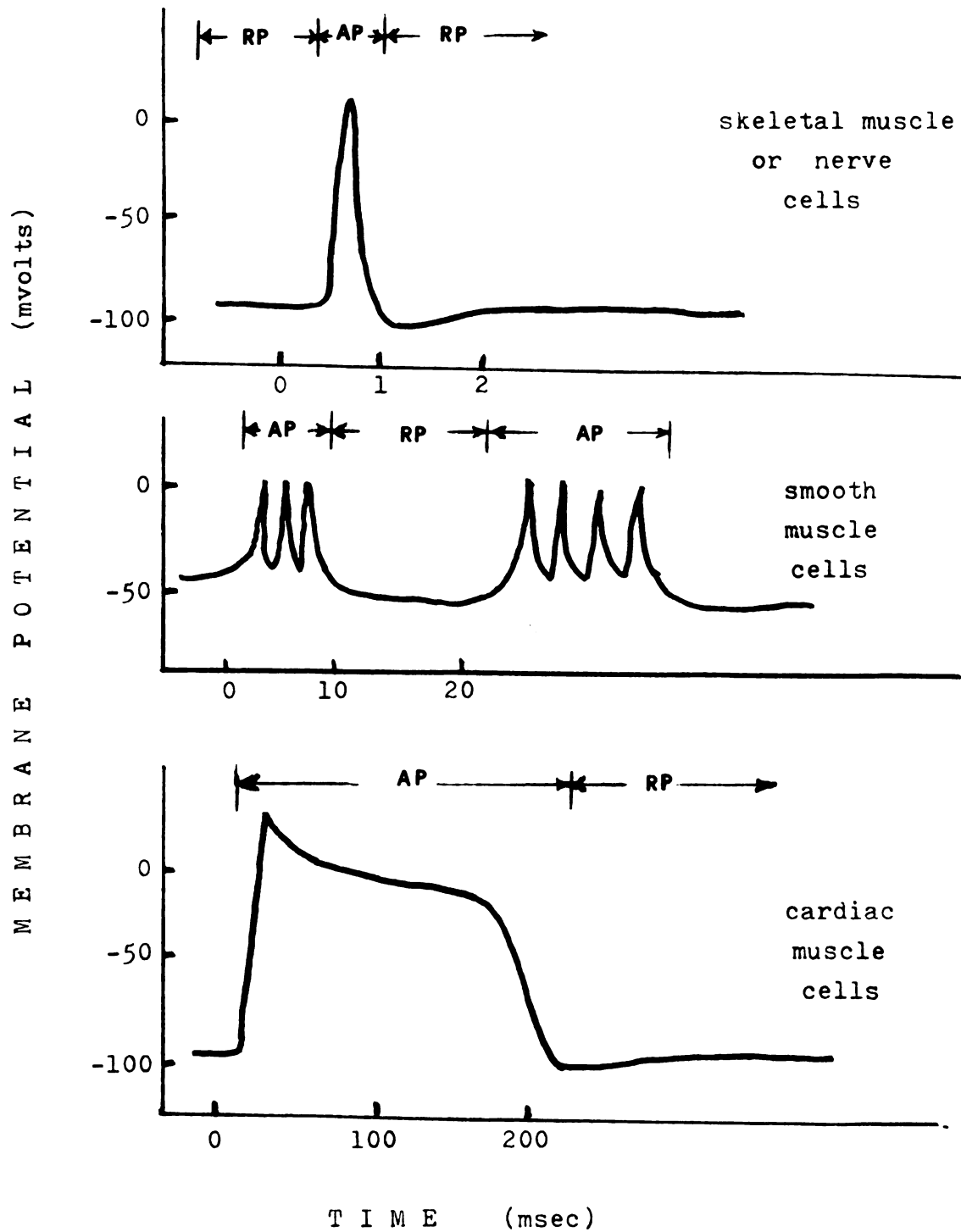


Figure 1. Schematic representation of resting potentials(RP) and action potentials(AP) in selected mammalian cells.

When the concentration of an ion in the blood perfusing a vascular bed is altered, the resistance to blood flow in that vascular bed changes. The qualitative effects of plasma ion concentration variations on vascular resistance are generally established. However, prior to this study, the quantitative and transient effects of changes in ion concentrations on resistance have not been extensively studied.

Changes in resistance to flow produced by altered ion concentrations are thought to be brought about by the effects of the ions on membrane potentials and the subsequent changes in tension developed by the vascular smooth muscle cells in the walls of the blood vessels. Changes in tension lead to changes in luminal diameter of these vessels. Their diameter (D) is directly related to resistance to flow (R) as can be seen by a modified form of the Hagen-Poiseuille equation for laminar flow of a Newtonian fluid through a circular tube:

$$R = \frac{-\Delta P}{Q} = \frac{128 \mu L}{D^4} .$$

Thus resistance to blood flow varies inversely with the fourth power of vessel diameter and linearly with viscosity  $\mu$  and flow rate  $Q$ .

If the relationship between ion concentrations and membrane potential could be predicted, then this would aid in explaining the mechanisms responsible for changing vascular resistance to blood flow, as well as understanding many other processes in cellular and nervous functioning.

A quantitative description of the events occurring during action potentials has been developed by Hodgkin and Huxley(49). Their work has greatly increased general understanding of action potentials, however a complete knowledge of the changes in the cell membrane that produce the action potentials is not yet available.

There have been several equations developed for predicting resting potentials and how they vary with ion concentrations(38,48,58,86). However, these equations are inadequate since they do not predict many experimentally observed changes in resting potentials. For example, previous methods predict a hyperpolarization when the extracellular potassium ion concentration ( $[K^+]_e$ ) is lowered, whereas some cells actually depolarize under this condition (24,39,88,90). Furthermore, there has been no method for predicting transient effects on membrane potential of ion concentration variations.

The purposes of the research presented in this thesis were to: 1) develop a general method of calculation that would accurately predict the appropriate directional and transient changes in resting membrane potential as functions of extracellular ion concentrations, 2) determine quantitatively the effects of changes in plasma ionic composition on vascular resistance to blood flow, and 3) use the method of predicting resting potentials to predict, and thus offer an explanation of, the mechanisms involved in observed change in resistance to blood flow when the concentration of an ion in the blood plasma is acutely varied.

These objectives were fulfilled and are considered separately in PARTS I, II, and III of this thesis. PART I discusses the factors which contribute to resting potential and develops a method of calculating transient changes in resting membrane potential when extracellular ion concentrations are varied. PART II presents the experimental effects of changes in plasma ion concentrations, osmolality and ouabain on vascular resistance to blood flow in skeletal muscle and coronary vascular beds of the dog. PART III presents the cellular mechanisms which produce the changes in resistance to blood flow when blood plasma  $[K^+]$  or osmolality is altered or when ouabain is administered. In addition, the transient changes in resistance produced by changing plasma  $[K^+]$  are predicted in PART III of this thesis.

PART I:

PREDICTING THE EFFECTS OF IONS ON

RESTING MEMBRANE POTENTIAL



## BACKGROUND

### Definition of Membrane Potential

A membrane potential is simply an electrical potential difference which exists across a cell membrane because of a separation of electrical charges. The charges may be either large ionized protein molecules, perhaps attached to the cell membrane, or simple ions such as  $\text{Na}^+$ ,  $\text{K}^+$ , or  $\text{Cl}^-$ .

The potential is maintained primarily by the relatively high resistance to ionic flow through the membrane. Changes in resting potential are due to net transmembrane ionic fluxes. For example, movement of cations into the cell causes hypopolarization (depolarization) whereas an anionic flux into the cell produces hyperpolarization. The opposite changes in potential occur for effluxes of the ions.

The cell membrane and electrical charge distribution are represented in Figure 2, where it is seen that the inside of the cell membrane is negatively charged with respect to the outside.

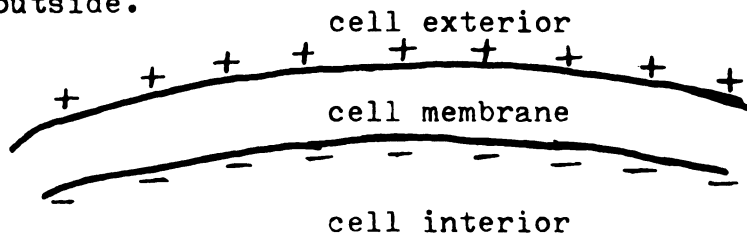


Figure 2. Schematic representation of a cell membrane showing distribution of electrical charges.

### Forces Which Act Upon Ions

In order to understand how membrane potentials are maintained and altered, it is necessary to consider the forces which are exerted on ions. These forces produce fluxes of the ions across the cell membrane and it is these fluxes which alter membrane potentials.

There are two forces which produce a passive diffusional movement of ions through the cell membrane: chemical concentration gradients and electrical gradients. If there are areas of unequal ion concentrations, the ions will tend to diffuse down their concentration gradients to an area of lower concentration. Since ions are electrically charged, an electrical gradient will tend to cause ions to migrate. With the interior of the cell negatively charged, cations will tend to diffuse into the cell whereas anions will tend to diffuse out of the cell. These electrical and chemical forces can be combined and are referred to as electrochemical forces.

If an ion is distributed at electrochemical equilibrium across a membrane, then there is no net diffusional flux of this ion across the membrane. The resting membrane potential at which this equilibrium exists is the equilibrium potential for that ion. Its value can be calculated from the Nernst equation (derived later) as follows:

$$E_n = \frac{R T}{F z_n} \ln \frac{[n]_e}{[n]_i}$$

where  $E_n$  = the equilibrium potential of ion  $n$ ,  
 $R$  = the gas constant,  
 $T$  = the absolute temperature,  
 $F$  = the Faraday = 96494 coulombs/gm mole,  
 $z_n$  = the valence of ion  $n$ .

Subscripts  $i$  and  $e$  refer to intracellular and extracellular, respectively.

If the equilibrium potential of an ion is more negative than the existing membrane potential ( $E_m$ ), there will be a net diffusional flux out of the cell if the ion is positively charged and into the cell if the ion is negatively charged. The reverse occurs when the equilibrium potential is less negative than membrane potential.

Some calculated Nernst equilibrium potentials are shown in Table 1 for a hypothetical smooth muscle cell. With the given ion concentrations, K ions will passively diffuse out of the cell while Na ions will diffuse into the cell. However, no net flux of Cl ions will occur. It can therefore be concluded that no forces other than those represented by the chemical and electrical gradients affect the movement of  $Cl^-$  across the membrane in this example. However, this is not the case for Na and K ions. With the passive diffusional loss of K ions from the cell and the gain of Na ions, there must be another force which acts on the Na and K ions in order to maintain the steady state concentrations of these ions in the cell. This force has come to be known as the "Na-K pump". It is an active, energy consuming mechanism

which transports K ions into the cell and Na ions out of the cell against their electrochemical gradients.

### The Na-K pump

Cells, in general, have a high concentration of K ions and a low concentration of Na ions inside them. Since the cell membrane is permeable to these ions and they are not at electrochemical equilibrium, there is a continuous passive diffusional loss of K ions from the cell and a gain of Na ions. These passive fluxes are balanced by an active, energy consuming transport of K ions into the cell and Na ions out of the cell. The mechanism responsible for this active transport is the afore mentioned Na-K pump (sometimes erroneously referred to as the Na pump), which is located in the sarcolemmal membrane of the cell.

The energy for active transport is supplied by the energy rich compound, adenosine triphosphate (ATP), which is produced by metabolic processes within the cell.

The actual process by which the ions are actively transported is still unknown, but an enzyme that is intimately related to the pumping mechanism has been identified in red blood cells, brain cells, and in the membranes of a great many other types of cells in a wide variety of species. This enzyme hydrolyzes ATP to adenosine triphosphate (ADP) and in the process releases energy. It is activated by  $\text{Na}^+$  and  $\text{K}^+$  and has therefore come to be known as Na-K activated adenosine triphosphatase or Na-K ATPase.

"It has different sites with affinities for cations: one where the affinity of  $\text{Na}^+$  exceeds the affinity for  $\text{K}^+$  and one where the affinity for  $\text{K}^+$  exceeds the affinity for  $\text{Na}^+$ . For maximum activity, one site must be occupied by Na ions and the other by K ions. The enzyme is a large lipoprotein with a molecular weight of 670,000 which requires  $\text{Mg}^{++}$  for activity and is inhibited by (many metabolic poisons as well as by the cardiac glucosides, including) ouabain. Its concentration in the cell membrane is proportionate to the rate of  $\text{Na}^+$  and  $\text{K}^+$  transport in the cells. Its properties closely resemble those of the Na-K pump and it must in some way be intimately associated with it."\*

If the Na-K pump transports one  $\text{K}^+$  into the cell for each  $\text{Na}^+$  that is extracted, then the pump is electroneutral since no net transfer of electrical charge occurs because of the pump. On the other hand, if more Na ions are transported out of the cell than K ions in (or vice versa), then the pump is electrogenic and contributes directly to resting membrane potential by generating an electrical current across the cell membrane.

As initially conceived in the early 1940's(86), it was thought that the pump transported only Na ions out of the cell and thus was electrogenic. Once it became established that the pump transported K ions into the cell at the same time as it transported Na ions out, it was generally believed that the pump was electroneutral. The idea of

---

\*W.F. Ganong(34), pp. 14-15.

electroneutrality became firmly entrenched with the successful prediction of resting membrane potentials by an equation (developed by Goldman(38) and Hodgkin and Katz(48)) which implicitly assumed electroneutrality.

Recently, however, it has been shown that the Na-K pump in red blood cells, fat cells, nerve cells, and muscle cells of many different species is electrogenic(2,20,21,22,27,39, 55,59,85,86,91,92). Thus it appears as if the Na-K pump is electrogenic in all cells.

One of the easiest and most conclusive ways to show that the Na-K pump of a given cell type is electrogenic is to show that the membrane hyperpolarizes when the intracellular sodium ion concentration ( $[Na^+]_i$ ) is slightly increased. This would produce a rapid depolarization if the pump were electroneutral. Another method is to show that a rapid depolarization occurs in the presence of a metabolic inhibitor. Also, the Na-K pump is electrogenic if reducing the  $[K^+]_e$  causes the cell to depolarize. However, failure of the cell to depolarize with reduced  $[K^+]_e$  does not imply that the pump is electroneutral.

The rate at which Na and K ions are actively transported is dependent upon the  $[K^+]_e$  and  $[Na^+]_i$ . Since the active transport is coupled, a decrease in  $[K^+]_e$  will not only reduce  $K^+$  uptake, but also reduce  $Na^+$  extrusion by the pump. Similarly for a decrease in the  $[Na^+]_i$ . Conversely, increases in the concentrations of these ions stimulate the activity of the pump.

The sensitivity of the Na-K pump to  $[K^+]_e$  and  $[Na^+]_i$  has been investigated by determining the ouabain-sensitive Na-K ATPase activity(31,91). It appears that the rate of active transport increases as the  $[K^+]_e$  is increased up to 10 mEq/l or as the  $[Na^+]_i$  is increased up to about 100 mEq/l. However, further increases in these concentrations have little affect on the pump, as seen in Figure 3.

The exchange ratio of the Na-K pump most often cited in the literature is 1.5 Na ions extracted per K ion taken up by the pump. However exchange ratios of 3:1 have also been reported(86). In general, it is not known what determines the coupling ratio nor whether this ratio is constant in a given cell.

### The Generation and Maintenance of Resting Membrane Potential

Cell membranes are, in general, more permeable to K ions than to Na ions ( $P_K/P_{Na} = 50-100$  if  $E_m = -90$  mvolts). This fact along with the existence of the Na-K pump are the major properties of the cell membrane responsible for the transmembrane electrical potential difference. Clearly, if there were no resistance to passive fluxes of ions across the membrane, then there could be no electrical potential difference across the membrane.

On the other hand, consider a cell membrane with equal but opposite concentration gradients of Na and K ions across the membrane,  $P_K/P_{Na} = 100$ , and  $E_m = 0$  at time  $(t) = 0$ . In a short time, 100 K ions will diffuse across the membrane

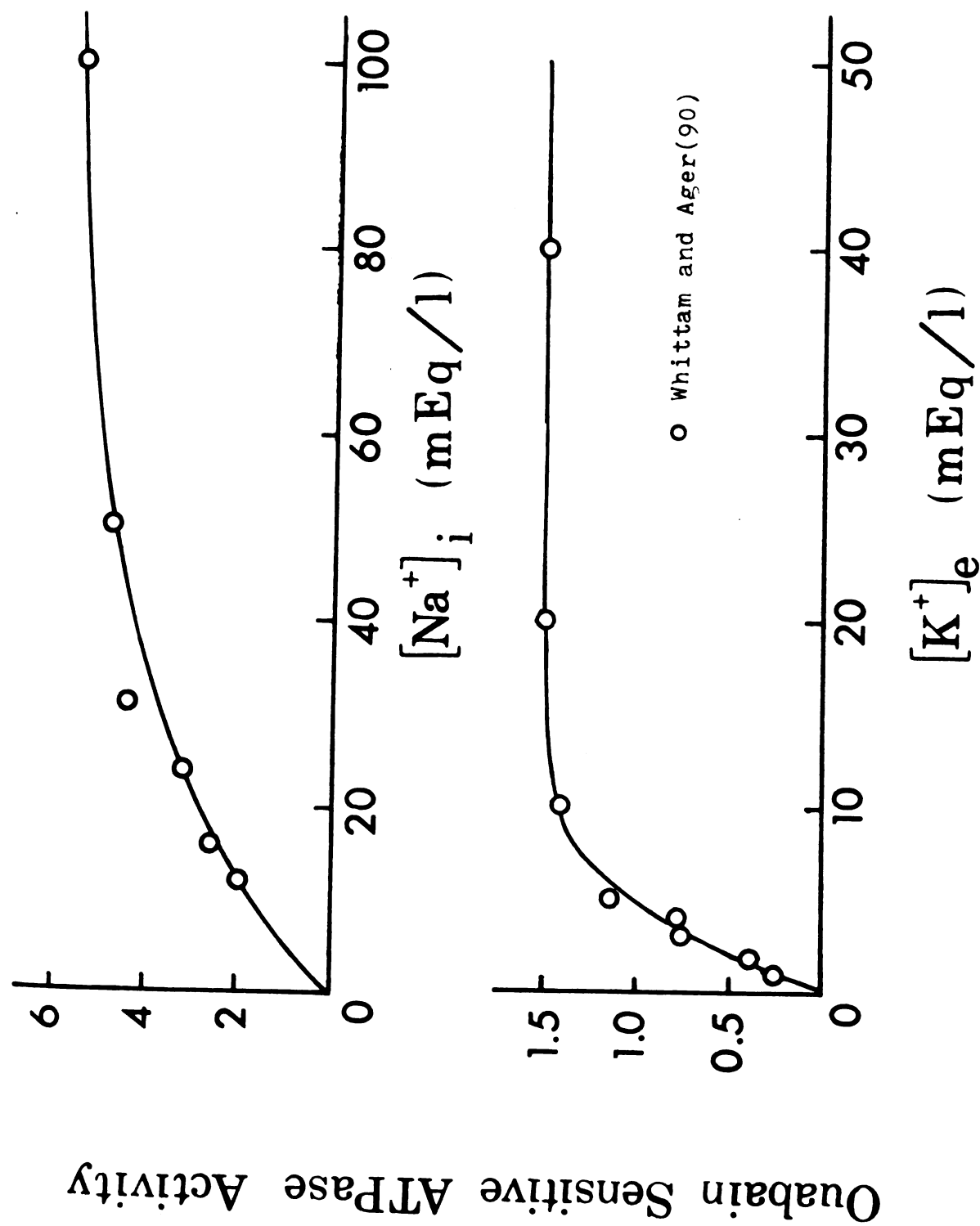


Figure 3. Effect of sodium and potassium concentration on ouabain sensitive Na-K ATPase activity.



compared with only one Na ion, resulting in a negative charge on the  $K^+$  side of the membrane. The negative charge increases the electrochemical driving force for  $Na^+$  while decreasing it for  $K^+$ . As diffusion proceeds, the membrane potential continues to increase and thus further increases the electrochemical gradient for  $Na^+$  while reducing it for  $K^+$ . The membrane rapidly (in the order of a few msec for biological membranes) becomes sufficiently charged so that only one  $K^+$  will cross the membrane for each  $Na^+$  and, if the concentrations are maintained constant, potential will no longer change even though the passive fluxes continue.

The portion of membrane potential in lining cells which is generated by the passive diffusion of ion across the cell membrane is referred to as the diffusion potential. The remaining fraction of membrane potential is generated by the electrogenic pump(s) which transport more charges in one direction across the membrane than in the opposite direction. Since metabolic energy is consumed by the electrogenic pump, this contribution to the total resting potential is referred to as the metabolic potential. The diffusion potential ( $E_{dif}$ ) and metabolic potential ( $E_{met}$ ) sum to produce the resting membrane potential:

$$E_m = E_{dif} + E_{met}.$$

The diffusion potential is a large fraction of  $E_m$  and thus  $E_{met}$  is usually small. For example, if  $E_m = -90$  mvolts,

$E_{dif}$  may equal -88 mvolts and  $E_{met} = -2$  mvolts. In general, as  $E_m$  becomes less negative,  $E_{met}$  increases and  $E_{dif}$  decreases. For example, if  $E_m = -50$  mvolts,  $E_{dif}$  may equal -40 mvolts and  $E_{met} = -10$  mvolts. These changes in  $E_{met}$  and  $E_{dif}$  as  $E_m$  becomes less negative are due to an increase in the sodium ion to potassium ion permeability ratio.

## PREDICTING RESTING MEMBRANE POTENTIALS

Because of their extreme importance in biological phenomena, it is important that we understand the processes and events which produce and alter resting membrane potentials. A knowledge of these processes and events can be demonstrated by a mathematical description of membrane potential. This description must be able to predict the steady state potentials as well as the changes in resting potential that occur when the concentrations of the naturally occurring ions are altered.

Membrane potential is a function of both the passive diffusion and active transport of ions across the cell membrane. Thus predicting resting membrane potentials as extracellular concentrations vary requires that the ionic fluxes due to the passive diffusion and active transport be calculated. The following sections examine the various methods of predicting ion fluxes and membrane potentials as well as considering the assumptions and applicability of each method.

## Nernst Equation: Electrochemical Equilibrium

### 1. Derivation

If an ion is distributed at electrochemical equilibrium across a membrane, then the sum of electrical plus chemical potentials of the ion on each side of the membrane will be equal:

$$z F E_1 + U_1 = z F E_2 + U_2. \quad (1)$$

The electrical potential  $E$  must be multiplied by  $F$ , the Faraday, in order to have units consistent with the chemical potential  $U$  and by  $z$ , the ion valence. Also

$$U = U_o + R T \ln a \quad (2)$$

where  $U_o$  represents the standard state chemical potential and  $a$  is the chemical activity of the ion. So that

$$zFE_1 + (U_o + RT \ln a_1) = zFE_2 + (U_o + RT \ln a_2). \quad (3)$$

Upon rearrangement, this yields the Nernst equation which gives the electrical potential difference across the membrane for any ion that is distributed at electrochemical equilibrium:

$$E_1 - E_2 = E_m = \frac{R T}{z F} \ln \frac{a_2}{a_1}. \quad (4)$$

This potential is referred to as the equilibrium potential for that ion. If it is assumed that the activity coefficient for the ion is the same on each side of the membrane, then the activity terms can be replaced by the appropriate concentrations  $C$ :

$$E_m = \frac{R}{z} \frac{T}{F} \ln \frac{C_2}{C_1} . \quad (5)$$

This is the most often used form of the Nernst equation.

## 2. Applicability

There were no assumptions made in the derivation of the Nernst equation, except that the ion under consideration is distributed across the membrane at electrochemical equilibrium, i.e., passively distributed. The simplification made by assuming that the activity coefficients on both sides of the membrane are equal should introduce little error. The total ionic concentrations on both sides of the membrane are approximately equal (.3 molal in mammals) and thus activity coefficients should be approximately equal and near 1.0. Note that no assumptions were made as to the membrane being homogeneous or the shape of the electrical potential profile through the membrane.

The Nernst equation can be used for predicting membrane potential if it has been established that the ion is at its equilibrium potential and if concentrations on both sides of the membrane are known. Alternately, the intracellular

concentration can be calculated from known  $E_m$  and extracellular ion concentration.

It now remains to be established which ions, if any, are passively distributed. In general, the criteria which must be satisfied are the following:

1. The ion must not be actively transported.
2. The ion must not be consumed or generated within the cell.
3. The ion must be in the bathing fluid sufficiently long.
4. Membrane permeability to the ion must be different from zero.

The ions to be excluded from an equilibrium distribution are  $\text{Na}^+$ ,  $\text{K}^+$ , and  $\text{Ca}^{++}$  since they are actively transported and  $\text{H}^+$  and  $\text{HCO}_3^-$  because they are generated or consumed within the cell. Of the ions which occur naturally and in relatively high concentrations,  $\text{Cl}^-$  is probably the only ion which may be distributed at electrochemical equilibrium.

In some cells, this is indeed the case. Studies in fat(64), liver(27), and skeletal muscle(50) cells showed that the  $\text{Cl}^-$  equilibrium potential and membrane potential are the same. However, there is evidence to indicate that the  $\text{Cl}^-$  may not be passively distributed in all tissues(23).

A comparison that is often made is between membrane potential and the potassium ion equilibrium potential ( $E_K$ ) at different extracellular potassium ion concentrations. This is sometimes a good approximation since the membrane permeability to  $\text{K}^+$  is relatively large and a major determinant of  $E_m$ . However,  $E_m$  should not be expected to

behave as a pure K electrode (i.e., vary exactly as  $E_K$ ) since other factors such as the Na-K pump and sodium ion permeability play a role in determining  $E_m$ . Nonetheless, since the  $[K^+]_i$  is easy to estimate and  $E_K$  is simple to calculate, a simple first approximation of  $E_m$  may be found by calculating  $E_K$ . For example, in skeletal muscle cells,  $E_K$  is often very close to  $E_m$  ( $E_K = -90$ ,  $E_m = -88$ ). However, in smooth muscle, fat and liver cells,  $E_K$  is very different from  $E_m$  ( $E_K = -90$ ,  $E_m = -50$ ).

### Nernst-Planck Equation for Ionic Fluxes

For biological membranes, the forces which cause passive movement of ions are those due to concentration gradients and electrical fields (electrical potential gradients). The diffusional flux of ion n ( $j_{n,dif}$ ) which occurs because of concentration gradients ( $\nabla C_n$ ) is expressed by Fick's law as

$$j_{n,dif} = -D_n \nabla C_n \quad (6)$$

where  $D_n$  is the diffusion coefficient for the ion.

If an electrical field ( $\nabla E$ ) is present, then, since ion velocity due to the electrical field is equal to  $\nabla E$  times the ion mobility ( $u_n$ ), the ionic flux will be

$$j_{n,el} = - u_n \frac{z_n}{|z_n|} C_n \nabla E. \quad (7)$$

The factor  $z_n/|z_n|$  takes care of the sign, which is in the direction of the negative gradient for cations and in the opposite direction for anions. The total flux when both diffusional and electrical forces are present is simply the sum of the individual fluxes:

$$j_n = - D_n \nabla C_n - D_n C_n z_n \frac{F}{R T} \nabla E. \quad (8)$$

(The units of  $j_n$  are moles per cross sectional area per time.) In this equation, the ionic mobility has been replaced in terms of diffusivity using the Einstein relation (65):

$$D_n = \frac{u_n R T}{z_n F}. \quad (9)$$

The above flux equation is converted into an expression for electrical current density by recognizing that each mole of ions carries a charge  $F z_n$ . Thus

$$J_n = - D_n z_n F (\nabla C_n + z_n C_n \frac{F}{R T} \nabla E) \quad (10)$$

and  $J_n$  has units of amperes per area.

These flux equations and variations of them are referred to as the Nernst-Planck equations. They are exact



theoretical descriptions of the events leading to the passive movement of ions at a point.

Unfortunately, because of the complexity of the electrical and chemical gradients within the membrane and at the membrane surfaces, the Nernst-Planck equation cannot be integrated directly and solved for the net ionic fluxes of an ion across the cell membrane.

### The Constant Field Flux Equation

#### 1. Derivation

Goldman made the assumption that the electrical field within the cell membrane is constant(38). In this case, the electrical potential increases linearly through the membrane and

$$\nabla E = \frac{dE}{dx} = \frac{E}{d} \quad (11)$$

where x represents position in the membrane and d is the membrane thickness. The result of this assumption is the Nernst-Planck equation (eqn 10) can be integrated directly. For ion n,

$$-J_n = D_n z_n F \frac{dM_n}{dx} + D_n z_n^2 \frac{F}{R T} M_n \frac{E}{d} \quad (12)$$

where  $M_n$  represents the concentration of the ion in the membrane. This is an ordinary first order separable

differential equation where the dependent variable is the concentration  $M_n$  and the independent variable is  $x$ .

Rearranging,

$$\frac{dM_n}{dx} = -\left(\frac{z_n F E}{R T d}\right) M_n - \frac{J_n}{D_n z_n F} \quad (13)$$

and solving for  $M_n$  as a function of  $x$  yields

$$M_n(x) + N \exp\left(-\frac{z_n F E x}{R T d}\right) = \frac{J_n R T d}{D_n z_n^2 F^2 E} \quad (14)$$

where  $N$  is a constant of integration.

The boundary conditions are

$$M_n(x=0) = M_{no} \quad \text{and} \quad (15a)$$

$$M_n(x=d) = M_{nd} \quad (15b)$$

The integration constant can be evaluated in terms of the concentration within the membrane. At  $x = 0$ ,

$$M_{no} = N - \frac{J_n R T d}{D_n z_n^2 F^2 E} \quad (16)$$

Substitution of  $N$  into equation 14 yields the constant field equation for the concentration profile within the membrane:

$$M_n(x) = M_{no} \exp\left(-\frac{z_n FEx}{RTd}\right) + \left(\exp\left(-\frac{z_n FEx}{RTd}\right) - 1\right) * \frac{J_n RTd}{D_n z_n^2 F^2 E}. \quad (17)$$

It can be seen that the concentration of an ion in the membrane is dependent upon surface concentrations, net flux of the ion, and the transmembrane electrical potential difference.

By applying the boundary condition at  $x = d$  and solving for  $J_n$ , we have

$$J_n = z_n^2 D_n \frac{FE}{RTd} \frac{M_{nd} - M_{no} \exp(-z_n FE/RT)}{\exp(-z_n FE/RT) - 1}. \quad (18)$$

Now it is assumed that the concentrations of the ions in the surfaces of the membrane are related to the concentrations in the fluids bathing the membrane by a constant  $b$ , called the partition coefficient (assumed equal on both sides of the membrane):

$$M_{no} = b_n C_{no} = b_n C_{ne} \quad (19a)$$

$$M_{nd} = b_n C_{nd} = b_n C_{ni} \quad (19b)$$

where  $C_{ne}$  and  $C_{ni}$  represent the concentrations of ion  $n$  in the extracellular fluid and the intracellular fluid, respectively.

By applying the partition coefficient assumption and defining the membrane permeability of ion  $n$  ( $P_n$ ) to be

$$P_n = \frac{D_n b_n}{d}, \quad (20)$$

eqn 18 becomes the widely used constant field equation for the net flux of an ion across the cell membrane:

$$J_n = P_n z_n^2 \frac{F^2 E}{RT} \frac{C_{ni} - C_{ne} \exp(-z_n FE/RT)}{\exp(-z_n FE/RT) - 1}. \quad (21)$$

Note that if any ion is distributed at electrochemical equilibrium, the net flux will be zero and the constant field flux equation reduces to the Nernst equation.

An important result of the constant field equation is that the concentrations of the ions within the cell membrane can be calculated. Figure 4 shows the concentration profiles for some of the ions in Table 1 as calculated from equations 17 and 21 with an assumed partition coefficient equal to 1.0. The concentrations vary exponentially with distance in the membrane as expected from eqn 17.

## 2. Applicability

There have been three main criticisms of the constant field flux equation (eqn 21): 1) the constant field assumption is incorrect, 2) the assumption that the partition coefficients on both sides of the membrane are equal is inaccurate, and 3) the permeability coefficients are not obtainable from fundamental microscopic membrane properties. The latter of these criticisms, true or not, has little bearing on the validity of eqn 21. Secondly,

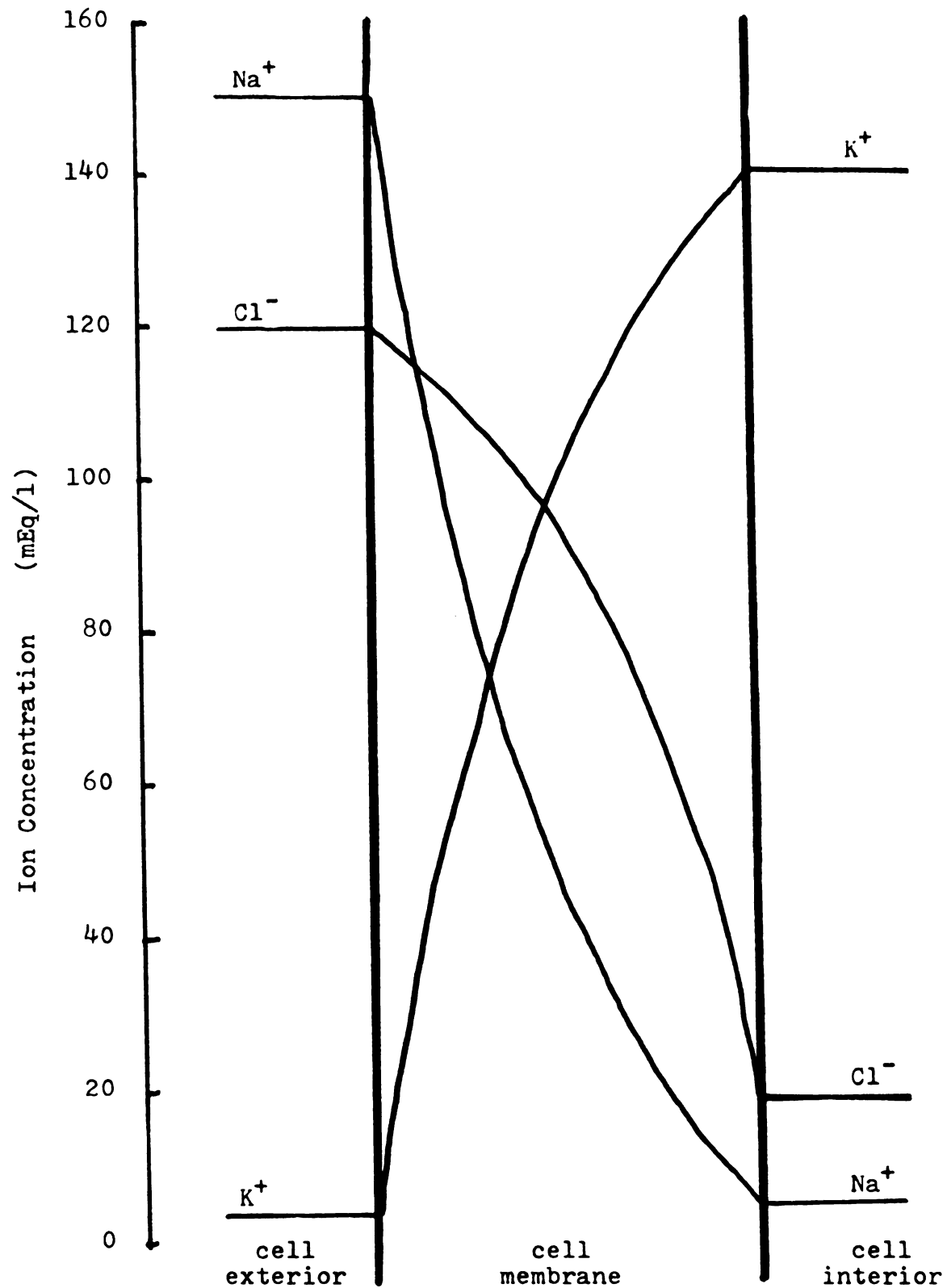


Figure 4. Ion concentrations in a cell membrane as calculated from the constant field equation.

there are no theoretical considerations which indicate that the partition coefficient on one side of a membrane would be unequal to the partition coefficient on the opposite side of the membrane. On the contrary, if the ions are passively diffusing through the membrane, the partition coefficients would be expected to be equal. Thus the second criticism will be ignored. At this point, it can be seen that the accuracy of the constant field flux equation is entirely dependent upon how close the electrical field in the membrane comes to being constant.

Cole(28) calculated electrical fields, based on a single ion model, and concluded that the assumption of a linear electrical potential was very good only for thin membranes ( $10 \text{ \AA}$ ). According to Plonsey(65), the constant field approximation is "fairly good for biological membranes and exact if the permeable ions are univalent and if the total ionic concentrations on each side of the membrane are equal."\* Zellman and Shi(93) calculated the concentrations of  $\text{Na}^+$ ,  $\text{K}^+$ , and  $\text{Cl}^-$  within the membrane based on the constant field assumption and then back calculated the electrical field from the charge density resulting from the differences in ionic concentrations. They examined the electrical field under various ion permeabilities, membrane potentials, membrane thicknesses, and ion concentration gradients and concluded that the constant field flux equation is very

---

\*R. F. Plonsey (65), p. 112.

good for biological membranes and is the best available approximation of ionic fluxes across biological membranes.

Thus, the constant field flux equation, eventhough only approximate, is not only a good approximation, but is also the best ionic flux equation presently available.

### The Goldman Equation

In a steady state there is, of course, no net flow of electrical current across the cell membrane. There are, however, continuous net passive transmembrane ionic fluxes of the ions not distributed at electrochemical equilibrium, primarily  $\text{Na}^+$ ,  $\text{K}^+$ , and, in some cells,  $\text{Cl}^-$ . If it is assumed that the sum of the electrical currents due to the passive movement of ions is zero, then

$$J_K + J_{\text{Na}} + J_{\text{Cl}} = 0 \quad (22)$$

where  $J_n$  is defined by eqn 21. By substituting the constant field flux equation into equation 22 and solving for  $E_m$ , we obtain

$$E_m = \frac{R T}{F} \ln \frac{P_K [\text{K}^+]_e + P_{\text{Na}} [\text{Na}^+]_e + P_{\text{Cl}} [\text{Cl}^-]_i}{P_K [\text{K}^+]_i + P_{\text{Na}} [\text{Na}^+]_i + P_{\text{Cl}} [\text{Cl}^-]_e} \quad (23)$$

This is the well known and widely used constant field equation for membrane potential, often referred to as the Goldman equation. Goldman(38) derived an equation for

biological membranes very similar to this. However, Hodgkin and Katz(48) first introduced the constant field equation (Goldman equation) as given here. Since then, many others have rederived it as well as several variations of it.

The Goldman equation has been extensively used for characterizing biological membranes and it has considerable merit because of its simplicity and relative accuracy. It is a definite improvement over the Nernst equation for the potassium equilibrium potential. In frog skeletal muscle, for example, the Goldman equations predicts within a few mvolts the membrane potential over the full range of  $[K^+]_e$ . In these cells, the electrogenic Na-K pump contributes only 1-3 mvolts to resting potential.

The major inaccuracy of the Goldman equation is the implicit assumption that the active transport system(s) within the cell membrane are electroneutral. This error is very obvious in smooth muscle cells where the electrogenic pump may contribute 10 or more mvolts to resting potential. In these cells, the Goldman equation fails to predict the normal resting potential as well as the appropriate potential changes as the  $[K^+]_e$  is varied.

When calculating membrane potentials, the error arising from neglecting the other ions that are naturally present is quite small since they are present in smaller concentrations and have lower membrane permeabilities. The error caused by neglecting the electrogenic Na-K pump recently has become



more obvious since it has been shown that probably all Na-K pumps are electrogenic (86) and in many cells this contributes significantly to resting membrane potential.

### Modifications of the Goldman Equation

If it is assumed that the Cl ion is distributed at electrochemical equilibrium as it is in certain cell types(27,50,64), then  $J_{Cl} = 0$  and

$$J_K + J_{Na} = 0 \quad (24)$$

The Goldman equation then reduces to

$$E_m = \frac{R T}{F} \ln \frac{P_K [K^+]_e + P_{Na} [Na^+]_e}{P_K [K^+]_i + P_{Na} [Na^+]_i} \quad (25)$$

The advantage of this equation is that it requires a smaller number of parameters for calculating membrane potential. Also, since the Cl ion is highly permeable and is not generally involved in a known active transport system, the equilibrium distribution should not be an unreasonable assumption.

Equation 25 can be used only for estimating membrane potential when the cell has been equilibrated in the bathing fluid. It should not be used to calculate membrane potential when extracellular ion concentrations are altered since any change in  $E_m$  will cause  $J_{Cl}$  to be unequal to zero.

As pointed out earlier, the basic failure of the Goldman equation is the assumption that active transport mechanism(s) are electroneutral. The electrogenic Na-K pump can be more accurately taken into account by assuming that

$$r J_K + J_{Na} + J_{Cl} = 0 \quad (26)$$

where  $r$  is the exchange ratio of the Na-K pump, i.e., the number of Na ions extruded from the cell per K ion taken into the cell. This produces the following form of the constant field equation:

$$E_m = \frac{R T}{F} \ln \frac{r P_K [K^+]_e + P_{Na} [Na^+]_e + P_{Cl} [Cl^-]_i}{r P_K [K^+]_i + P_{Na} [Na^+]_i + P_{Cl} [Cl^-]_e} \quad (27)$$

This equation is an improved form of the constant field equation. Eventhough it adequately takes into account the contribution of the electrogenic Na-K pump to resting potential, it has the disadvantage that it is only applicable during steady state conditions and is not suited for transient potential predictions when the extracellular ion concentrations are changed.

Another as yet relatively unexplored form of the Goldman equation is derived by assuming that the sum of all passive currents is equal to the current produced by the electrogenic Na-K pump(59):

$$J_K + J_{Na} + J_{Cl} = J_p. \quad (28)$$

This reduces to

$$E_m = \frac{RT}{F} \ln \frac{P_K [K^+]_e + P_{Na} [Na^+]_e + P_{Cl} [Cl^-]_i + J_p (RT/E_m F)}{P_K [K^+]_i + P_{Na} [Na^+]_i + P_{Cl} [Cl^-]_e + J_p (RT/E_m F)}. \quad (29)$$

This is unquestionably the best form of all the constant field potential equations since the steady state passive currents must be equal to electrogenic currents. Furthermore, this is a very good approximation during unsteady state conditions except during action potentials. Equation 29 is generally applicable for predicting resting membrane potential and can be used during both unsteady and steady state conditions. Since  $E_m$  appears explicitly on both sides of eqn 29, it must be solved by trial and error. However, with the availability of computers, this is a minor inconvenience.

In order to use eqn 29, a method of calculating the current generated by the electrogenic pump is needed. Assuming that the coupling ratio of the pump is constant,  $J_p$  will vary linearly with the rate of active transport:

$$J_p = J_{po} A \quad (30)$$

where  $J_{po}$  is the steady state  $J_p$  and  $A$  represents the activity of the Na-K pump.  $A$  will, of course, equal 1.0 under steady state conditions.

In general, the Na-K pump is stimulated by increases in either  $[K^+]_e$  or  $[Na^+]_i$  and is inhibited by decreases in these concentrations. Thus A is a function of  $[K^+]_e$  and  $[Na^+]_i$ . The ouabain sensitive Na-K ATPase activity of Whittam and Ager(91) is a measure of the sensitivity of the Na-K pump to  $[Na^+]_i$  and  $[K^+]_e$ . The equations

$$a_K = 1.5 \left( 1 - \frac{[K^+]_e + 2.5}{2.5} \exp(-.45[K^+]_e) \right) \quad (31)$$

$$a_{Na} = 5.7 \left( 1 - \exp(-.035[Na^+]_i) \right) \quad (32)$$

approximate their data as seen by the lines in Figure 3.

The activity of the Na-K pump is then

$$a = a_K * a_{Na} \quad (33)$$

and

$$A = a / a_o. \quad (34)$$

$a_o$  is the steady state value of a.

$J_{po}$  is calculated from the steady state resting membrane potential  $E_{mo}$  which is calculated from equation 27. Eqn 27 can be rearranged to give

$$J_{po} = \frac{E_{mo} F b \exp(E_{mo} F/RT) - c}{R T (1 - \exp(E_{mo} F/RT))} \quad (35)$$

$$\text{where } b = P_K[K^+]_e + P_{Na}[Na^+]_e + P_{Cl}[Cl^-]_i \quad (36)$$

and 
$$c = P_K[K^+]_i + P_{Na}[Na^+]_i + P_{Cl}[Cl^-]_e. \quad (37)$$

$J_{po}$  can also be expressed in terms of  $r$ , but the resulting expression is more complicated than eqn 35 and has no additional benefits.

In summary of equation 29, it is now possible to calculate the resting membrane potential of a cell when the extracellular ion concentrations are varied and include in the calculations the contribution of the electrogenic Na-K pump. The calculation procedure is as follows:

- 1) Calculate  $a$  and  $a_o$  from eqns 31, 32, and 33.
- 2) Calculate  $J_{po}$  from eqns 35, 36, and 37 using the  $E_{mo}$  calculated from eqn 27.
- 3) Calculate  $J_p$  from eqns 30 and 34.
- 4) Solve eqn 29 by trial and error for  $E_m$ .

Figure 5 compares the resting potentials calculated from the Nernst equation, the Goldman equation and equation 29 for skeletal muscle and smooth muscle cells when the  $[K^+]_e$  is varied from 0 to 150 mEq/l. The normal  $[K^+]_e$  is 4 mEq/l. Note that the discrepancy between the three equations is less for the skeletal muscle than for the smooth muscle cells.

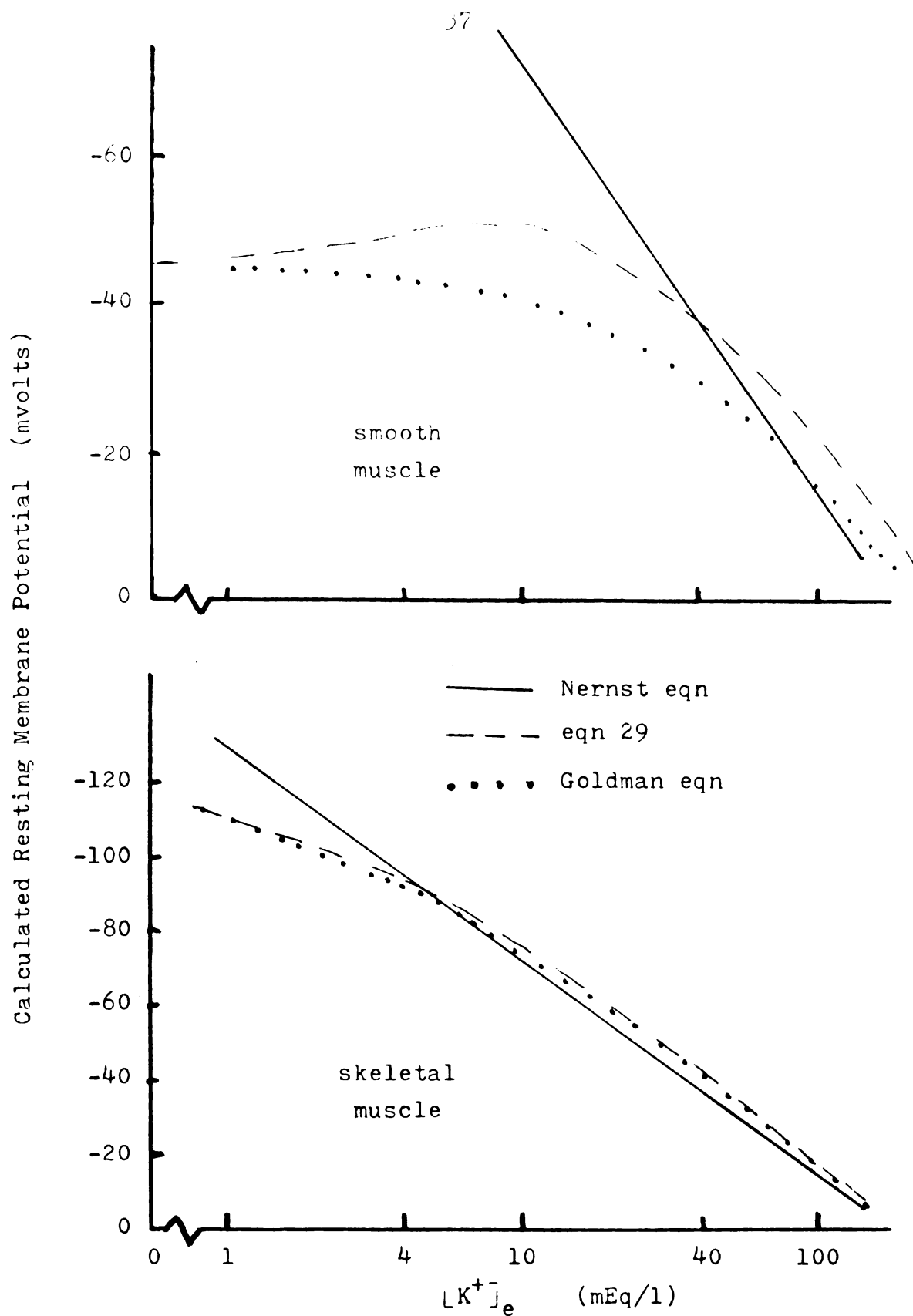


Figure 5. Calculated effects of potassium ion on resting potential in skeletal and smooth muscle .

General Method of Predicting Changes in Resting Membrane Potential: A Model

Each of the previously presented methods for calculating membrane potential has certain advantages as well as disadvantages. One criticism of all the potential equations is that they do not allow for the changes in intracellular ion concentrations that do occur. In general, intracellular concentrations are determined experimentally under normal conditions and then assumed to remain constant when the cell is bathed in fluid of various ionic compositions. In practice, intracellular ion concentrations can change quite rapidly. For example, Thomas(84,85) has shown that the  $[Na^+]_i$  can increase by as much as 17% per minute. A second shortcoming of the previous equations is that they predict an instantaneous change in membrane potential whenever the extracellular ion concentrations are altered. Membrane potential generally decays exponentially from the initial to the new potential, indicating the time required for electrical charges to transverse the cell membrane(84).

The transient changes in intracellular concentrations and membrane potential can be predicted by using the instantaneous ionic fluxes, both passive and active, in performing the calculations. Change in membrane potential is simply the charge flow  $Q$  divided by membrane capacitance  $C$ :

$$E_m = E_{m0} + Q / C \quad (38)$$

where  $Q$  is the sum of the electrical currents due to passive and active ion fluxes. Intracellular concentrations are calculated from a material balance on the ions. However, the mathematics become much more complex and cannot be expressed as a single equation. A computer must be employed to solve such complex mathematics. This approach was used in developing a model for predicting resting membrane potentials.

### Description of the Model

The cell is modeled as a volume of intracellular fluid of known composition separated from extracellular fluid (also of known composition) by a semipermeable membrane. Typical intracellular and extracellular concentrations are given in Table 1. The initial resting potential must be known as well as ion permeabilities and cell surface area. Only Na, K and Cl ions are considered.

### Calculation of Passive Fluxes

Passive fluxes are calculated from the constant field flux equation (eqn 21), which relates the passive molar flux of ion  $n$  ( $M_{n,pas}$ ) crossing the membrane to ion permeability, membrane potential and electrochemical driving forces:

$$M_{n,pas} = J_{n,pas} / F z_n. \quad (39)$$



### Calculation of Active Fluxes

Initial (steady state) active fluxes ( $M_{n,o,act}$ ) of  $Na^+$  and  $K^+$  must be equal and opposite passive fluxes and are calculated from equation 39. Changes in rate of active ion transport are calculated from the ouabain sensitive Na-K ATPase activity of Whittam and Ager(91) as was given by equations 31 and 32. Active molar fluxes are then expressed as

$$M_{n,act} = M_{n,o,act} \frac{a}{a_o}. \quad (40)$$

It is assumed that chloride is not actively transported.

### Calculation of Intracellular Concentrations and Cell Potential

The intracellular concentration of ion n at any time (t) is affected by changes in cell volume and the net flux of the ion across the membrane:

$$[n]_i = \frac{V_o}{V} [n]_{i,o} + \int_0^t \frac{A}{V} (M_{n,pas} + M_{n,act}) dt, \quad (41)$$

where A is the cell surface area.

Cell water space (V) is affected by osmotic effects. Water flow across the membrane is directly proportional to water permeability and osmolality (osm) difference. Cell water space is expressed as

$$V = V_o + \int_0^t A P_{HOH} (osm_i - osm_e) dt \quad (42)$$

where A is assumed constant.  $Osm_i$  is expressed as

$$osm_i = osm_{i,o} \frac{V_o}{V} + \int_0^t \frac{A}{V} \sum (M_{n,pad} + M_{n,act}) dt \quad (43)$$

Potential at any time is equal to the initial potential plus total charge which has crossed the membrane divided by the membrane capacitance:

$$E_m = E_{m,o} + \frac{F}{C} \int_0^t \sum z_n (M_{n,pas} + M_{n,act}) dt \quad (44)$$

The above equations (39-44) when taken together and solved simultaneously are referred to as "the model." Since direct analytical integration of these equation is clearly impossible, these equations were numerically integrated on a CDC 6500 digital computer. Extracellular concentration changes used in the model are step changes.

### Computer Techniques

A relatively small number of ions crossing the cell membrane can very rapidly produce substantial changes in membrane potential while causing very little change in intracellular concentrations. Thus, it was necessary to use small time increments in performing the calculations in order to maintain membrane potential stability. The time increment was chosen to be 1 msec initially and was increased to a maximum of 1 sec during the calculations.

However, as a measure to insure stability, the time increment was reduced when appropriate to prevent membrane potential from changing by more than 0.5 mvolt per increment. This was necessary in order to avoid oscillations in membrane potential. Furthermore, stability was further improved by doing all calculations in double precision, which computes approximately 29 decimal digits on the CDC 6500 computer, compared with 15 decimal digits during single precision calculations.

In order to calculate change in membrane potential, the computer initializes constants from the user supplied steady state data on the cell. Then the extracellular concentrations are altered. The sequence of calculations used to predict subsequent changes in resting membrane potential is shown in the algorithm of Figure 6. Euler's method of integration was used.

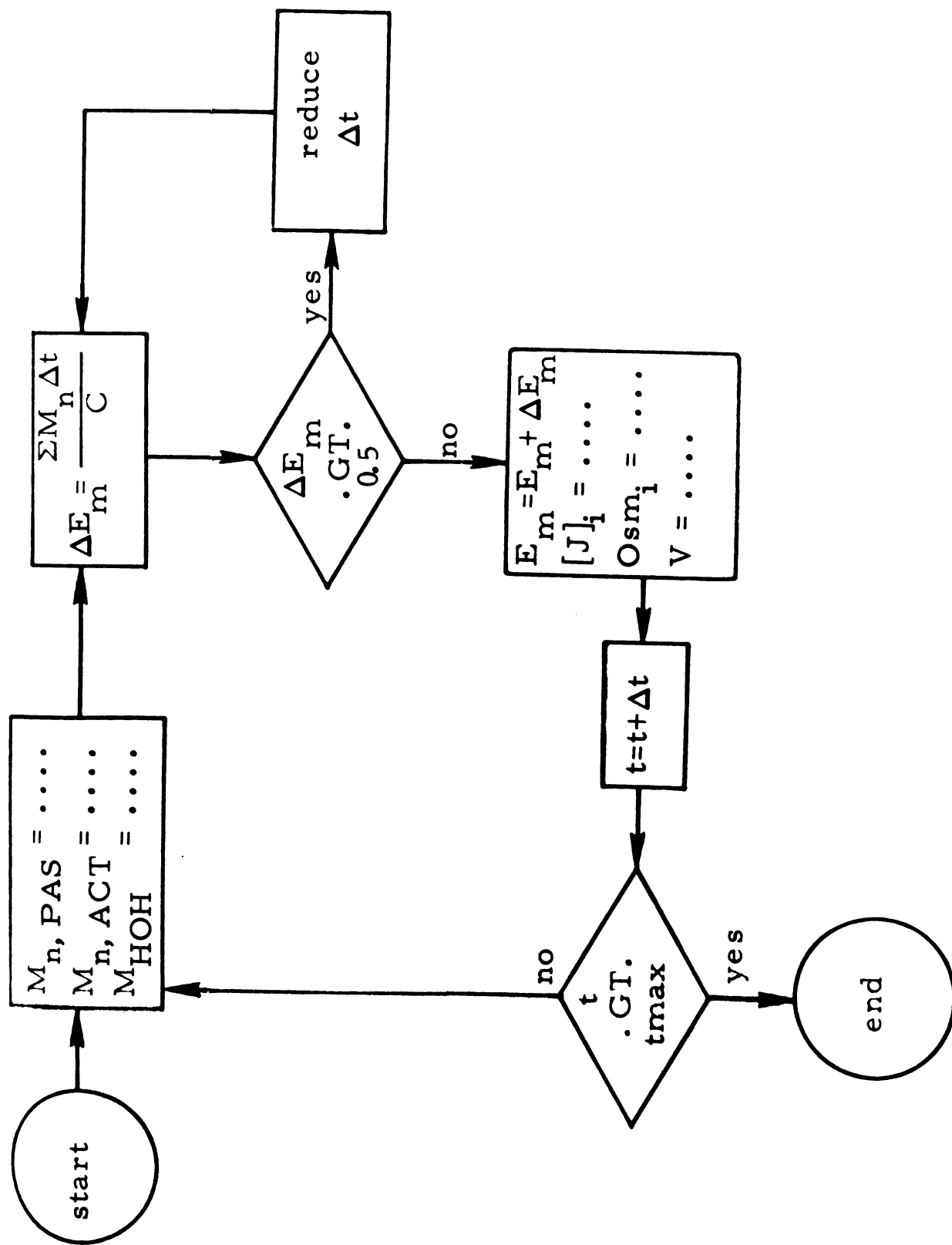


Figure 6. Algorithm showing sequence of calculations performed by the model.

## CALCULATED AND EXPERIMENTAL MEMBRANE POTENTIALS

There are two important aspects of calculating membrane potential from theory. The first of these is of course in attempt to predict the experimentally observed potentials. Most of the calculated potentials which will be discussed are devoted to this aspect.

A second area of interest is in predicting phenomena which have not as yet been experimentally observed and reported in the literature. Such calculations should stimulate additional research with the hopes of observing the predicted phenomena.

### Effect of Extracellular $K^+$

One of the most commonly used conditions under which resting membrane potential is experimentally determined is as a function of extracellular potassium ion concentration. Figure 7 shows the calculated potential of a snail neurone when that cell is subjected to a step change in  $[K^+]_e$  from 1.6 to 25 mEq/l produced by isoosmotic substitution of  $K^+$  for  $Na^+$ . The calculated ion fluxes that occurred during this time are shown in Figure 8. The fluxes are positive if influxes and negative if effluxes. (Ion permeabilities and initial intracellular ion concentrations used in this and the

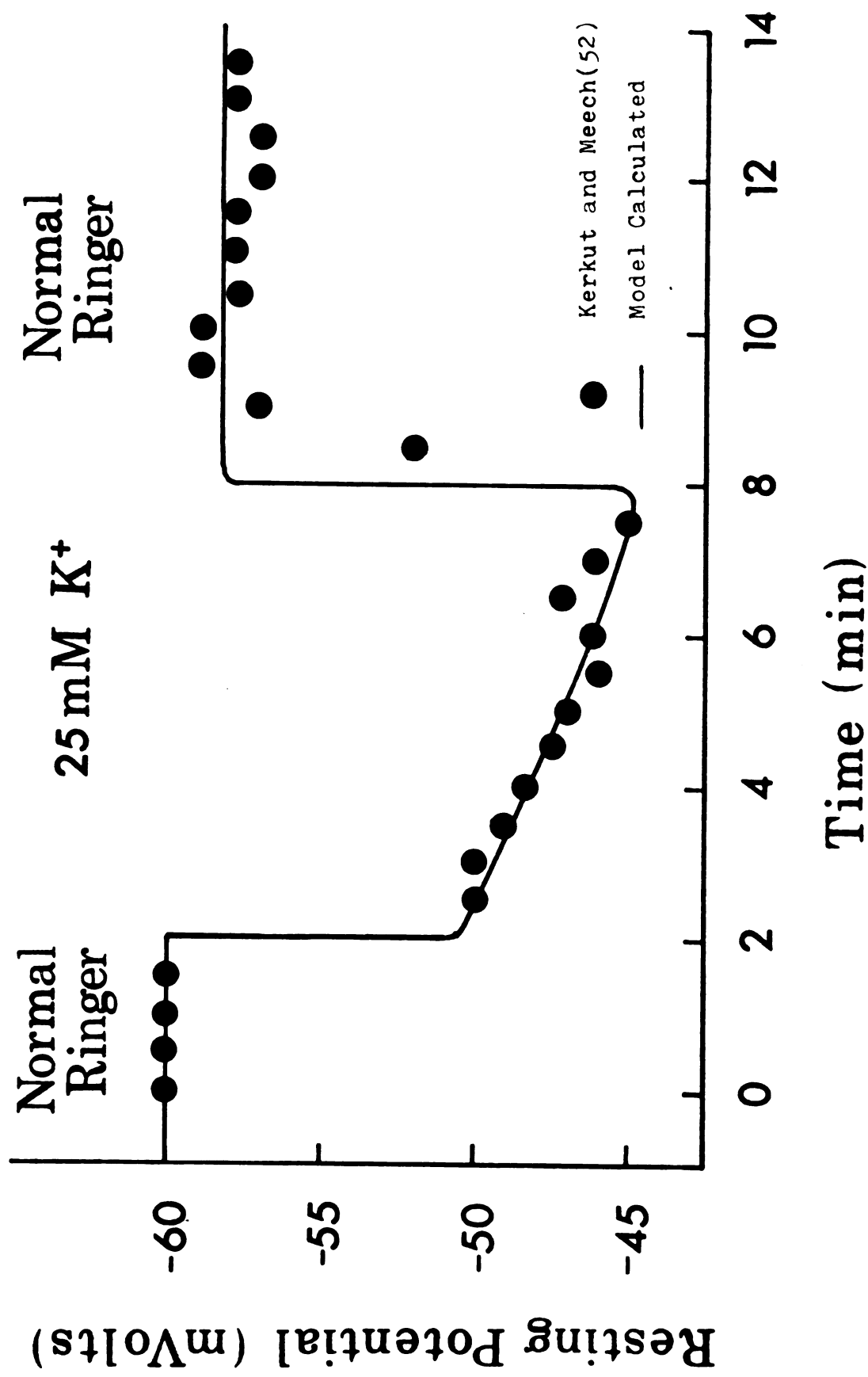


Figure 7. Changes in resting potential of snail neurone in response to a step increase in  $[K^+]_e$  and return to the normal  $[K^+]_e$ .

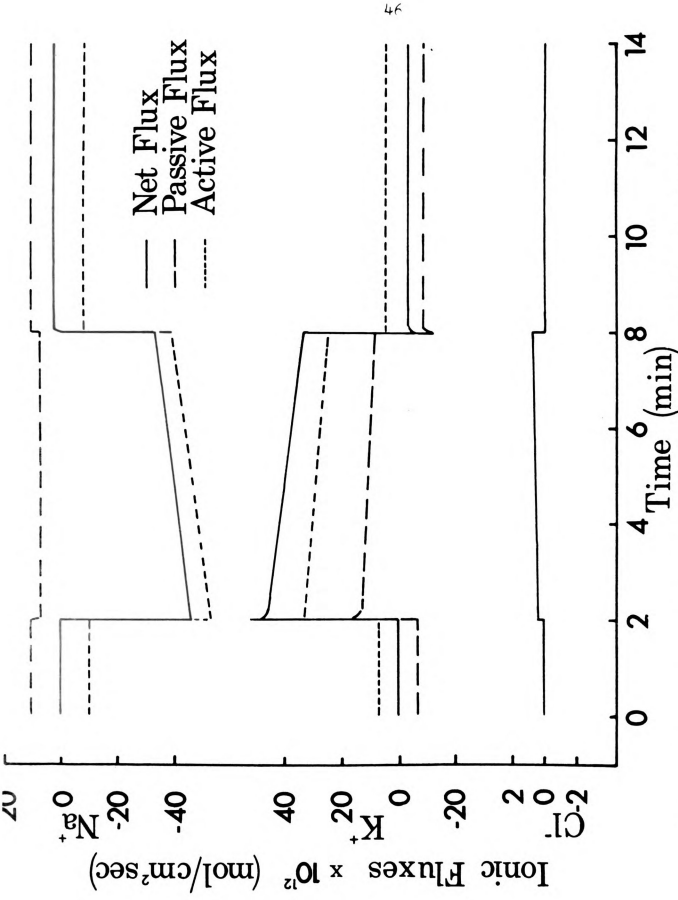


Figure 8. Changes in ionic fluxes on snail neurone in response to a step increase in  $[K^+]_o$  and return to normal.

following calculations are given in Table 2.) Depolarization of the neurone results, even though the electrogenic Na-K pump is stimulated, since the increased  $[K^+]_e$  stops the passive  $K^+$  efflux and causes a passive  $K^+$  influx as shown in Figure 8. Note that initially there is a large, rapid change in potential. After this, potential changes only slowly as intracellular ion concentrations change. Both the experimental resting potentials of Kerkut and Meech(52) (filled circles) and the calculated values (solid line) are shown. The predicted gradual depolarization following the initial rapid depolarization is caused by slowing of the electrogenic Na-K pump with decreased  $[Na^+]_i$  and by continuously changing passive fluxes of all ions. The  $[Na^+]_i$  decrease results from increased active extrusion (caused by elevated  $[K^+]_e$  stimulating the electrogenic pump) and from the decreased passive influx (caused by a decreased electrochemical gradient) of  $Na^+$ . The changes in passive fluxes result from changes in intracellular concentrations and membrane potential.

Upon returning  $[K^+]_e$  to normal, the cell repolarizes to -58.5 mvolts, but not to the initial -60 mvolts. The model indicates that slowing of the electrogenic Na-K pump by the decreased  $[Na^+]_i$  is responsible for the failure of the cell to completely repolarize. The simulated potential returns to -60 mvolts only very slowly as  $[Na^+]_i$  returns to its initial value.



Table 2. Permeabilities and intracellular concentrations used in the simulations.<sup>†</sup>

Cell	$P_K \times 10^7$	Ref.	$P_{Na} \times 10^7$	Ref.	$P_{Cl} \times 10^7$	Ref.	$[K^+]_i$	Ref.	$[Na^+]_i$	Ref.
snail neurone	4.2	59*	0.55	59*	0.63		90	59	3	84
molluscan neurone	1.0	38*	.034	38*	0.01		230	39	70	
guinea-pig taenia coli	1.1	21	0.18	21	0.67	21	145		5	
guinea-pig portal vein	1.1		0.26		0.67		145		5	

<sup>†</sup>P in cm/sec, [ ] in mEq/l.

\* Only  $P_{Na}/P_K$  given.

Figure 9 is a graph of experimental(39) (filled circles) and predicted (solid line) molluscan neurone membrane potential over a wide range of  $K^+_e$  concentrations. The simulated depolarizations that occur at low  $K^+_e$  concentrations are due to slowing of the electrogenic Na-K pump. Those that occur at high  $K^+_e$  concentrations are due mostly to changes in passive ion fluxes since the Na-K pump activity changes very little as  $K^+_e$  concentrations are raised above 10 mEq/l (Fig. 3). The contribution that the pump makes to resting membrane potential of this cell can be seen in Fig. 9 by comparing the predicted potential with that calculated from the Goldman equation (dashed line). Note that the measured membrane potential of Gorman and Marmor(39) obtained in the molluscan neurone agrees with that predicted by the model over the physiological range. The cause of the discrepancy between predicted and experimental potentials at high  $K^+_e$  concentrations is unknown.

#### Hyperpolarization After Exposure to Zero $K^+$

Several cell types hyperpolarize beyond normal resting potential when the extracellular fluid is returned to normal after exposure to  $K^+$ -free bathing fluid or after cold storage(39,55,88). Figure 10 shows the simulated recovery of guinea-pig portal vein (solid line) after a one hour exposure to  $K^+$ -free bathing fluid. The membrane hyperpolarizes to -66 mvolts when the  $[K^+]_e$  is returned to normal

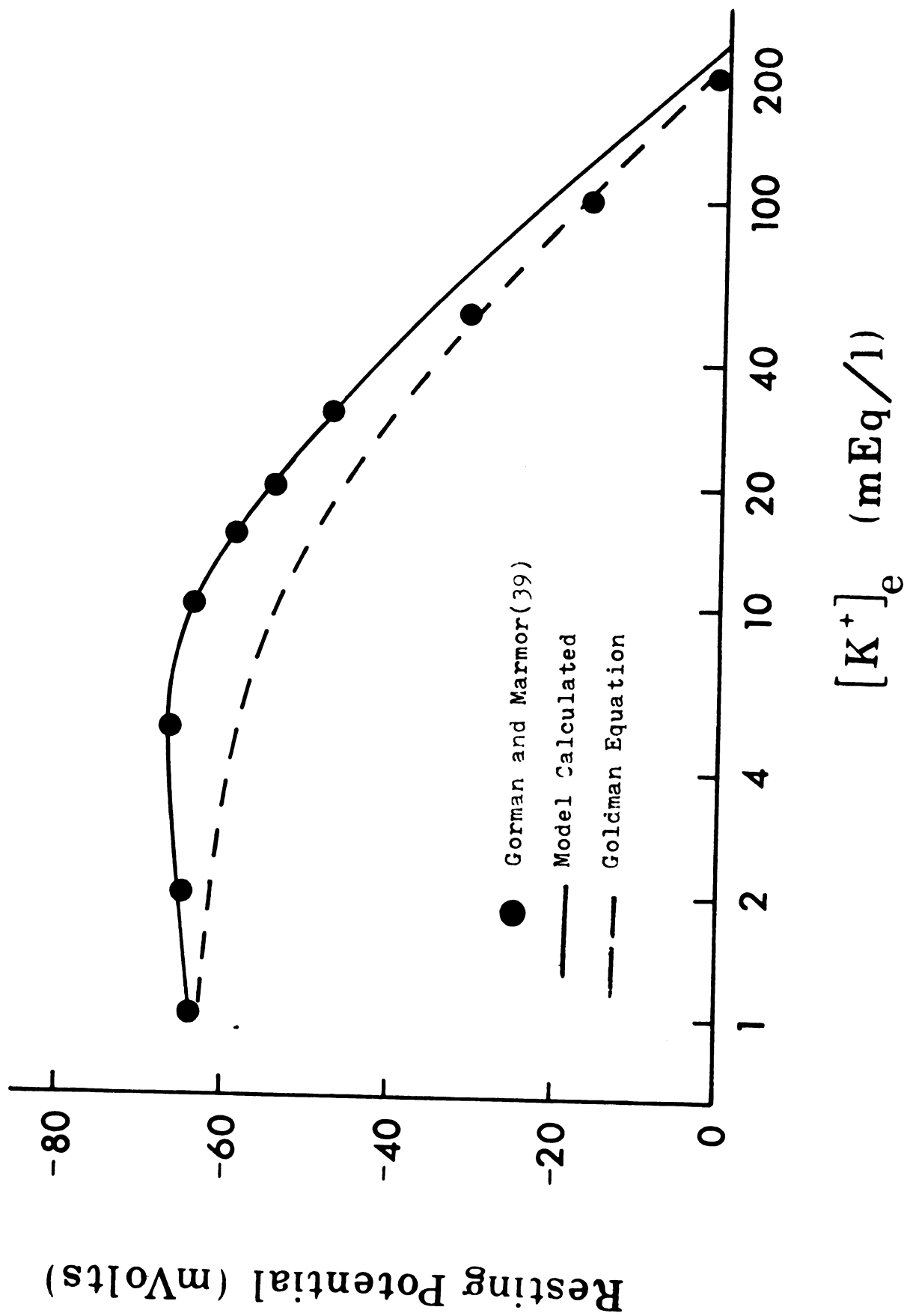


Figure 9. Steady state resting potential of molluscan neurone at various  $K^+_e$  concentrations.

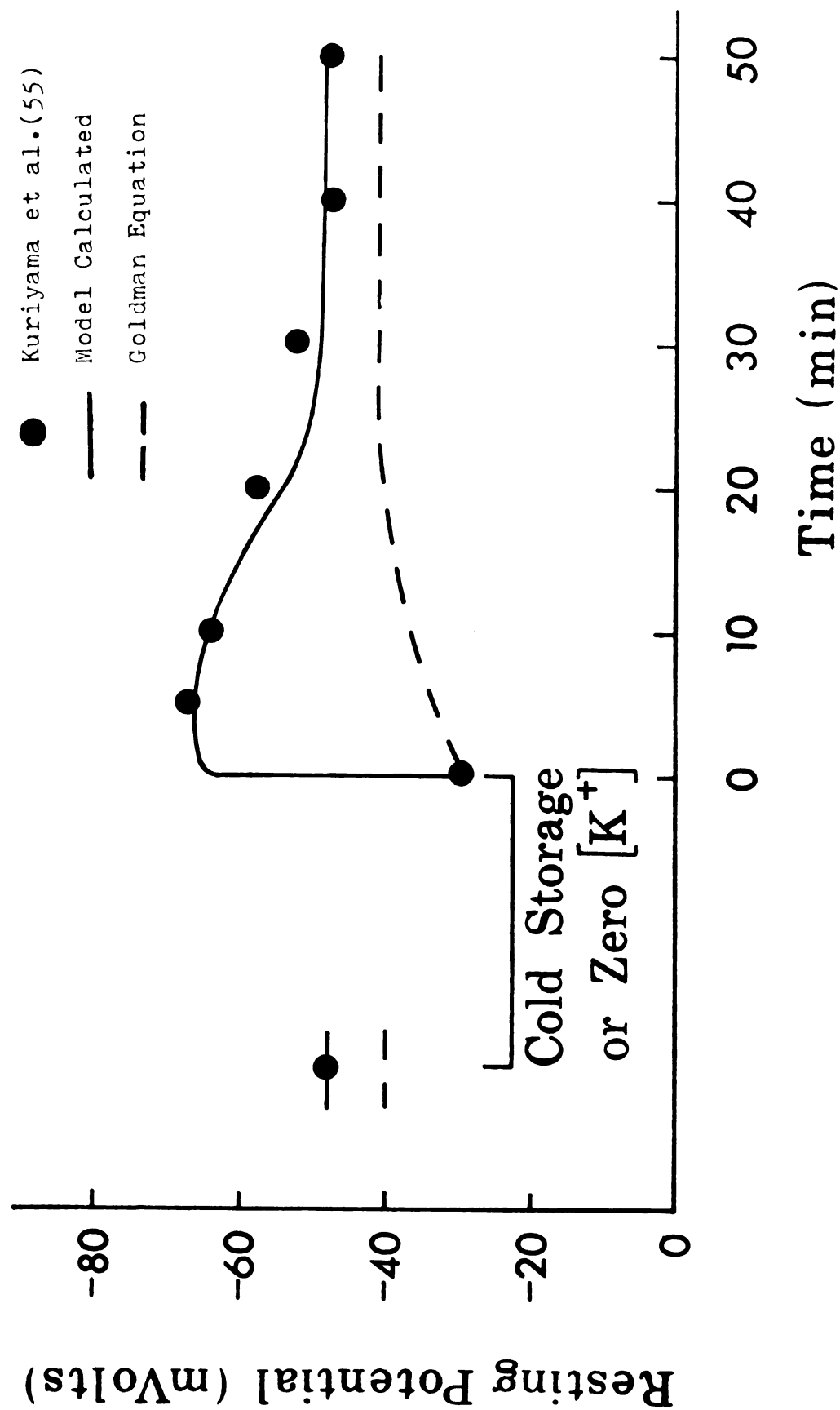


Figure 10. Resting potential of guinea-pig portal vein during recovery from  $Na^+$  loading.

and then returns to its initial value. The simulated data for guinea-pig portal vein are compared with the experimental potentials of Kuriyama et al(55) which were recorded upon returning temperature to normal after 3-5 hours of cold storage. Approximately 30 minutes are required for the simulated potential to return to its initial value.

Membrane potentials calculated from the Goldman equation (dashed line) are also shown.

Removal of extracellular potassium or cold storage inhibits the Na-K pump's active extrusion of  $\text{Na}^+$  and active uptake of  $\text{K}^+$ , causing  $[\text{Na}^+]_i$  to increase while  $[\text{K}^+]_i$  decreases. Upon return to the normal bathing solution, the increased  $[\text{Na}^+]_i$  stimulates the electrogenic pump to a higher than normal activity and hyperpolarization beyond the initial resting potential occurs. (Although not shown in Figure 10, the cell hyperpolarizes beyond the K ion equilibrium potential, indicating the presence of an electrogenic pump.) Note that the increase in pumping rate also hastens the return of intracellular Na and K ion concentrations to normal.

### Effect of $\text{Cl}^-$

Kerkut and Meech(52) showed that snail neurones will depolarize by 4.5 mvolts when the  $[\text{Cl}^-]_e$  is changed from 118 to 25 mEq/l (by substituting with acetate) while further reduction in the  $[\text{Cl}^-]_e$  causes no increase in the level of depolarization of the membrane. The data of Kerkut and

Meech (open circles) and simulated membrane potential of snail neurone (solid line) are shown in Figure 11.

(Acetate was assumed to be an impermeable anion for the simulation.) Predicted potentials were -46.9, -46.4 and -46.0 vmolts at chloride ion concentrations of 25, 10 and 0.1 mEq/l, respectively. The depolarization that occurs in the model simulation results from passive efflux of  $\text{Cl}^-$  from the cell.

#### Effect of Deficient $\text{Na}^+$

Snail neurone and marine molluscan neurone hyperpolarize in response to complete replacement of extracellular  $\text{Na}^+$  with Tris(39,52). Guinea-pig taenia coli hyperpolarizes in response to partial replacement of  $\text{Na}^+$ , but replacement of 90% or more of the  $\text{Na}^+$  causes taenia coli to transiently hyperpolarize followed by depolarization(18). Guinea-pig portal vein also hyperpolarizes with decreased  $[\text{Na}^+]_e$ , but the resting potential is little effected by complete removal of  $\text{Na}^+_e$ (55).

The model predicts hyperpolarization at all levels of  $\text{Na}^+$  deficiency, due to the decreased influx of  $\text{Na}^+$ . At 100%  $\text{Na}^+$  removal, the calculated membrane potential eventually equals  $E_K$  as all of the  $\text{Na}^+$  is lost from the cell. The lower portion of Figure 12 shows the calculated steady state effects of sodium deficiency on the resting membrane potential of guinea-pig taenia coli over the range of 0 to 100%  $\text{Na}^+$  removal. The upper portion of Figure 12 shows the transient

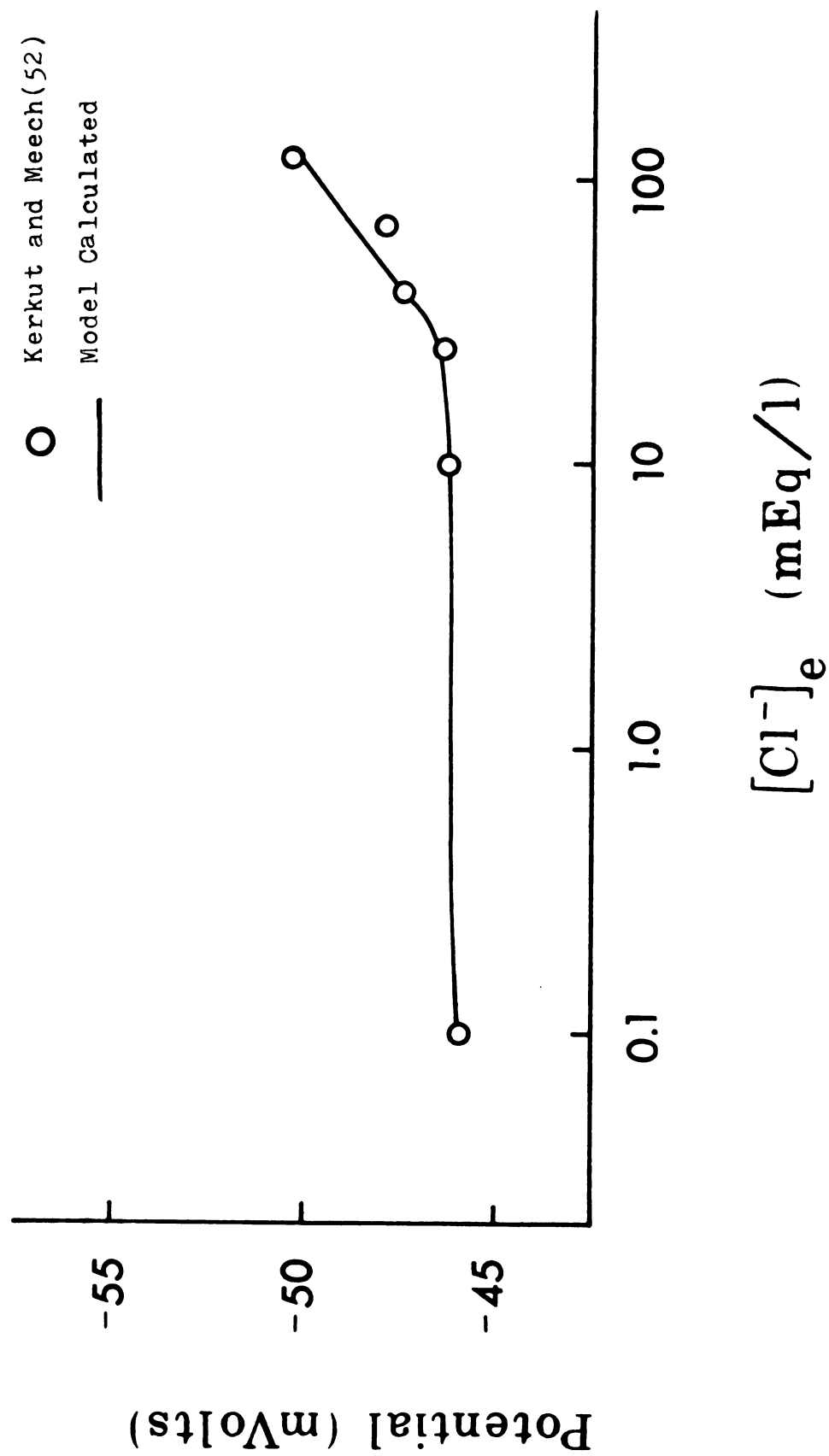


Figure 11. Resting potential of snail neurone at various  $\text{Cl}^-$  concentrations.

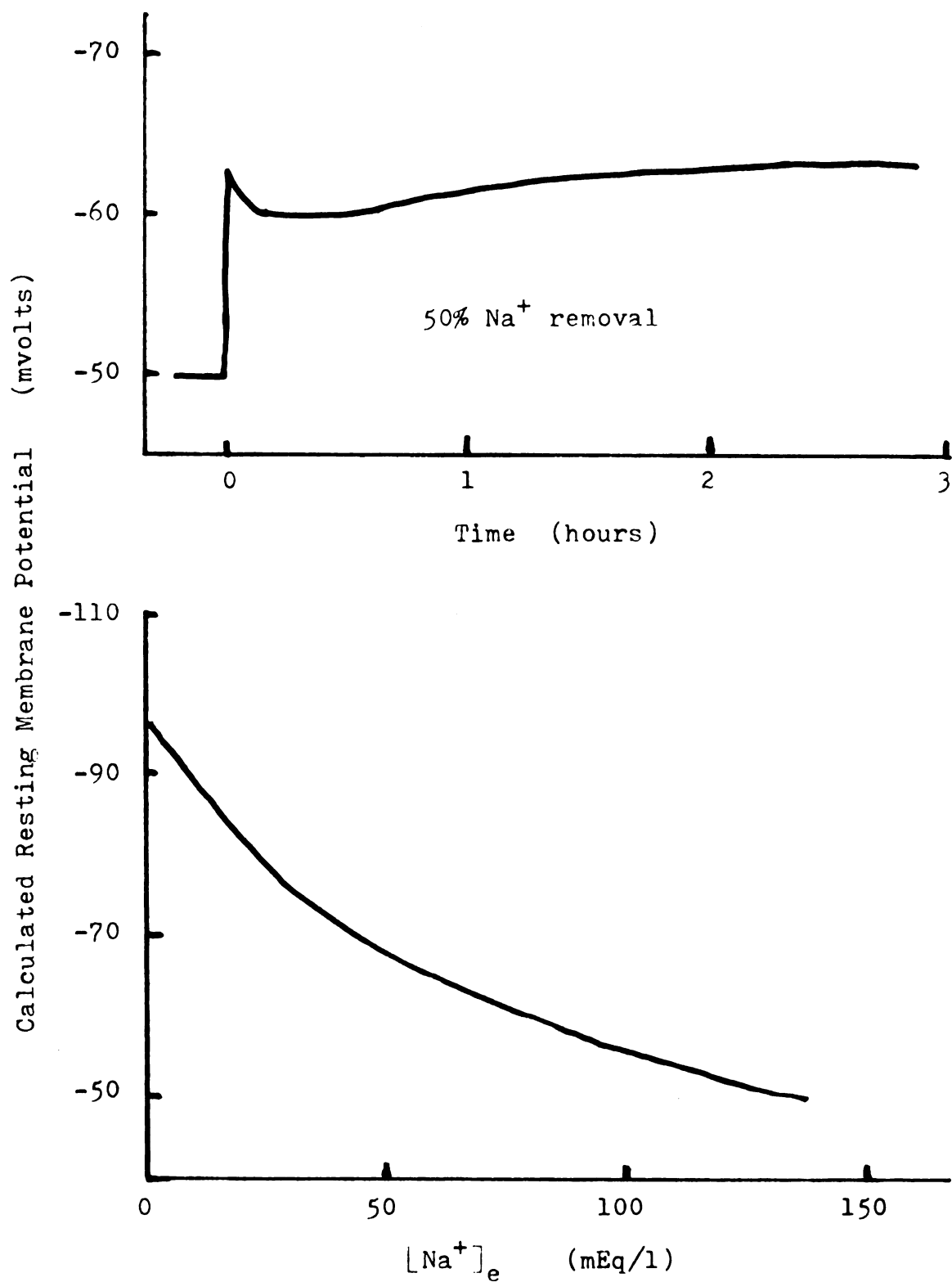


Figure 12. Calculated transient and steady state effects of sodium deficiency on resting potential of guinea-pig taenia coli.



effects of 50%  $\text{Na}^+$  removal in the same tissue. The initial hyperpolarization is due to a decreased  $\text{Na}^+$  influx while the slight depolarization following the initial hyperpolarization is due to the decreasing  $[\text{Na}^+]_i$  slowing the electrogenic pump. The late slow hyperpolarization is due to a slow loss of  $\text{K}^+$  from the cell.

### Effects of Tonicity

#### 1. Increased Tonicity with Increased $\text{Na}^+_e$

Bulbring and Kuriyama(18) reported depolarization in guinea-pig taenia coli smooth muscle of 4 to 8 mvolts and then partial repolarization when the cells were subjected to 1.5 times normal tonicity produced by addition of  $\text{Na}^+$  in combination with ethanesulphonate (presumed an impermeant anion). The model simulation predicts a depolarization of 7 mvolts and then partial repolarization of 6 mvolts after five minutes under these conditions as showed in Figure 13.

The initial depolarization results from the positive charge carried into the cell by an increased passive influx of  $\text{Na}^+$ . The partial repolarization is caused by the stimulating effect the increasing  $[\text{Na}^+]_i$  has on the electrogenic Na-K pump and by the increased  $\text{K}^+$  efflux due to the increased  $[\text{K}^+]_i$ . Both passive influx and loss of cell water increase  $[\text{Na}^+]_i$  while only water loss increases the  $[\text{K}^+]_i$ .

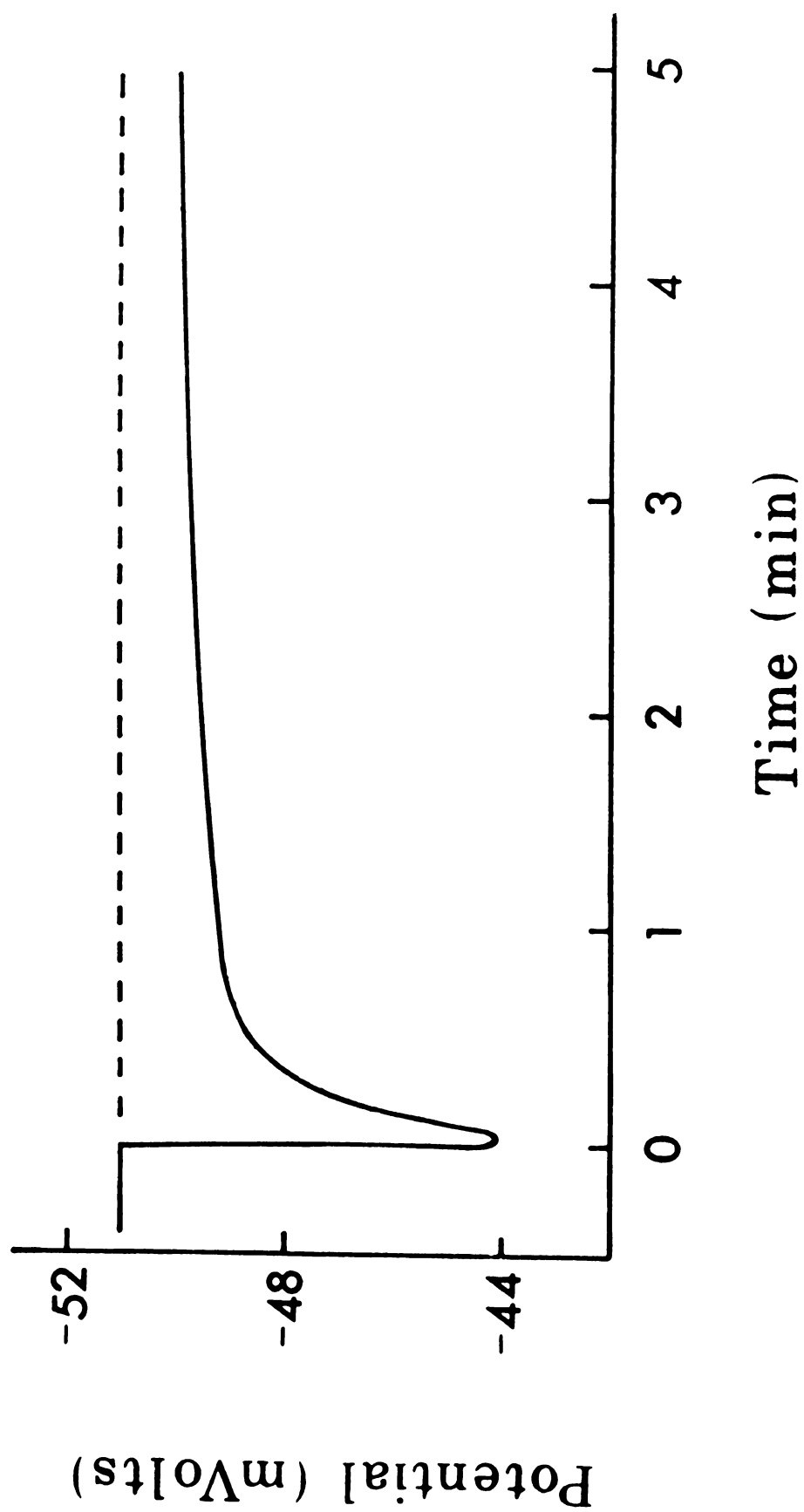


Figure 13. Calculated effects of increased tonicity and  $[Na^+]_e$  on resting potential in guinea-pig taenia coli.

## 2. Increased Tonicity with Constant $\text{Na}^+_e$

Tomita(87) reported guinea-pig taenia coli has a normal resting potential of -51 mvolts and will hyperpolarize to -63 mvolts when the tonicity of the extracellular fluid is doubled by addition of sucrose. Model simulation predicts that taenia coli will gradually hyperpolarize, becoming constant at -70 mvolts only after 30 minutes under these conditions, as seen in Figure 14. Hyperpolarization results from the effects of loss of cell water. Though  $[\text{Na}^+]_i$  increases and stimulates the electrogenic pump, a more important factor is the change in passive flux of  $\text{K}^+$  due to the increased  $[\text{K}^+]_i$ .

The cause of the discrepancy between the predicted -70 mvolts and the experimental -63 mvolts is not known. Perhaps changes in membrane permeabilities(24) or time of measure may be involved.

### Effect of Membrane Capacitance

It should be noted that membrane capacitance is not a determining factor of resting potential, as might be expected from the relationship between potential, charge crossing the membrane and membrane capacitance:

$$E_m = E_{mo} + Q / C.$$

Nerve cells have capacitances of approximately 1.0

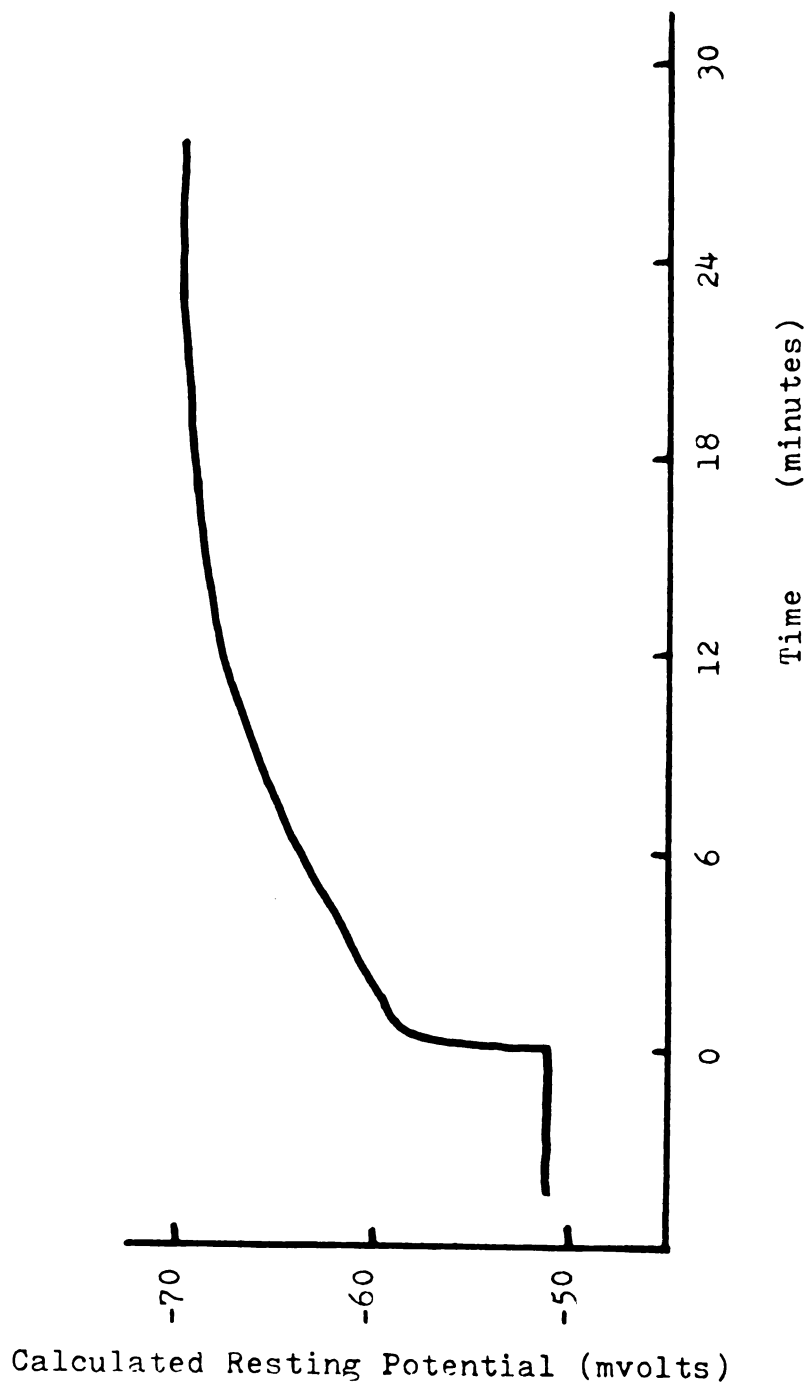


Figure 14. Calculated changes in resting potential of guinea-pig taenia coli upon doubling normal tonicity with sucrose.

ufarad/cm<sup>2</sup>(65), striated muscle 10 ufarad/cm<sup>2</sup>(65) and smooth muscle 2.5 ufarad/cm<sup>2</sup>(1). Simulated membrane potentials for each of the above capacitances in the same cell are shown in Figure 15. The eventual potential reached in response to a step change in  $[K^+]_e$  is independent of membrane capacitance. Only during the first two seconds after a step change in extracellular concentrations are the simulated potentials different. Thus ion distribution across the membrane, not capacitance, is the determinant of resting membrane potential.

#### Na-K Exchange Ratio

One feature of the model is that the Na-K exchange ratio of the pump is calculated in all simulations. Whittam and Ager(91) measured the Na-K exchange ratio in human red blood cells and found an average of 1.5 Na ions extruded by the pump for each  $K^+$  taken up and in some cells the ratio was as high as 2.53:1. The exchange ratio in frog skeletal muscle may be as high as 3:1(2). Thomas(85) has estimated an exchange ratio of 1.5 to 1.33:1 in snail neurone. The simulated exchange ratios were 2.35:1 for marine molluscan neurone, 1.92:1 for guinea-pig taenia coli and 1.56:1 for snail neurone.

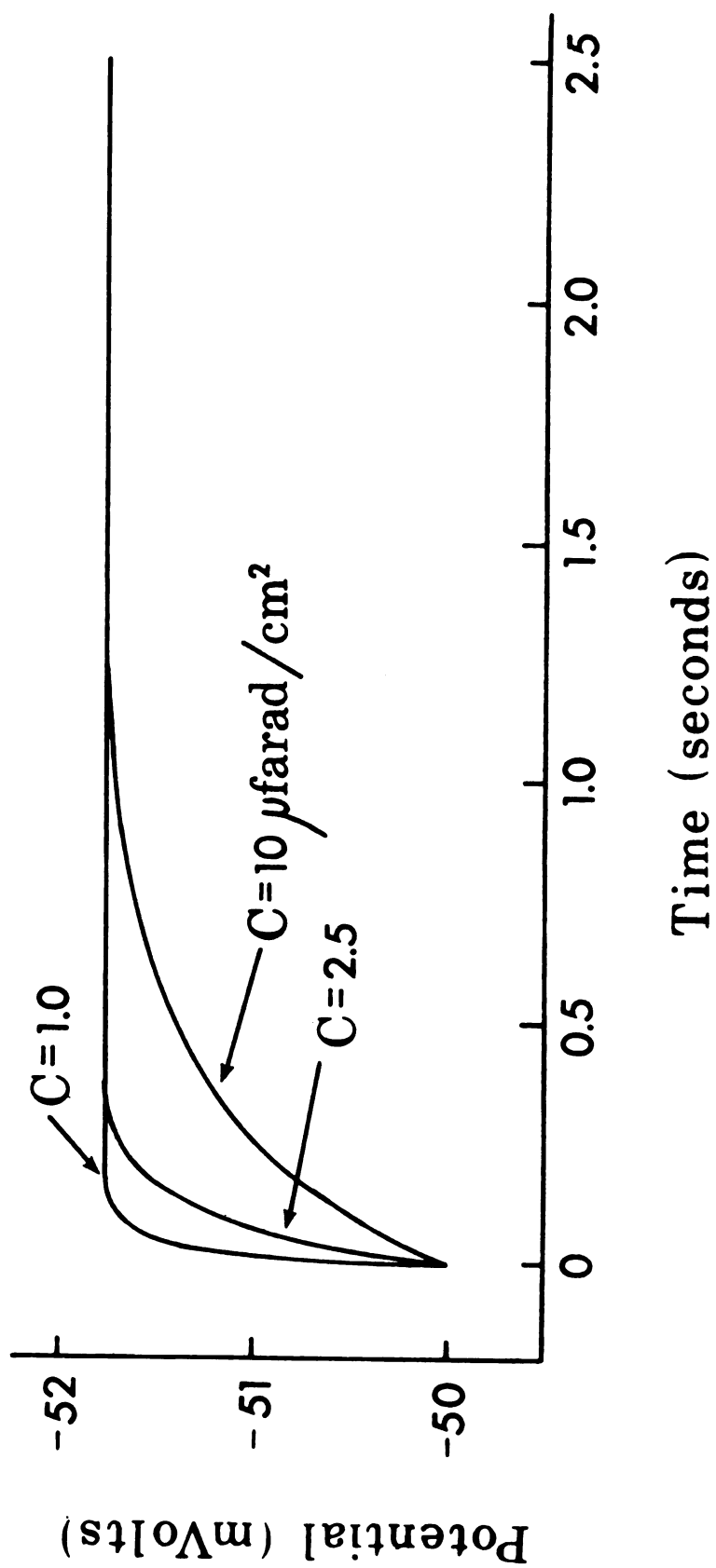


Figure 15. Effect of membrane capacitance ( $C$ ) on time course of potential change simulated in the same cell for the same change in  $[K]_e$ .

## PREDICTED CHANGES IN CELL VOLUME AND INTRACELLULAR ION CONCENTRATIONS

Thus far, only membrane potential changes as predicted by the model have been considered. However, as seen in the development of the model, continuous changes in cell volume and intracellular ion concentrations are also simultaneously calculated. The reason for the neglect of predicted volume and intracellular concentrations is that there are very few experimental data in the literature of sufficient accuracy for comparison. In general, there are no available techniques for continuously recording changes in cell volume and cell ion concentrations. However, there are two exceptions to this general rule.

First, with stirred red blood cells, cell volume can be continuously monitored photometrically. Figure 16 shows the calculated changes in red cell volume when the tonicity of the bathing fluid is increased to 1.49 times normal by addition of sucrose. The time course of the volume change calculated with the model agrees very closely with experimental data(66) and with the calculated volume changes of Devi, et al.(30), who have developed a computer model which predicts red cell volume change. However, their model is based solely on water fluxes and does not take into

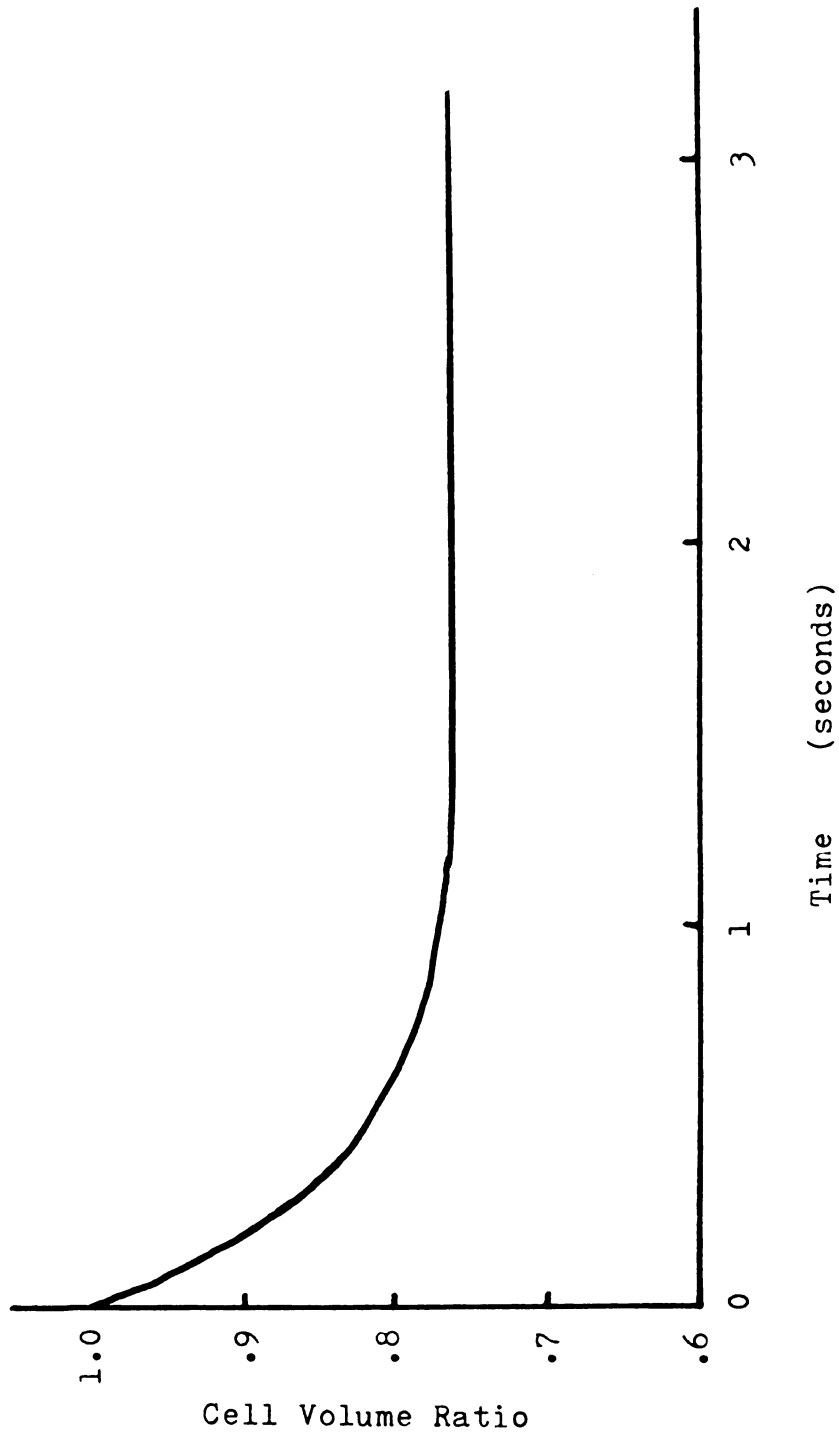


Figure 16. Calculated changes in red blood cell volume when tonicity is suddenly increased to 1.49 times normal.



account the effects of the loss of intracellular ions which occurs when the bathing solutions are changed(15).

It is possible for cell volume to change eventhough tonicity is constant. Figure 17 is an example of a calculated volume change which occurs because of the loss of ions from the cell when the extracellular sodium concentration is reduced by 50% (replaced with a nonpermeating ion). Changes in both passive and active fluxes are responsible for the net loss of ions.

The second exception is that it is now possible to continuously record  $[Na^+]_i$  with Na sensitive microelectrodes in large cells. Calculated (solid line) and experimental (85) (filled circles)  $[Na^+]_i$  of a snail neurone are showed in Figure 18. When the extracellular  $K^+$  was removed, the Na-K pump was inhibited, allowing the  $[Na^+]_i$  to increase. Note that, upon returning the  $[K^+]_e$  to normal, the experimental  $[Na^+]_i$  decreased at a faster rate than predicted by the model. This suggests that the Na-K pump in the snail neurone is actually more sensitive to  $[Na^+]_i$  than assumed in the model.

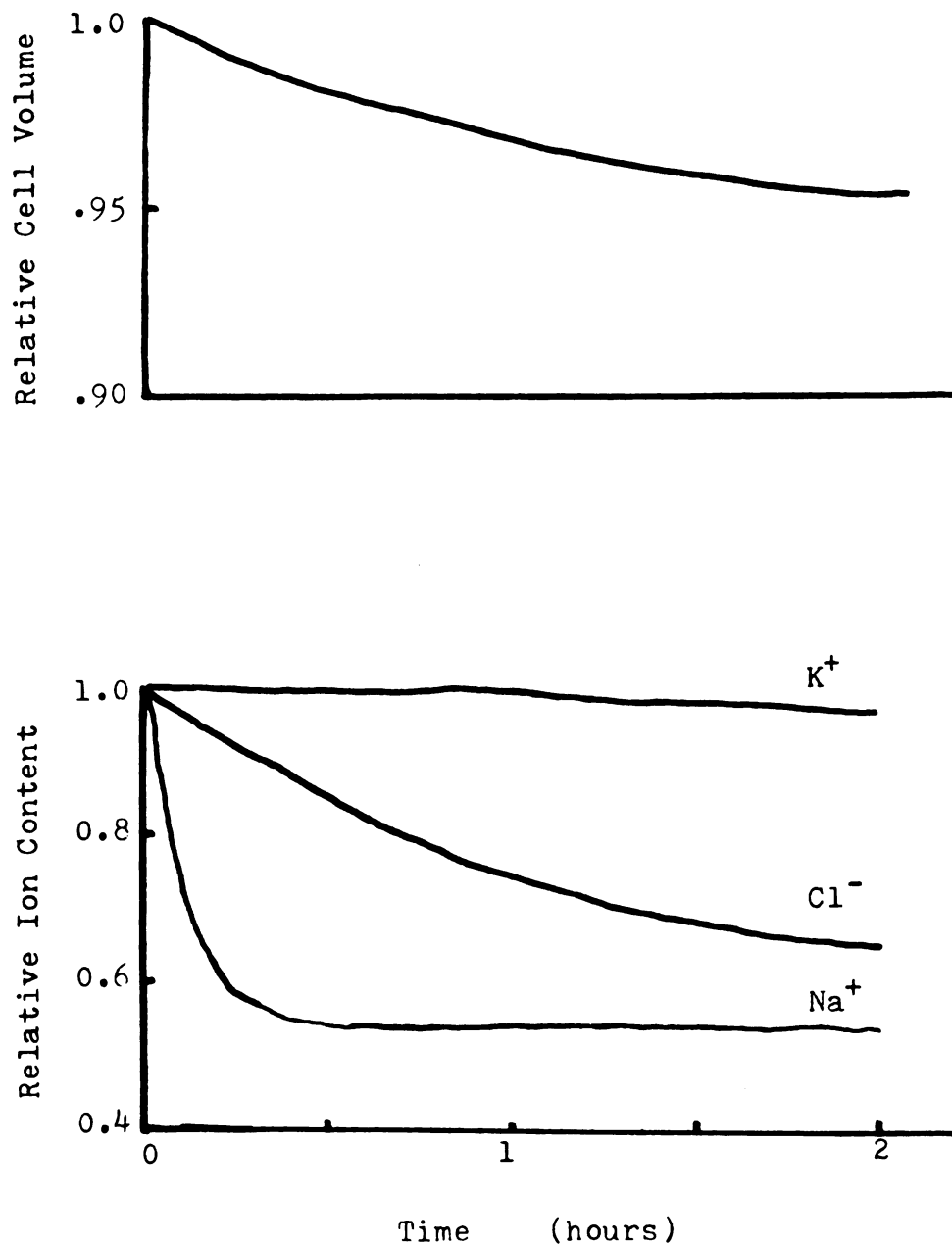


Figure 17. Decrease in cell volume and ion content caused by a reduction in  $[Na^+]_e$ .

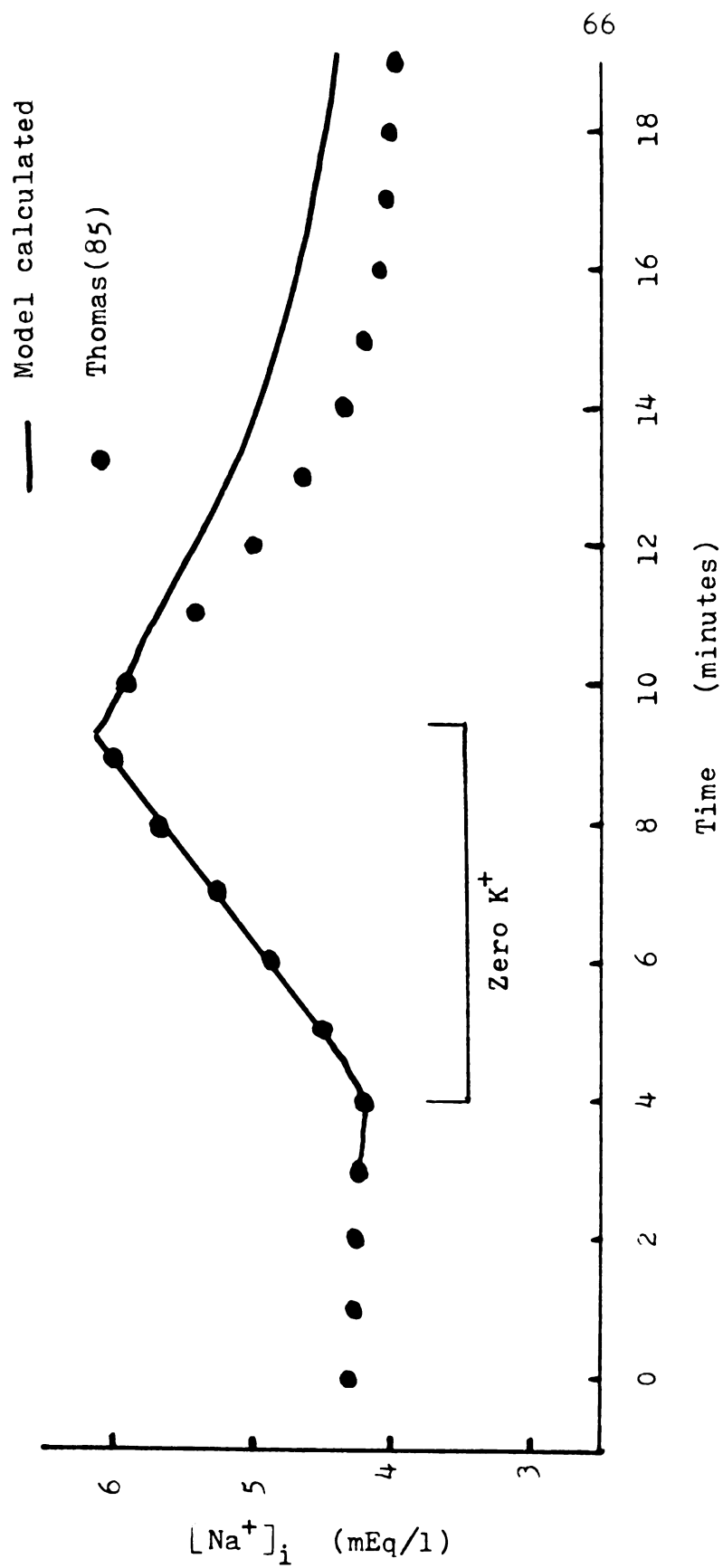


Figure 18. Effect of potassium ion free bathing fluid on intracellular sodium ion concentration in snail neurone.

## DISCUSSION OF THE MODEL FOR PREDICTING RESTING POTENTIALS

There were many assumptions made in the development of this model and most, if not all, can be questioned. However, it must be noted that with the data available and reasonable assumptions, the model predicts with striking accuracy not only the potential changes but also the time course of these changes.

Of prime importance is the use of the model in explaining and testing the mechanisms responsible for membrane potential changes. Based on an electrogenic Na-K exchange pump and available data, the model can predict most observed changes in potential and thus offer a possible explanation of the responsible mechanisms.

It is important to note that if the Na-K pump had been assumed electroneutral, experimental changes in resting could not have been predicted. (Appropriate transient changes in  $P_{Na}/P_K$  could explain certain potential changes, however the hyperpolarization after exposure to zero  $K^+$  bathing fluid, for example, would be unexplained.) While steady state potentials can sometimes be explained with an electroneutral pump, the unsteady state data available in the literature can be predicted by our model only when we introduce the electrogenic characteristic of the Na-K pump.

The simulation can be used to predict the contribution of the electrogenic Na-K pump to both transient and steady state potentials as shown in Figure 9. As the  $[K^+]_e$  increases, the contribution of the pump to predicted resting potential gradually increases, reaches a maximum and then decreases. The initial increase is due to speeding of the electrogenic pump and the maximum corresponds approximately to the point where further increases in the  $[K^+]$  no longer increase the activity of the pump, as seen in Figure 3. The decrease in contribution of the electrogenic pump to resting potential at high  $K^+_e$  concentrations is due to a loss of  $Na^+_i$ , resulting in a suppression of the pump.

During the unsteady state, the contribution of the pump to resting potential can be much greater than under steady state conditions. As seen in Figure 10, the steady state contribution of the pump to portal vein potential is about 7.5 mvolts. However, with  $Na^+$  loading of the cell, the pump contribution increases to 35 mvolts, followed by a decay back to 7.5 mvolts as the  $[Na^+]_i$  decreases to the steady state value.

In all of the previously calculated potentials, it was assumed that the membrane permeabilities to all ions remained constant. However, it has been shown in guinea-pig taenia coli that  $P_K$  and  $P_{Na}$  increases as the cell gains Na and loses K(24). In general, the factors which control membrane permeability are unknown.

Although several parameters describing the cell are needed for this model in order to calculate changes in resting membrane potential, most of these parameters are available in the literature. When experimental values of ion permeabilities, initial intracellular ion concentrations, etc., could not be found or when literature values varied widely, the parameters were chosen such that the model provided a "fit" of experimental membrane potentials.

One of the major difficulties faced when simulating membrane potential of a cell type with the model is lack of data. Ion permeabilities and intracellular ion concentrations are not generally known. As our knowledge and understanding of cell processes increase, it becomes increasingly more important that complete studies be made which include simultaneous measurements of potentials, intracellular concentrations, membrane permeabilities, and other cell properties. Only under these conditions can an accurate, detailed analysis be done.

PART II:

THE EFFECTS OF IONS, OSMOLALITY AND OUABAIN  
ON VASCULAR RESISTANCE TO BLOOD FLOW

## SUMMARY OF CALCULATING RESTING POTENTIALS

The factors which produce fluxes of ions across a cell membrane have been discussed and described mathematically. In addition, several methods of calculating resting membrane potential have been derived and discussed. With the model that was developed, it is now for the first time possible to predict transient changes in resting potential as extracellular ion concentrations are varied. In order to predict experimental changes in resting potential, both the passive ion fluxes, due to electrochemical driving forces, and the active ion fluxes, due to the Na-K pump, must be calculated.

The mechanisms responsible for the changes in resting potential have been examined. While calculating membrane potentials, it has become obvious that the Na-K pump must be electrogenic in all of the types of cells which were studied. Furthermore, the electrogenic pump contributes significantly to resting potential in many cell types, especially during the unsteady state. It appears that the Na-K pump is electrogenic in all cell types.



It is well established that changing the plasma concentration of the major cations ( $K^+$ ,  $Mg^{++}$ ,  $Ca^{++}$ , and  $H^+$ ) alters vascular resistance to blood flow. In addition, resistance changes when the total plasma concentration (plasma osmolality) is altered. The effects of changing plasma ion concentrations and osmolality on resistance are of interest since plasma ionic and osmolality changes are known to occur in many normal and pathological conditions (exercise, shock, hypertension, etc.).

Past studies(c.f.,45,46) showed that acute local increases in plasma  $[K^+]$ ,  $[Mg^{++}]$  or osmolality decrease resistance in almost every systemic vascular bed. These effects are well established since the concentrations can be easily increased by direct infusion into the blood.

The effects on resistance of decreasing the plasma  $[K^+]$ ,  $[Mg^{++}]$  or osmolality have also been previously studied. The data indicate that low  $[K^+]$  increases resistance in the canine forelimb and kidney(44), whereas reducing  $[Mg^{++}]$  does not affect resistance(44). Furthermore, reducing plasma osmolality increases resistance(61,81). However, these results are not easily interpreted since the concentrations were reduced by a dilutional technique which produced other secondary blood changes such as reduced hematocrit, reduced blood viscosity, altered plasma binding of cations, etc. In addition, the dilutional technique used in the hypo-osmolality experiments also reduced the plasma concentration of all ions. It is possible that the observed changes in

resistance are, in part, related to one or more of the secondary abnormalities.

Studies on the heart suggest that low  $[K^+]$  may increase myocardial contractile force, but is without affect on coronary resistance(44). The effects of hypoosmolality on the heart and on coronary resistance have not been previously examined.

In order to fully understand the mechanisms responsible for the changes in resistance when plasma ion concentrations are altered, the detailed quantitative effects of ion concentration variations on vascular resistance to flow must be known. In general, the qualitative effects of elevated ion concentrations and osmolality are established. However, the quantitative and transient effects on vascular resistance of abnormally low concentrations of the major cations and of low osmolality are not well established.

In the present studies, hemodialysis was used to alter the plasma ion concentrations and to reduce osmolality. The experiments were performed in attempt to determine and quantify the effects of reducing plasma  $[K^+]$ ,  $[Mg^{++}]$ ,  $[Na^+]$  and osmolality on resistance in the skeletal muscle and/or coronary vascular beds of the dog. In some instances, the effects of elevated  $[K^+]$  were also investigated. In order to examine the cellular mechanisms which produce the changes in resistance, ouabain was used to inhibit active transport by the Na-K pump.

## LITERATURE REVIEW

### Potassium

Some of the earlier studies which indicate that  $K^+$  may be important in blood flow regulation are those in 1934 and 1935 which showed that the  $[K^+]$  in the venous blood of skeletal muscle increased when the muscle was active(8) or when the flow rate to the muscle was reduced(9). "Shortly thereafter it was found that the potassium ion, administered into the coronary artery, can produce coronary vasodilation."\* Since then, it has been shown that "a slight increase (1-4 mEq/liter) in the plasma  $[K^+]$  of the blood perfusing all of the systemic vascular beds studied, except perhaps the hepatic, produces a decrease in vascular resistance to blood flow. From studies of segmental resistances in the forelimb and intestine, it appears the site of dilation is limited mainly to small vessels just proximal to the capillaries. Increasing the blood  $[K^+]$  to higher levels (above 10 mEq/liter) produces a pronounced constriction of the large arteries."† "Furthermore, it has been shown that local reduction in plasma  $[K^+]$  produces a rise in resistance to flow through kidney, limb and gracilis muscle."\*

---

\*Haddy, F.J., and J.B. Scott(46), p. 694-695.

†Scott, J.B., et al.(75), p. 1403.

In the heart, locally increasing the plasma  $[K^+]$  causes a reduction in coronary vascular resistance and myocardial contractile force(73). However, there have been very few studies on the effects of local hypokalemia in the in situ, working heart since that change has been difficult to produce. Haddy, et al.(44), using the dilutional method, reported that local hypokalemia tends to increase myocardial contractile force, but the effect was of questionable significance and coronary vascular resistance was unaffected by hypokalemia.

### Magnesium

The acute local effect of increasing arterial plasma  $[Mg^{++}]$  by a factor of 2 to 3 is a reduced resistance(26, 61,72,83). From segmental resistance studies in the forelimb and intestine, it was concluded that the dilation is primarily due to an increased arteriole diameter(75).

Using the dilution technique, it has been concluded that lowering the plasma  $[Mg^{++}]$  by approximately 40% is without affect on vascular resistance in the forelimb, heart and kidney(44). While this suggests that reducing plasma  $[Mg^{++}]$  produces no effect on resistance, the data are not conclusive because of the disadvantages of the dilutional technique used in those studies.

## Sodium

The study of specific effects of  $\text{Na}^+$  is difficult because plasma  $[\text{Na}^+]$  cannot be significantly increased without increasing osmolality as well. In one study, Overbeck, et al.(61) showed that the changes in resistance observed with increased  $[\text{Na}^+]$  paralleled tonicity changes and not  $[\text{Na}^+]$ .

The effects of acute local reduction in plasma  $[\text{Na}^+]$  under isotonic conditions have not been extensively studied because of the difficulties involved in producing that change. Overbeck, et al.(61), using the dilution technique, failed to demonstrate any effect of hyponatremia on vascular resistance. Thus it appears that the Na ion per se is not acutely vaso-active.

Studies with isolated tissues, however, indicate that the  $\text{Na}^+$  may play a role in regulating muscle tension. Reducing the  $[\text{Na}^+]_e$  while maintaining tonicity constant alters membrane potential in several cell types(18,39,52,55). Furthermore, it is well established that  $\text{Na}^+$  and  $\text{Ca}^{++}$  compete for binding sites on the cell membrane. It appears that competition for these binding sites is important in regulating membrane stability. Altering  $[\text{Na}^+]_e$  or  $[\text{Ca}^{++}]_e$  has no affect on muscle tension as long as the  $[\text{Na}^+]^2$  to  $[\text{Ca}^{++}]$  ratio is not altered. If this ratio decreases, then tension increases and vice versa.

### Osmolality

The effects of acute local increases in plasma osmolality on resistance to blood flow through intact vascular beds and on the myocardium are now well established. In general, hyperosmolality decreases vascular resistance and increases myocardial contractile force(36,45). A notable exception is that hyperosmolal NaCl infusion into the coronary artery transiently decreases contractile force(36).

The acute effects produced by local decreases in plasma osmolality have also been examined in several vascular beds (35,36,45,61,81), but these studies do not include the coronary vasculature nor the effects of hypoosmolality on the myocardium. Moreover, while hypoosmolality has been reported to increase vascular resistance(35,36,61,81), the results are not as easy to interpret as those during hyperosmolality because dilutional techniques have been employed to create the abnormality. Thus, hypoosmolality has always been studied in the presence of other blood changes, e.g., hypokalemia, hypocalcemia, hyponatremia, reduced hematocrit, etc. It is possible that the elevated resistance is, in part, related to one or more of these secondary abnormalities.

### Ouabain

Ouabain is a glycoside which is well known and widely used for its ability to inhibit active transport by the

Na-K pump(31,91). It appears that this drug slows the pump by competitively binding to the extracellular potassium sites. The rate of inhibition increases with increasing concentration of the glycoside but decreases if the  $[K^+]$  is raised in the presence of very low concentrations of the inhibitor(92).

Ouabain is also well known for its ability to increase contractile force of the heart. This and other related glycosides are used clinically in attempt to increase the strength of the heart. It appears that the increase in contractile force is a result of inhibiting the Na-K pump (37,56,69). In this regard, concomitant with the changes in contractile force produced by ouabain administration are a loss of potassium from the myocardial cells and a gain of sodium(c.f.,16).

Another affect of ouabain is that it increases vascular resistance to blood flow in systemic and coronary vascular beds(29,71). Bloor et al.(29) have shown that intracoronary administration of ouabain increased vascular resistance during both systole and diastole.

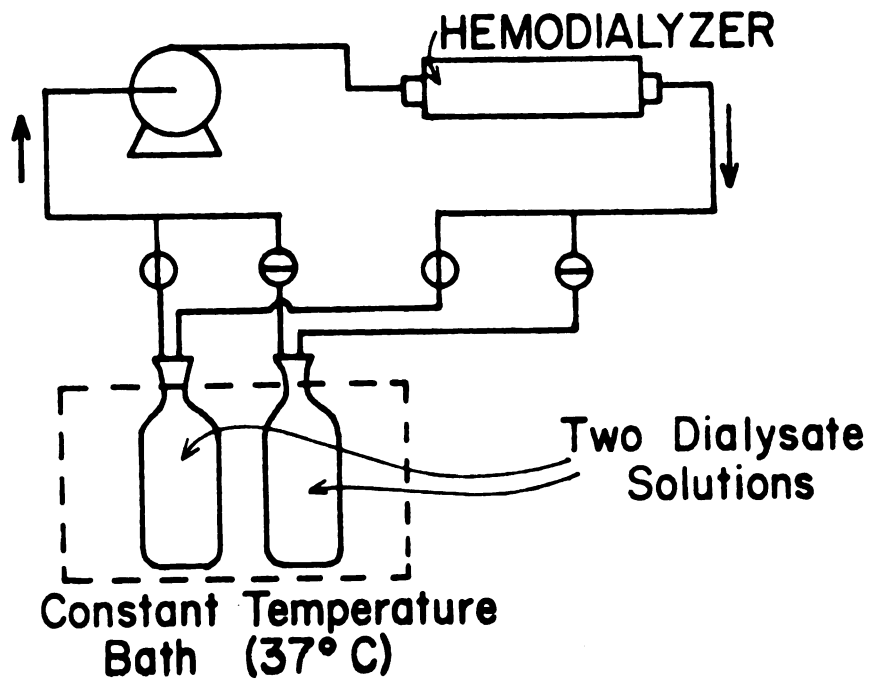
## METHODS

Mongrel dogs weighing 15-40 kg were anesthetized by intravenous injection of sodium pentobarbital (33 mg/kg), ventilated with a mechanical positive pressure respirator via an intratracheal tube, and anticoagulated by intravenous sodium heparine (5 mg/kg).

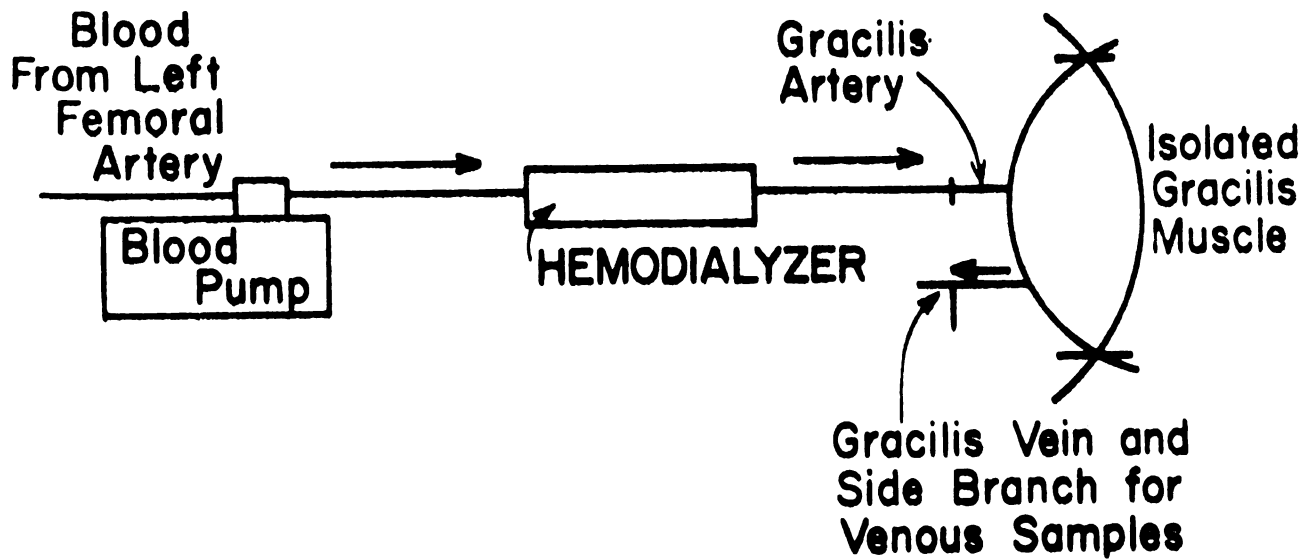
### Gracilis Muscle Preparation

The right hindlimb gracilis muscle was surgically exposed and isolated from the body between its origin and insertion except for the main gracilis artery, vein and nerve. The origin and insertion were ligated (for detailed procedure, see Nagle et al.(60)). A cannula was placed in a side branch of the gracilis vein to allow sampling of venous blood. The left femoral artery was ligated and a constant displacement finger-type blood pump was interposed between the proximal segment of the femoral artery and a hemodialyzer. The dialyzer was flushed with saline and then filled with arterial blood. Blood leaving the dialyzer entered the gracilis artery (as seen in Figure 19b) and blood flow rate was adjusted so that the perfusion pressure was approximately equal to systemic pressure. Flow rate





(a) Dialysate Circuit



(b) Blood Circuit

Figure 19. Blood and dialysate flow circuits used in the gracilis muscle experiments.

ranged from 5 to 33 ml/min in different experiments, depending on muscle size and initial resistance, but was maintained constant in any given experiment. Inlet and outlet dialyzer pressures and perfusion and systemic pressures were monitored continuously on a direct-writing oscillograph.

### Heart Preparation

The heart was exposed by opening the chest between the 4th and 5th ribs. Using a previously described surgical procedure(36), the left common coronary artery was cannulated with a curved metal cannula via the left subclavian artery. An extracorporeal circuit containing a constant output blood pump and a hollow fiber hemodialyzer was inserted between the left femoral artery and the cannulated left common coronary artery. Initially flow was adjusted so that coronary perfusion pressure was approximately equal to systemic pressure. Left ventricular contractile force was measured by attaching a strain gauge arch directly to the surface of the left ventricle. Systemic pressure, coronary perfusion pressure, contractile force and lead II of the EKG were continuously monitored on a direct writing oscillograph.

In the initial series of experiments, blood flow to the left common coronary artery was held constant with a blood pump. Thus changes in coronary perfusion pressure indicate changes in resistance to flow.

In the second series of experiments, the left common coronary artery was perfused at constant pressure. Thus changes in coronary blood flow indicated changes in vascular resistance. Surgical procedures were the same as in the constant flow experiments, except a second extracorporeal circuit containing a macroelectrode for measurement of coronary sinus oxygen tension ( $P_{O_2}$ ) was inserted between the coronary sinus and the jugular vein. A Y-tube was also inserted between the dialyzer and the coronary artery. One branch of the Y supplied blood to the coronary and the other branch, which contained a variable resistor to control perfusion pressure, diverted blood to a reservoir. The reservoir blood was continuously returned to the femoral vein via gravity feed. Initially the pump flow through the dialyzer was set at a rate approximately twice the coronary flow (56-194 ml/min) at a perfusion pressure of approximately 100 mm Hg.

#### Forelimb Preparation

The right brachial artery, forelimb nerves, and brachial and cephalic veins were dissected free at a level 3-5 cm above the elbow. Collateral flow to the limb was abolished by including all other structures in tourniquets. The humerus was sectioned and bone wax was applied to the exposed ends. A finger-type blood pump was interposed between the right femoral artery and a hemodialyzer.

Blood leaving the dialyzer entered the brachial artery. Initially flow rate was adjusted so that perfusion pressure was approximately equal to systemic pressure and this flow was maintained throughout the experiment.

### Altering Blood Plasma Ion Concentraions

Hemodialysis was used to alter blood plasma ion concentrations. The blood and dialysate flow schemes used in gracilis muscle experiments are shown in Figure 19. As the blood passes through the dialyzer, it is physically separate from a circulating dialysate fluid. However, the small ions and molecules in the two liquids can passively exchange across the porous dialyzer membranes.

During the control period, the dialysate fluid has approximately the same ionic makeup as normal plasma as seen in Table 3. Consequently, the plasma undergoes essentially no concentration changes as it passes through the hemodialyzer. By switching to a dialysate of different composition, the plasma concentration of an ion can be selectively raised or lowered without affecting other variables such as hematocrit, nonelectrolyte concentrations, blood viscosity, etc. For example, by replacing the 4 mEq/l of  $K^+$  in the dialysate with  $Na^+$ , the plasma  $[K^+]$  can be dramatically reduced. It is seen from Table 3 that a 50% change in  $[K^+]$  alters the  $[Na^+]$  by only  $1\frac{1}{3}\%$ . This change can be considered negligible in comparison with the change in  $[K^+]$ .

Table 3. A comparison of blood plasma composition and control dialysate composition.

Blood Plasma Composition			Control Dialysate Composition		
1. Blood Cells					
2. Plasma Proteins					
3. Organic Substances					
4. Inorganic Substances:					
			Membrane		
H <sub>2</sub> O					H <sub>2</sub> O
Na <sup>+</sup>	150			146	Na <sup>+</sup>
K <sup>+</sup>	4			4	K <sup>+</sup>
Mg <sup>++</sup>	2			2	Mg <sup>++</sup>
Ca <sup>++</sup>	5			5	Ca <sup>++</sup>
Cl <sup>-</sup>	103			131	Cl <sup>-</sup>
HCO <sub>3</sub> <sup>-</sup>	29			21	HCO <sub>3</sub> <sup>-</sup>
Others	19			5	Others

Concentrations in meq/liter

In the heart and gracilis muscle experiments, the perfusing blood was made hyperkalemic and/or hypokalemic (by altering the amount of  $K^+$  in the dialysate solution) and hypoosmolal (by reducing the amount of NaCl in the dialysate). Typical dialysates for a hypoosmolality experiment are a control Ringer's solution at 300 mOsm/kg (Table 3) and two additional Ringer's solution at 250 and 200 mOsm/kg. In some of the gracilis muscle experiments, the perfusing blood was also made hyponatremic (low on  $Na^+$ ) by adding sufficient mannitol to the above mentioned hypoosmotic dialysates such that the blood was isoosmolal as it left the hemodialyzer. Finally, in one series of gracilis muscle experiments, the blood plasma  $[Mg^{++}]$  was reduced by replacing the dialysate  $Mg^{++}$  with  $Na^+$ .

The dialysates used during the heart experiments were the same as those in the gracilis muscle experiments (Table 3), except each contained 1 gm glucose/liter of solution.

The dialysate containers were placed in a constant temperature bath at  $37^{\circ}C$  so that the blood was isothermal as it entered the vascular bed under study. In addition, the dialysate was circulated at a constant rate of approximately  $600\text{ cm}^3/\text{min}$ .

### Monitoring Resistance

Changes in vascular resistance to blood flow are conveniently monitored by recording either 1) changes in the pressure required to pump a constant flow rate through the vascular bed (changes in perfusion pressure), or 2) changes in blood flow rate while the perfusion pressure is maintained constant. (Ignoring the venous pressure introduces only a few percent error since venous pressure is low and constant(c.f., 61).) Since the latter of these methods of recording resistance changes was the more difficult to do experimentally, we chose to use the former method in most experiments. During the heart experiments in which perfusion pressure was held constant, coronary flow rate was determined every minute by measuring the flow to the reservoir and subtracting this from the total pump flow (measured at the end of the experiment).

In all experiments, the organ was initially perfused with blood dialyzed against the control Ringer's solution until all monitored variables were constant. Then the dialysate was switched to another solution in which the concentration of selected ion(s) had been altered. After a new steady state had been reached or after a predetermined amount of time, the dialysate was returned to the control solution and the variables were once again allowed to become constant.

## Hemodialyzers

Two types of hemodialyzers were used. During the gracilis muscle experiments, two parallel-plate dialyzers similar in design to that developed by Babb and Grimsrud (7,35,36,37) as an artificial kidney were used. In this design, the Cuprophase PT 150 membrane is supported by foam nickel metal.\* The porous metal allows the dialyzer fluid to flow through its structure while maintaining rigid support for the membrane. This dialyzer design is illustrated in Figure 20. With transfer areas of approximately 200 and 1000 cm<sup>2</sup>, these dialyzers were suited for low flow experiments (5-50 ml/min).

During the heart and forelimb experiments, a commercial Cordis-Dow artificial kidney was used. It is a hollow fiber hemodialyzer with a transfer area of approximately 1 m<sup>2</sup> and is suited for larger flows (50-300 ml/min).

## Analysis

Samples were taken from the blood entering the dialyzer and entering the organ in all experiments. In addition, during the gracilis muscle and constant pressure heart experiments, the effluent blood was also sampled.

---

\* Available commercially from General Electric Company, Detroit, Michigan.



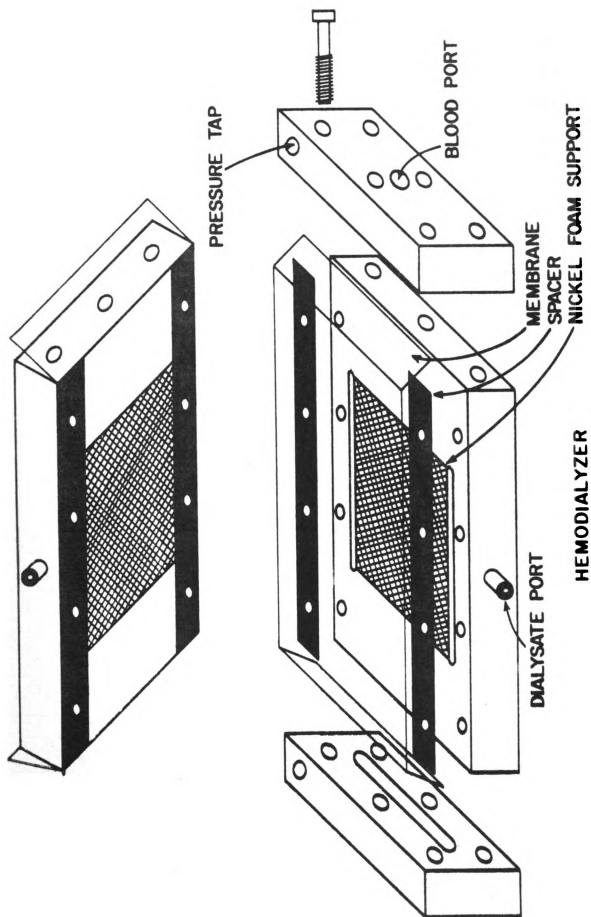


Figure 20. Exploded view of hemodialyzer.

These samples were analyzed for plasma  $[K^+]$  and  $[Na^+]$  by flame photometry,  $[Ca^{++}]$  and  $[Mg^{++}]$  by atomic absorption, osmolality by freezing point depression, hematocrit via microcentrifugation and pH with a Radiometer pH meter.

The data were statistically analyzed using Student's t test modified for paired replicates. All changes are referred to as significant if  $P < 0.05$ . Correlation coefficients for the data were calculated using standard linear regression analysis techniques(33).

## EXPERIMENTAL RESULTS

### Potassium

#### 1. Gracilis Muscle

A typical response of the gracilis muscle to low plasma  $[K^+]$  is illustrated in Figure 21. The arrow indicates the point at which the dialysate solution was switched from the control Ringer's solution to one containing zero potassium. After a time lag of about 1 minute, muscle perfusion pressure began to rise and leveled off in another 2 minutes. The absence of an immediate rise in perfusion pressure after switching dialysates is attributed mostly to the fact that the gracilis muscle was still perfused with normokalemic blood from the connecting tubing and outlet of the hemodialyzer. When the dialysate was returned to control, perfusion pressure simply returned to the prehypokalemia value.

The resistance response of the gracilis muscle to an elevated plasma  $[K^+]$  is quite different from the response to a reduced  $[K^+]$ , as seen in Figure 22. The arrow in the top tracing indicates the time at which the dialysate was switched from the control dialysate to one containing 8.4 mEq/l of  $K^+$ . This increased the plasma  $[K^+]$  of the blood

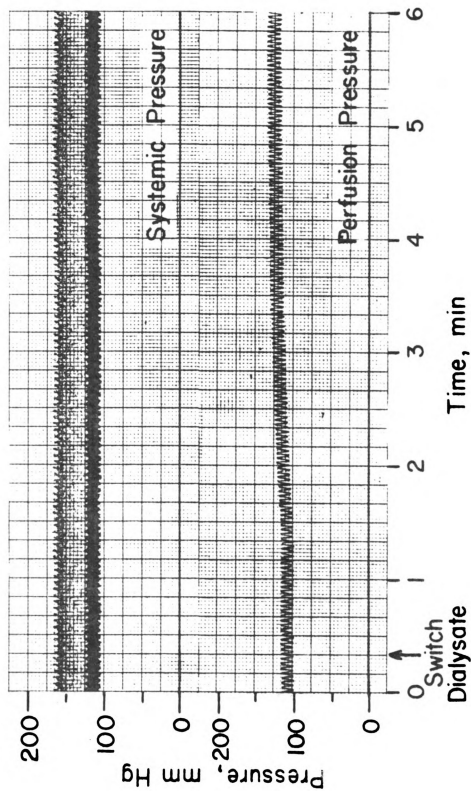


Figure 21. Typical Response of Gracilis Muscle to Hypokalemia.

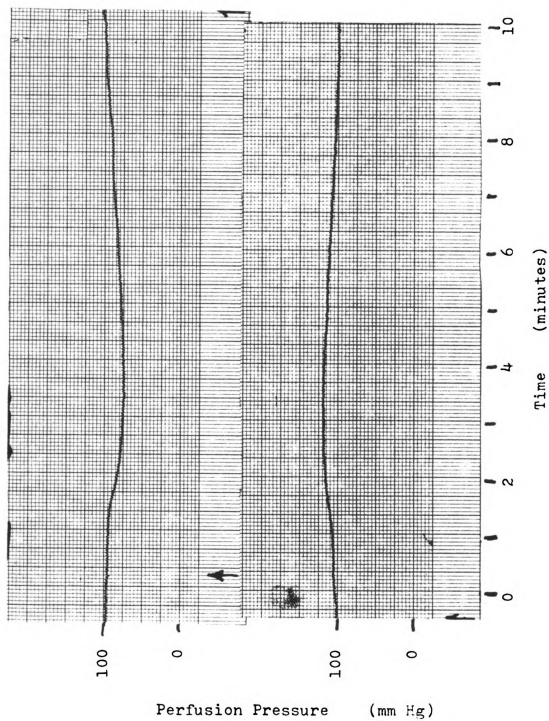


Figure 22. Effects of hyperkalemia on gracilis muscle perfusion pressure.

perfusing the gracilis muscle from 3.7 mEq/l to 5.6 mEq/l. Resistance initially decreased when the muscle was perfused with hyperkalemic blood. In approximately  $3\frac{1}{2}$  minutes, resistance reached a minimum and then began to increase eventhough the plasma  $[K^+]$  was not changing. After 10 minutes of hyperkalemic perfusion, resistance was greater than the control resistance. The effects of returning to the control dialysate at this time are shown in the bottom tracing in Figure 22. (This is a direct continuation of the upper tracing.) It is seen that resistance increased further and then returned to the control value after approximately 10 minutes.

Figure 23 summarizes the results of the short term (2-5 min) hypokalemic and hyperkalemic perfusion of the gracilis muscle vasculature. For the range of plasma  $K^+$  concentrations considered, approximately 0.2 to 8.0 mEq/l, the regression analysis relationship between percent change in arterial plasma  $[K^+]$  (x) and percent change in resistance (y) is  $y = -0.240 x$  with a correlation coefficient (r) equal to 0.958. The data for the hypokalemic perfusion are plotted as the average of the "on" (change elicited by switching from the control to experimental dialysate) and "off" responses to hypokalemia in each animal. No significant difference was obtained when the on and off responses were plotted separately. For the hyperkalemic perfusions, the data in Figure 22 represent the maximum reduction in resistance in each animal. When the change in resistance

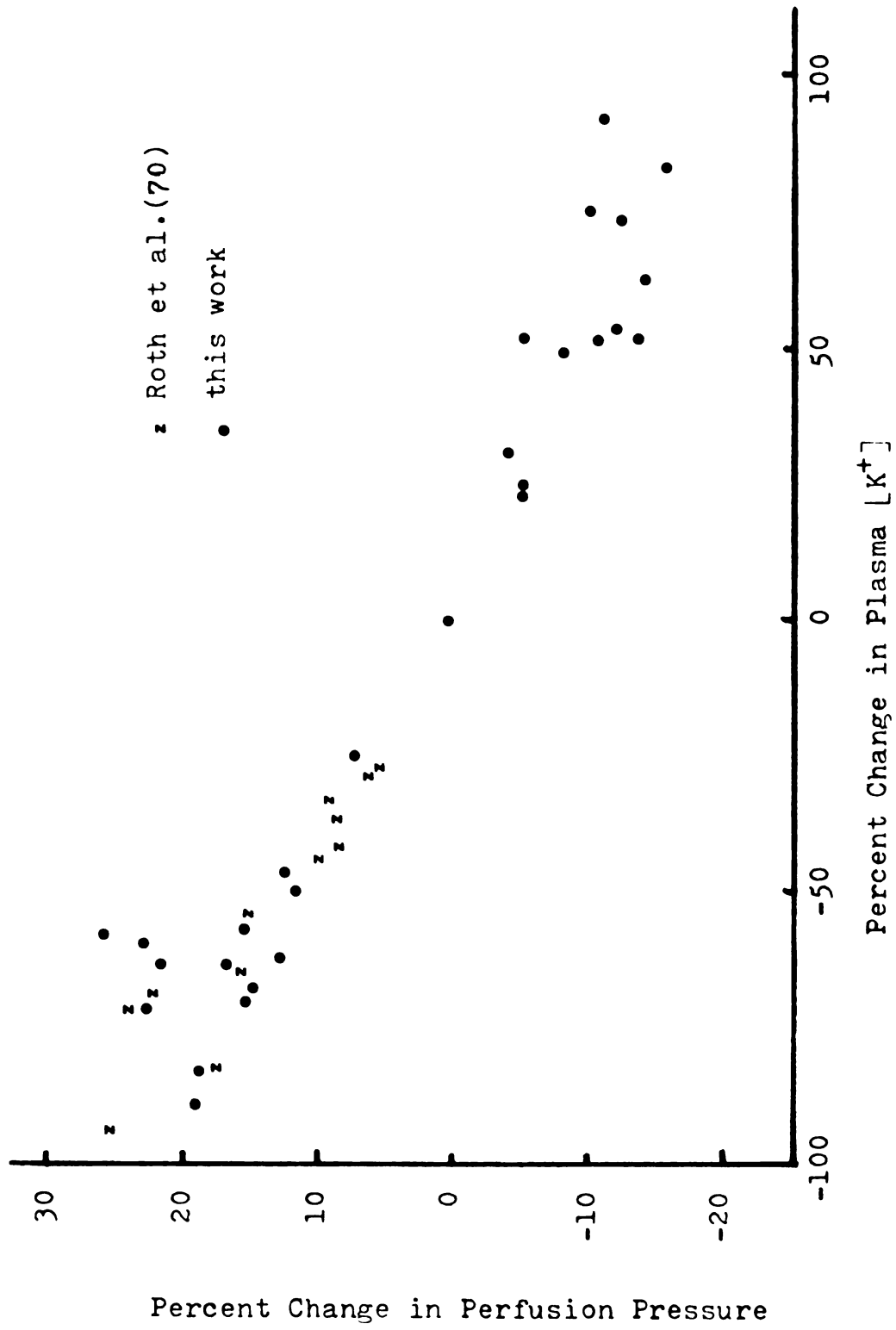


Figure 23. Effects of altering plasma [ $K^+$ ] on gracilis muscle perfusion pressure.

was compared to the venous plasma  $[K^+]$  leaving the muscle, the correlation was poor ( $r=0.387$ ).

Considering the effects of elevated and reduced plasma  $[K^+]$  separately, regression analysis shows that, for the hypokalemia data,  $y = -0.261 x$  with  $r = 0.774$  and, for the hyperkalemia data,  $y = -0.179 x$  with  $r = 0.709$ . This suggests that the gracilis muscle vasculature response to a reduction in  $[K^+]$  below normal is greater than the response to an equal increase in  $[K^+]$  above normal by almost 50% (0.261 compared to 0.179). (See appendix for tabulated data.)

## 2. Heart

A typical response elicited by local hypokalemia during constant flow perfusion of the left common coronary artery is shown in Figure 24. Upon reducing the plasma  $[K^+]$  of the blood perfusing the coronary artery from 3.4 to 1.6 mEq/l, there were simultaneous, large increases in both ventricular contractile force and coronary vascular resistance, while systemic pressure was little affected. Upon returning the plasma  $[K^+]$  to control, the responses quickly disappeared.

Individual data from 10 such animals are shown in Figures 25 and 26. (Solid lines connecting open circles represent data taken from the same animal before ouabain administration. Filled circles represent effects after ouabain administration. The dashed lines connect the pre to post ouabain responses.) It can be seen that acute local hypokalemia always produced an increase in coronary



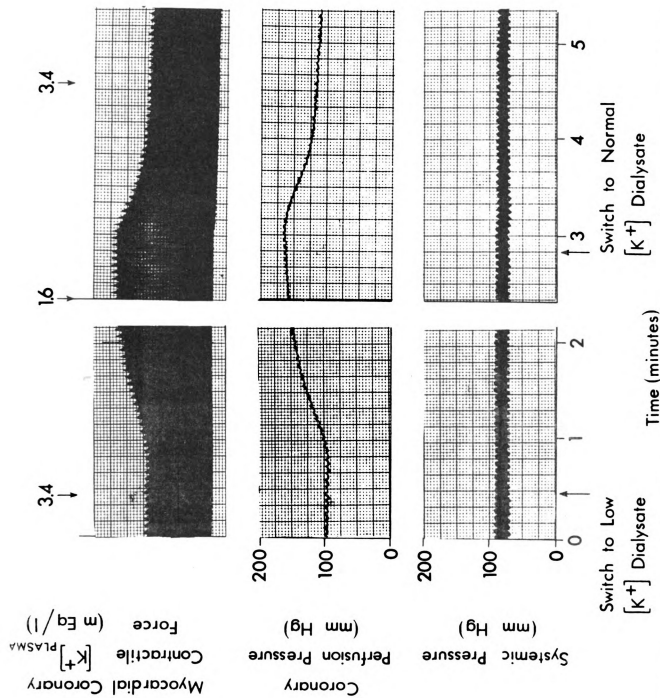


Figure 24. Typical effects of local hypokalemia on left ventricular contractile force, coronary vascular resistance and systemic arterial pressure during perfusion of the coronary vasculature with constant flow.

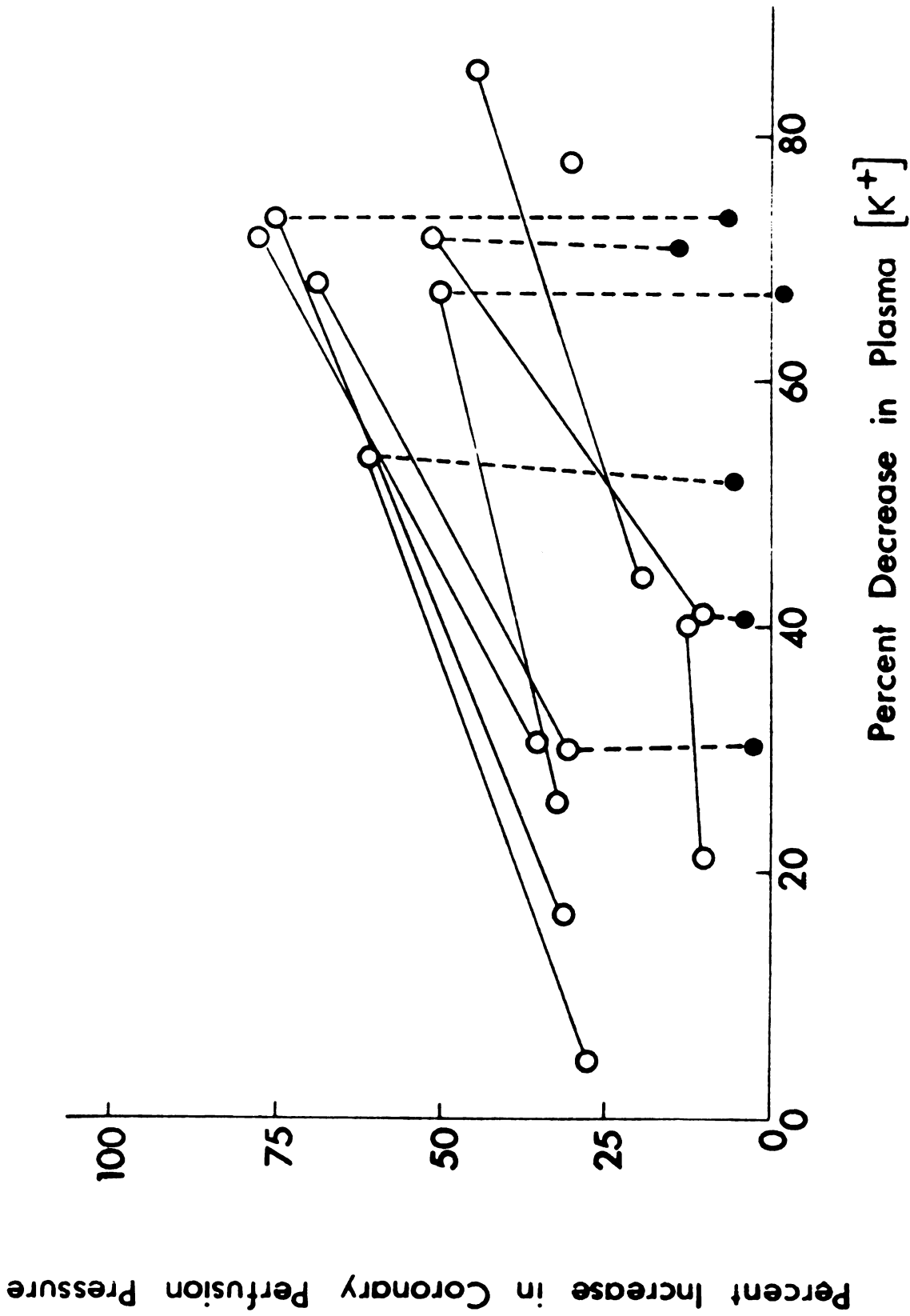


Figure 25. Changes in coronary perfusion pressure produced by reducing coronary arterial plasma  $[K^+]$  at constant coronary flow.

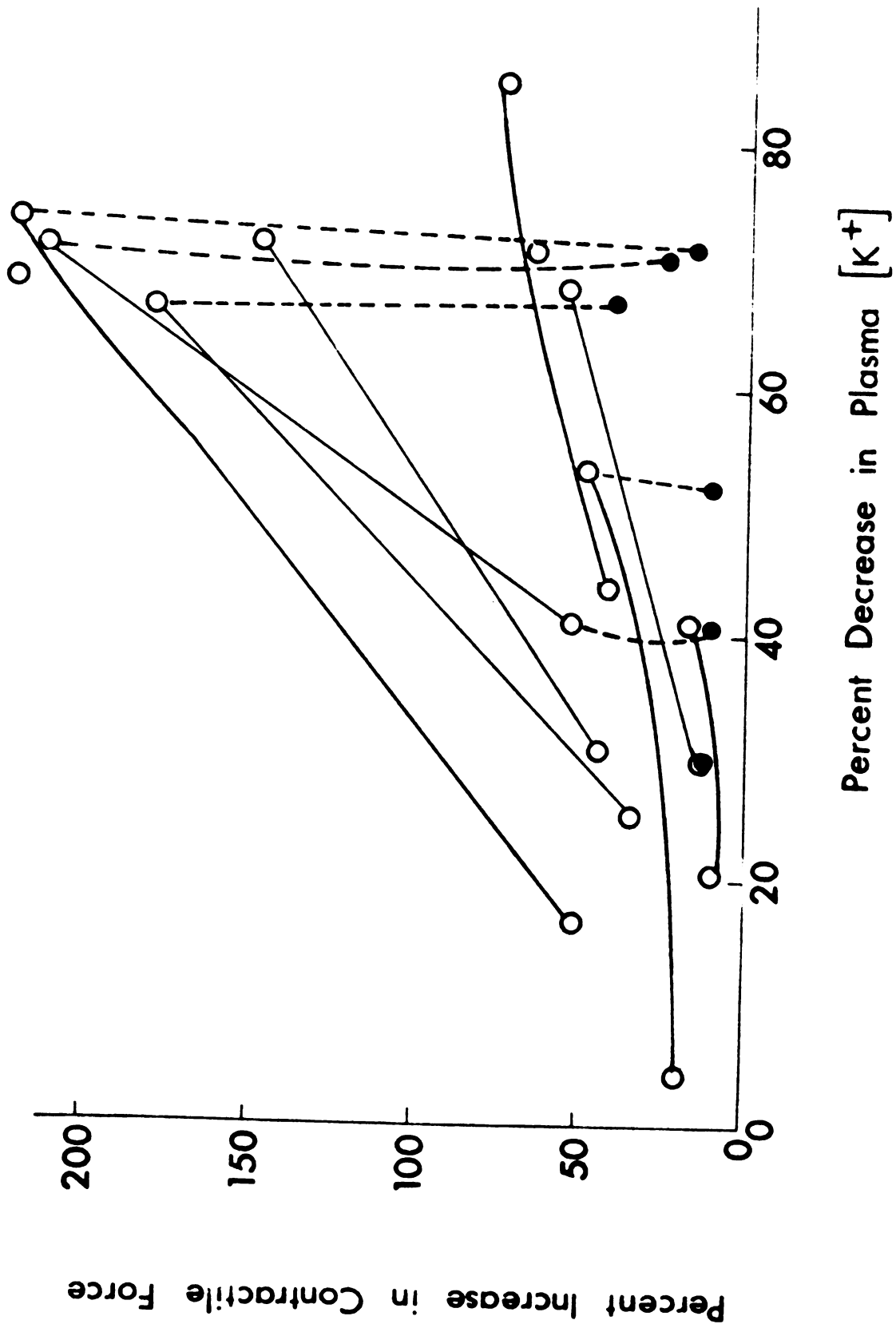


Figure 26. Changes in left ventricular contractile force produced by reducing coronary arterial plasma  $[K^+]$  at constant coronary flow.

vascular resistance and myocardial contractile force. In some animals, a reduction of the plasma  $[K^+]$  by approximately 75% produced a 75% increase in vascular resistance (Fig. 25) and a 200% increase in contractile force (Fig. 26). With two different levels of hypokalemia, the larger reduction in plasma  $[K^+]$  produced the greater increase in resistance and contractile force in each animal.

There was a strong correlation between percent change in length of the QT interval (x) and percent change in heart contractile force (y) as seen in Figure 27:  $y = 8x$  with  $r = 0.827$ . Again, the larger increases in QT interval were produced by the greater reduction in  $[K^+]$  in each animal. However, in some instances, hypokalemia caused a disappearance or reversal of the T wave and consequently QT interval could not be determined.

On the average, a 47% reduction in plasma  $[K^+]$  during constant coronary flow produced (after approximately 3 minutes) a 76% increase in left ventricular contractile force ( $P < .0001$ ), a 39% increase in coronary vascular resistance ( $P < .0001$ ), a 12% increase in QT interval ( $P < .001$ ), no change in heart rate, and only an insignificant ( $P > .4$ ) 3% increase in systemic arterial pressure. Upon returning the plasma  $[K^+]$  to normal, all variables returned to values not significantly different from their controls ( $P > .1$ ).

During constant pressure perfusion of the left common coronary artery, acute local hypokalemia immediately reduced coronary blood flow and coronary sinus oxygen tension and

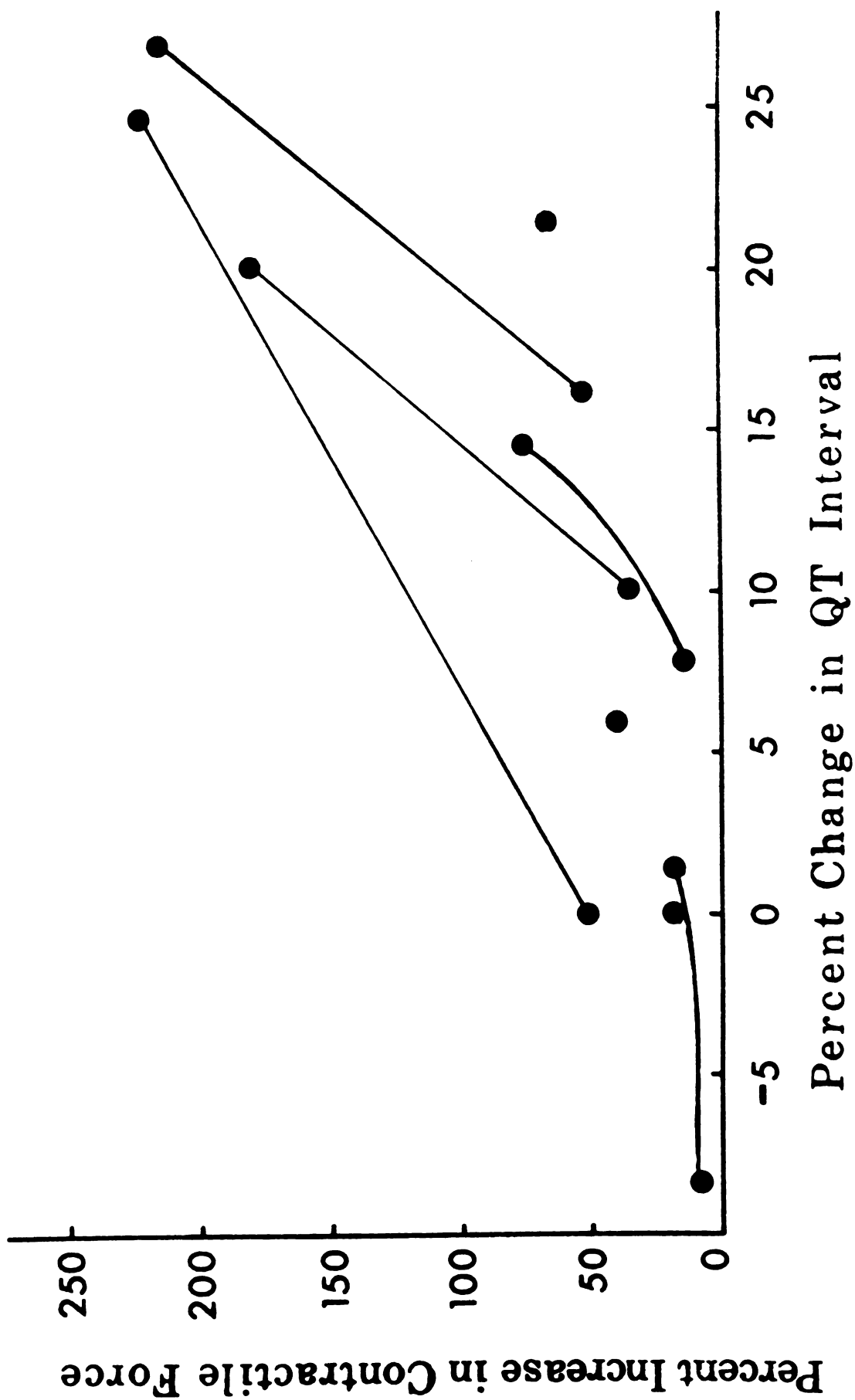


Figure 27. Effects of local hypokalemia on QT interval and myocardial contractility at constant coronary flow.

elevated myocardial contractile force. There was, however, no change in systemic arterial pressure. Average data for two levels of hypokalemic perfusion (5 min duration) are shown in Figure 28. It is evident that on the average the fall in coronary blood flow and increase in myocardial contractile force were greater during the more severe period of hypokalemia. This was also the case for coronary sinus  $O_2$  tension. These responses were quickly reversed upon return to the control dialysate.

The average effects of prolonging the duration of hypokalemic perfusion to 20 minutes are shown in Figure 29. During the hypokalemic perfusion, an average of 68% of the plasma  $K^+$  was removed from the blood perfusing the coronary artery. This caused a gradual increase in contractile force which became constant at a 37% increase after 12 minutes of hypokalemia. Systemic pressure decreased slightly throughout the perfusion period and became significantly different from the control value ( $P < .05$ ) after 12 minutes. The changes in coronary sinus  $P_{O_2}$  mimicked the changes in coronary flow, both of which initially decreased significantly ( $P < .025$ ), returned to control after approximately 8 minutes, and then rose well above control ( $P < .05$ ) by the end of the 20 minute hypokalemic perfusion period.

After 20 minutes, the plasma  $[K^+]$  was returned to control. Contractile force returned to the control value within 5 minutes. Systemic arterial pressure decreased further and remained different from the prehypokalemia

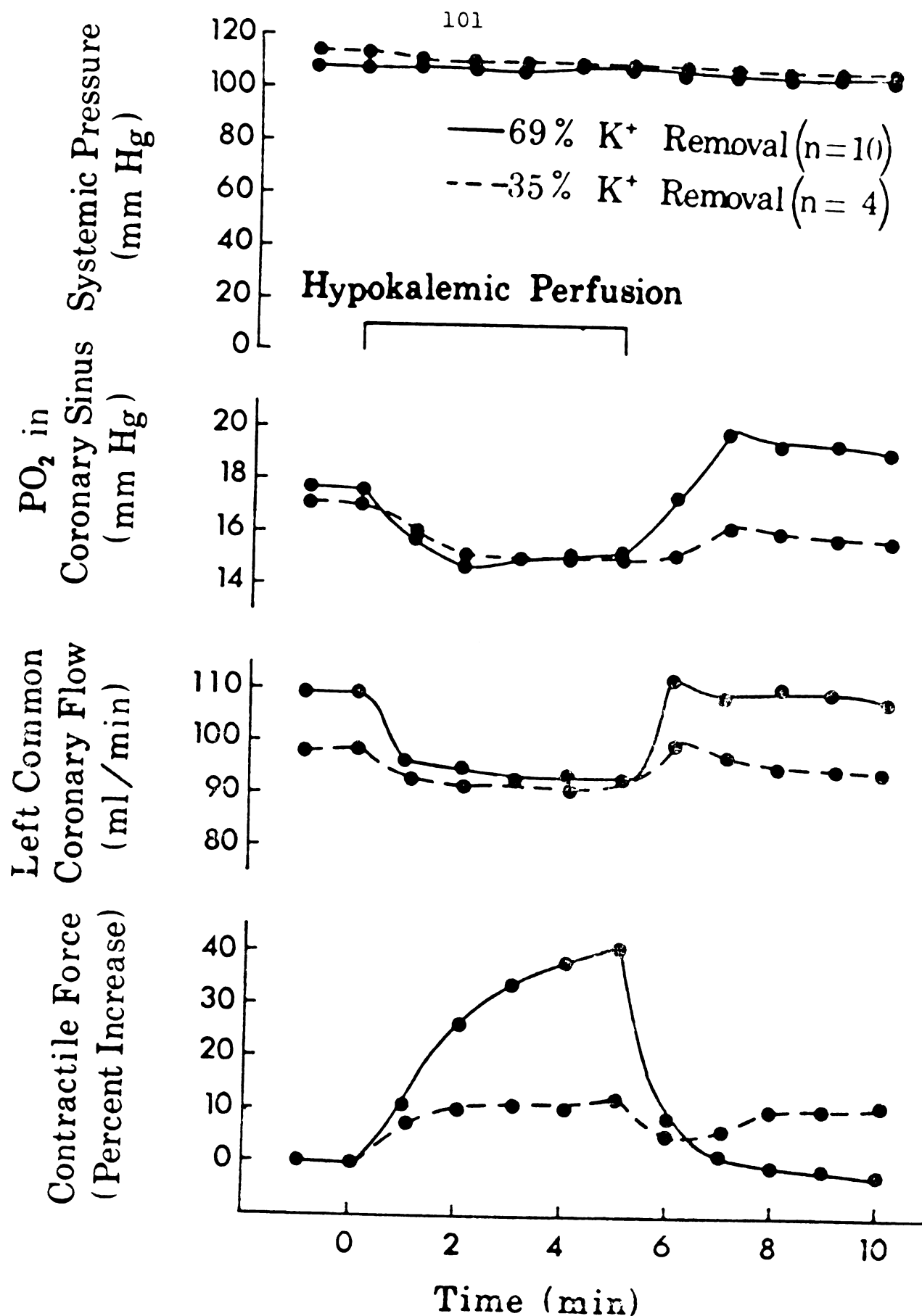


Figure 28. Average effects of local hypokalemia on the myocardial and coronary vessels produced during constant coronary perfusion pressure.

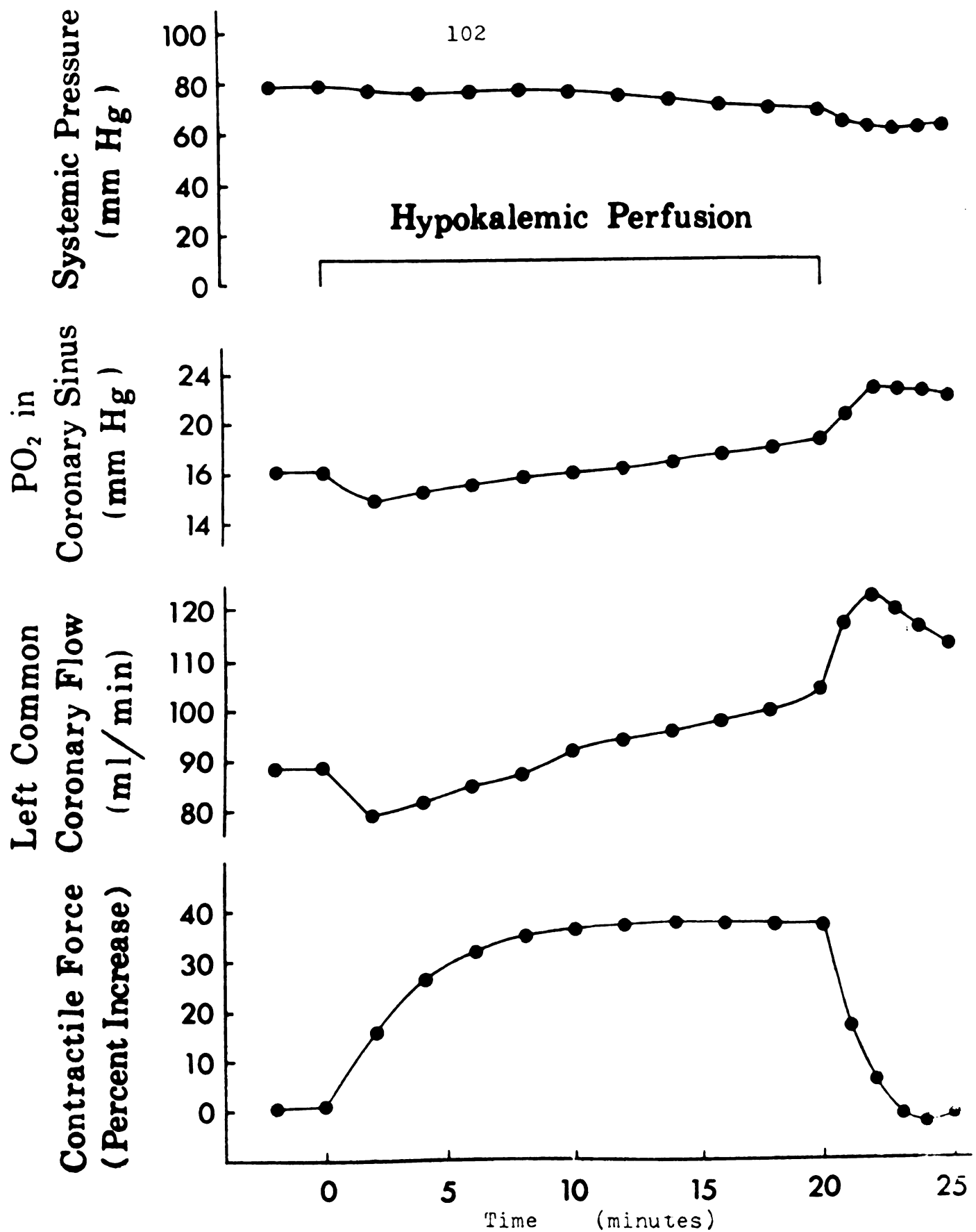


Figure 29. Average effects (n=8) of prolonged hypokalemia on the myocardium and coronary vessels produced while maintaining coronary perfusion pressure constant.



value. Both coronary flow rate and coronary sinus  $P_{O_2}$  rose further.

### Magnesium

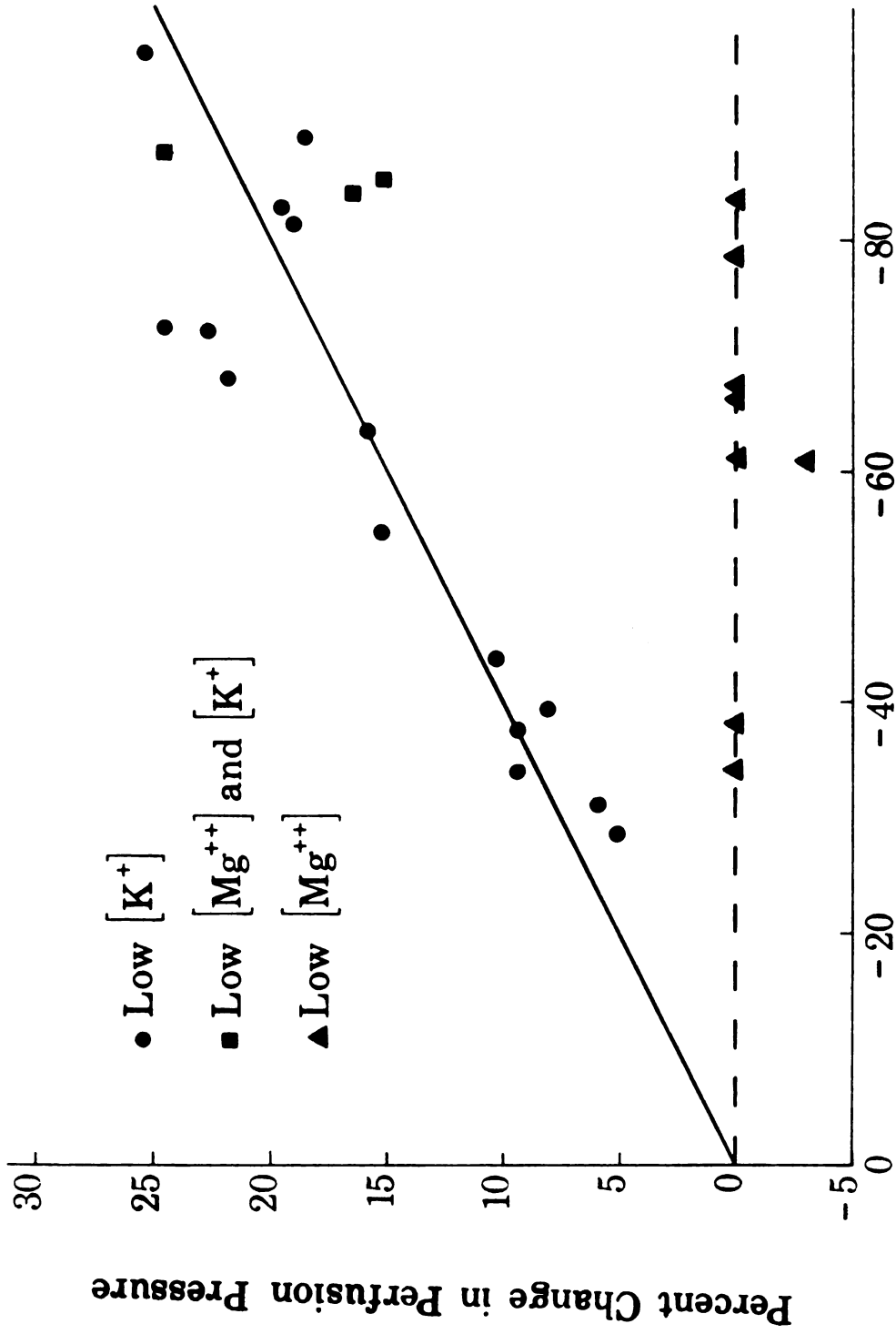
Figure 30 shows the result of 7 hypomagnesemia experiments. Each point is the averaged 5-10 minute response relative to control for a single gracilis muscle preparation. Removal of 33% to 84% of the plasma  $Mg^{++}$  affected vascular resistance in only one experiment. In that experiment, the gracilis responded with a decrease in resistance initially, but failed to respond on further exposures to hypomagnesemia.

Three of the above experiments included simultaneously perfusing the gracilis muscle with hypokalemic and hypomagnesemic blood. On the average, removal of 65% of the  $Mg^{++}$  and 86% of the  $K^+$  from the blood plasma produced a 21% change in perfusion pressure. From Figure 30 it can be seen that this increase in perfusion pressure corresponds to an 86% decrease in plasma  $[K^+]$ . Thus the  $[K^+]$  decrease alone can account for the increase in pressure.

### Hypoosmolality

#### 1. Gracilis Muscle

Figure 31 shows typical responses of two gracilis muscles to two different levels of hypoosmolality. When the dialysate was changed from normo to hypoosmotic, gracilis



Percent Change in  $[K^+]$  and/or  $[Mg^{++}]$  Relative to Control

Figure 30. Effects of low plasma  $[Mg^{++}]$  on gracilis muscle perfusion pressure compared to the effects of low plasma  $[K^+]$ .

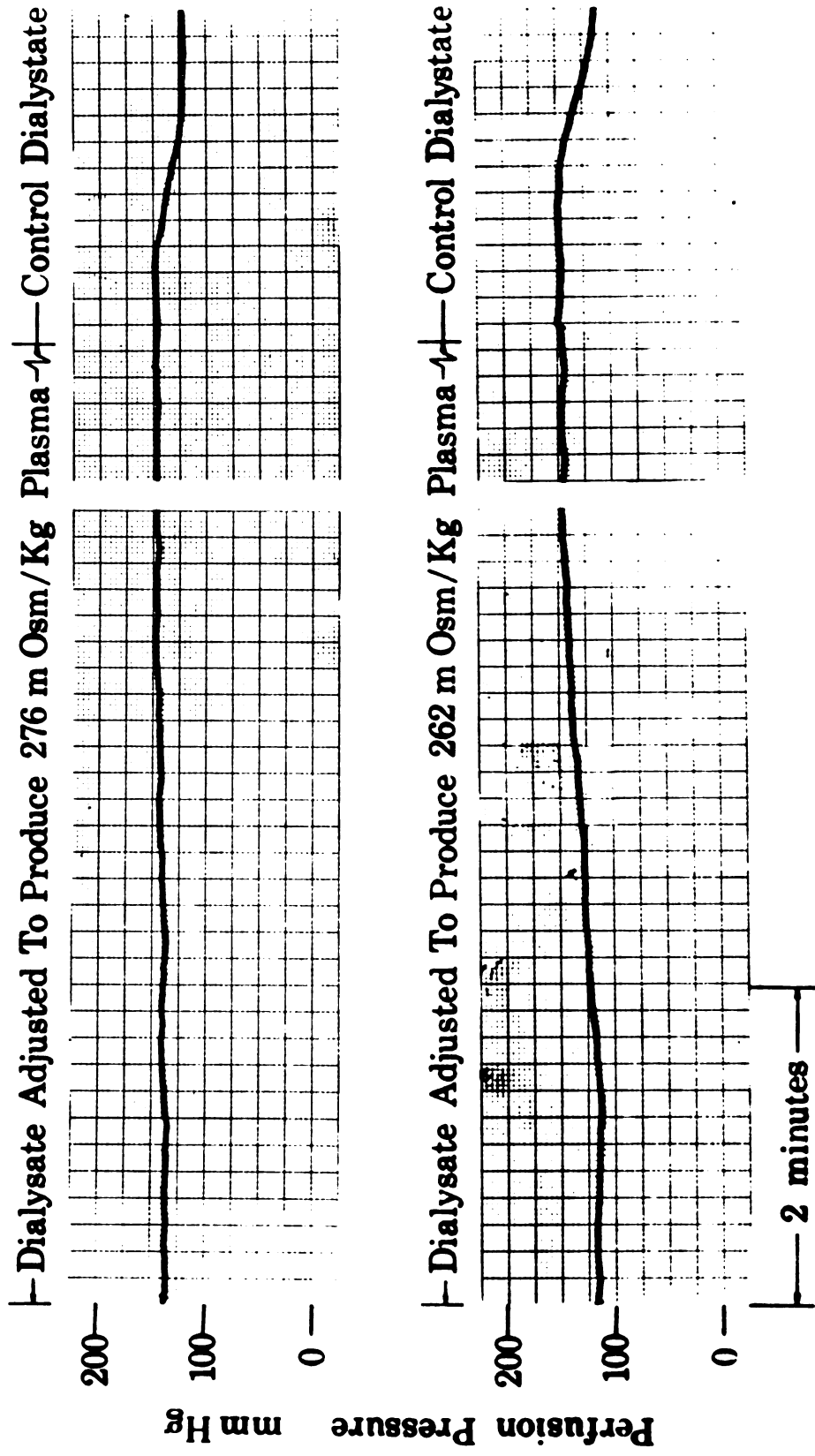


Figure 31. Typical responses of gracilis muscle to hypoosmotic perfusion.

artery perfusion pressure gradually increased after a short time lag and reached a steady state within 4-5 minutes. The short delay in pressure response agrees very well with the calculated time it took for the hypoosmolal blood to reach the muscle. Upon returning the dialysate to control, perfusion pressure promptly returned to the initial value. Note that the more severe hypoosmolality caused the greater increase in perfusion pressure.

Figure 32 shows that the relationship between plasma osmolality and vascular resistance is linear over the range of 300 to 225 mOsm/kg. The regression analysis relationship between percent change in vascular resistance (y) and osmolality (x) is  $y = -2.0 x$  with a correlation coefficient (r) equal to 0.95. The change in gracilis artery perfusion pressure in Fig. 32 is the average of the "on" (steady state change elicited by switching from control to experimental dialysate) and "off" responses. There were no significant differences between the two responses.

## 2. Heart

During constant flow perfusion of the left common coronary artery, hypoosmolality always increased coronary vascular resistance as seen in Figure 33. (The solid line connecting the filled circles represents data taken in the same animal.) In 8 of 9 animals, the greater reduction in plasma osmolality produced the larger increase in resistance. On the average, coronary vascular resistance increased 33% in response to a 7.5% decrease in plasma osmolality.

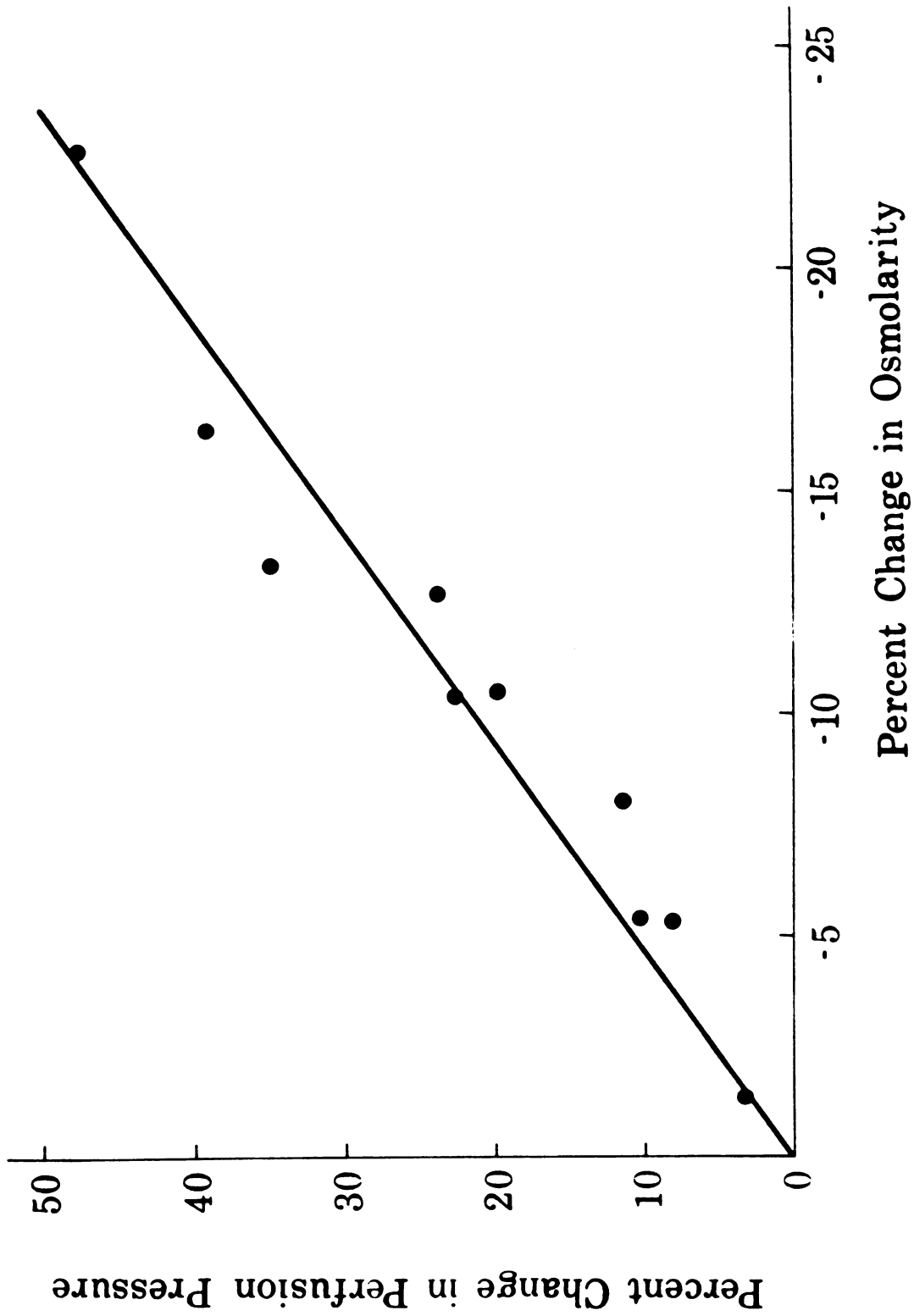


Figure 32. Effects of plasma hypoosmolality on gracilis muscle perfusion pressure.

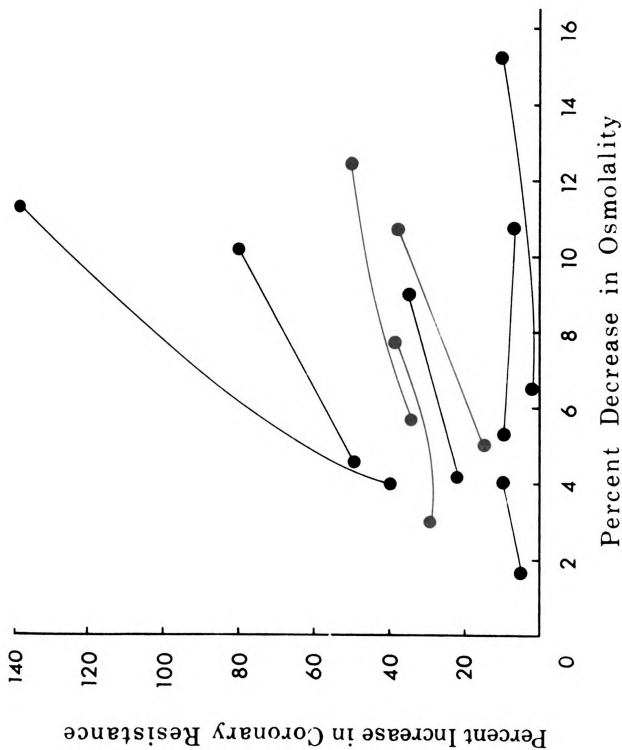


Figure 33. The effects of local plasma hypoosmolality on coronary perfusion pressure produced during constant coronary flow.

However the responses do not correlate well ( $r=0.498$ ). The data are the average of the "on" and "off" responses in each animal. As in the gracilis muscle, there were no significant difference between the two responses.

Concomitant with the increased coronary vascular resistance was an increased contractile force in each animal, as seen in Figure 34. In 5 of 8 animals, the increase in contractile force was greater with the more severe hypo-osmolality. On the average ( $n=9$ ), a 7.5% decrease in osmolality produced a 20% increase in contractile force. However the correlation between change in contractile force and osmolality was also poor ( $r=0.51$ ). There were also simultaneous decreases in the QT interval (Figure 35). On the average ( $n=7$ ), the QT interval decreased by 12% when contractile force was increased by 18%. The largest increase in contractile force was accompanied by the greatest decrease in QT interval.

The effects of reducing plasma osmolality by an average of 20 mOsm/kg while perfusing the left common coronary artery at constant pressure are shown in Figure 36. Hypo-osmolality significantly increased contractile force, however the initial increase waned with time. Associated with the rise in contractile force and fall in left common coronary flow rate ( $P < .0001$ ) was a decrease in coronary sinus oxygen tension ( $P < .005$ ). Also systemic pressure was slightly reduced. When the coronary artery was again perfused with normoosmotic blood, contractile force and

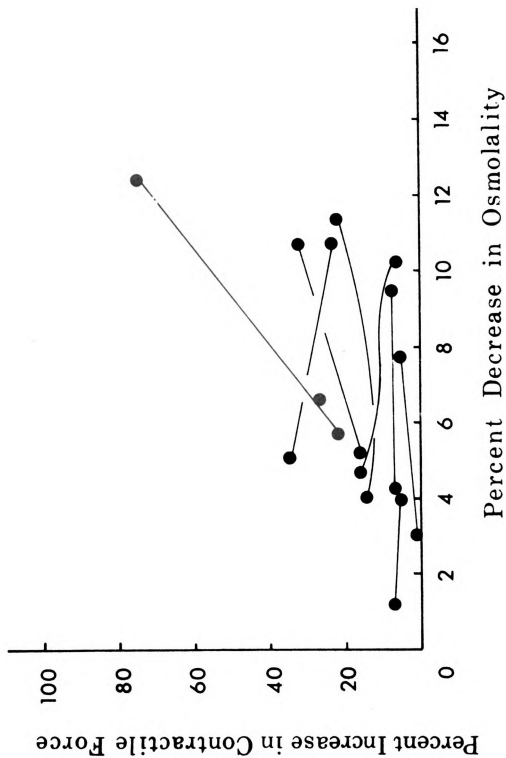


Figure 34. The effects of local plasma hypoosmolality on myocardial contractile force produced during constant coronary flow.



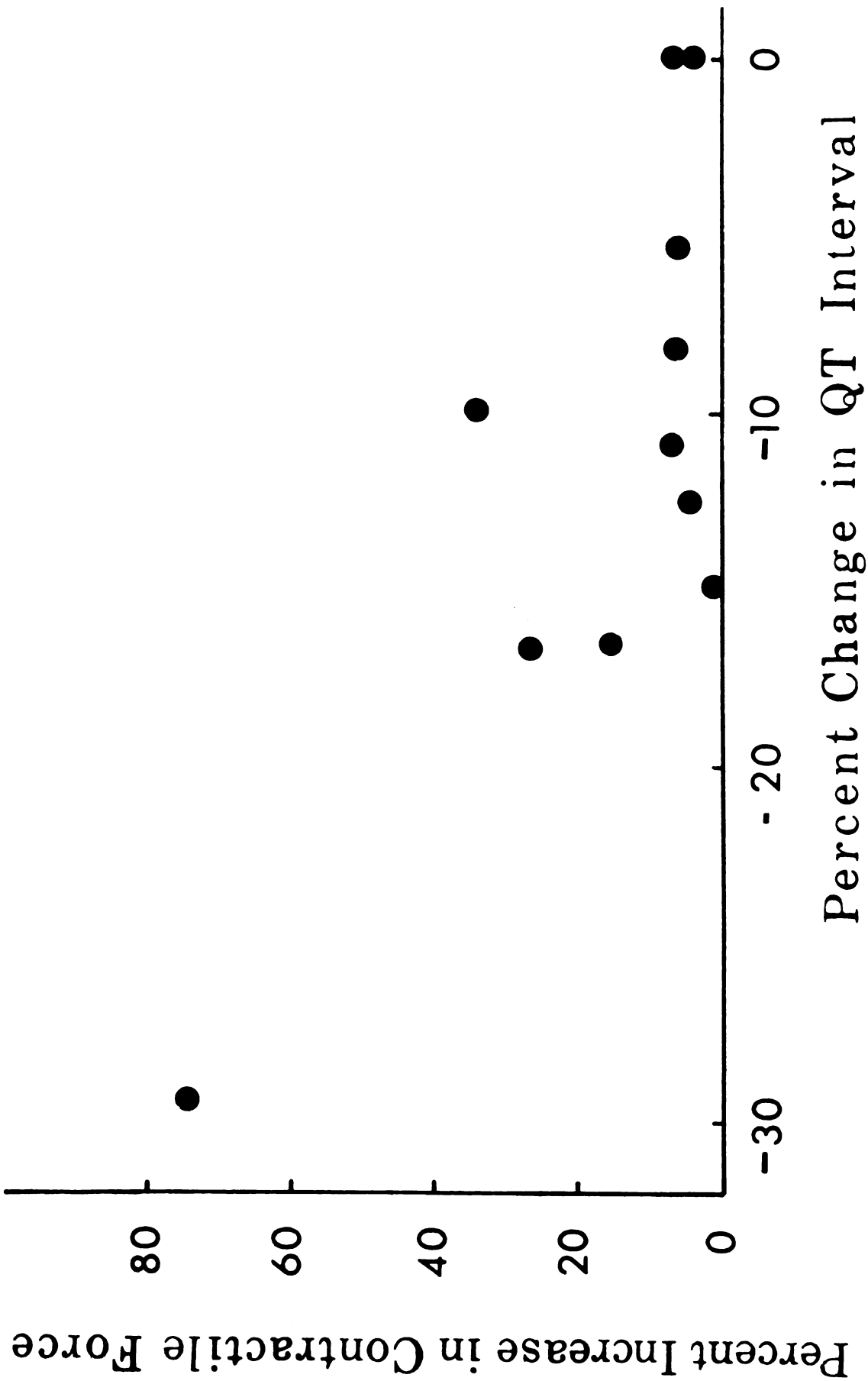


Figure 35. Simultaneous changes in QT interval and contractile force produced by hypotensive perfusion of coronary artery at constant flow.

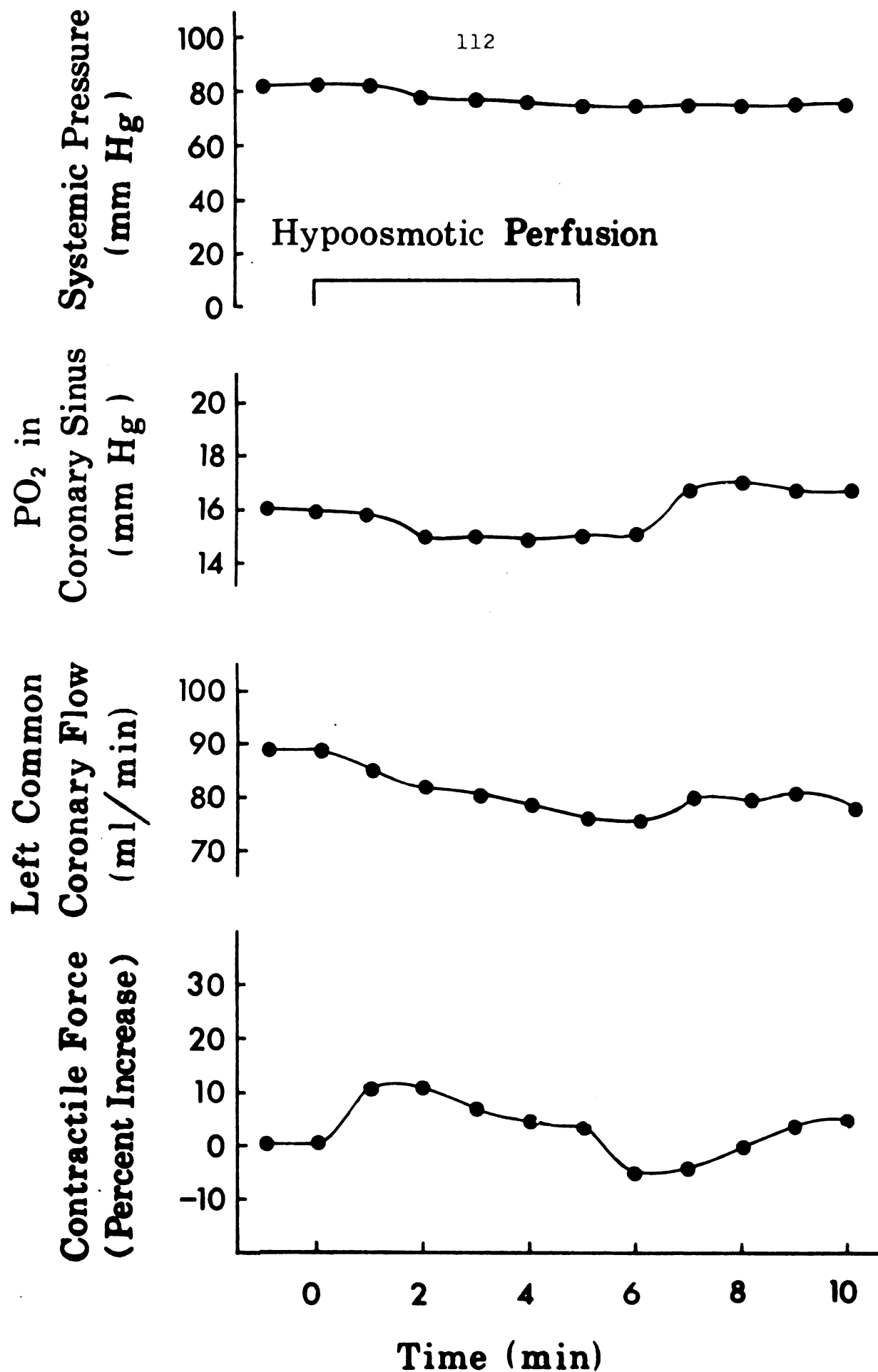


Figure 36. Effects of local hypoosmolality on myocardium and coronary vessels produced during constant pressure perfusion of coronary artery.

coronary sinus  $P_{O_2}$  returned to their initial values. Coronary flow increased but failed to return to the control value and systemic pressure remained reduced.

### Sodium

The effect on gracilis artery perfusion pressure of partial replacement of the plasma NaCl with mannitol is shown in Figure 37. Reducing the plasma  $[Na^+]$  and  $[Cl^-]$  while maintaining the blood isoosmolal produced a slow increase in resistance to flow. For example, in the top tracing there was a 28% decrease in plasma  $[Na^+]$  and roughly a 20 mm Hg rise in perfusion pressure. However returning the dialysate to control produced variable results. As seen in the top tracing, perfusion pressure did return to control when the plasma  $[Na^+]$  and  $[Cl^-]$  were returned to normal. This was not the case for the lower two tracings. In the middle trace, perfusion pressure failed to respond to the control dialysate and in the bottom trace pressure continued to rise after returning to the control dialysate. In these experiments the dialyzer produced no measureable change in blood hematocrit and pH, or in plasma  $[K^+]$  or  $[Ca^{++}]$ .

As seen by the filled circles in Figure 38, hyponatremia always produced an increase in resistance in each animal. The correlation coefficient between percent reduction in  $[Na^+]$  and percent increase in perfusion pressure ( $r=0.793$ ) suggests that resistance increases approximately linearly as the

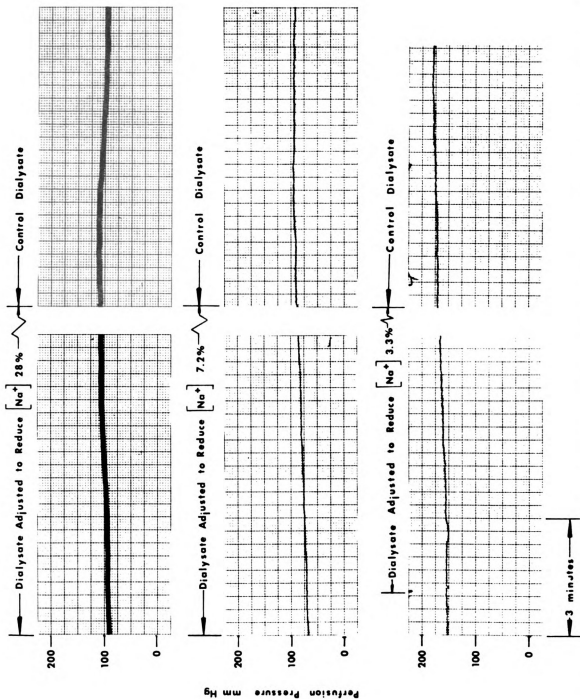


Figure 37. Effects of hyponatremia on gracilis muscle perfusion pressure.

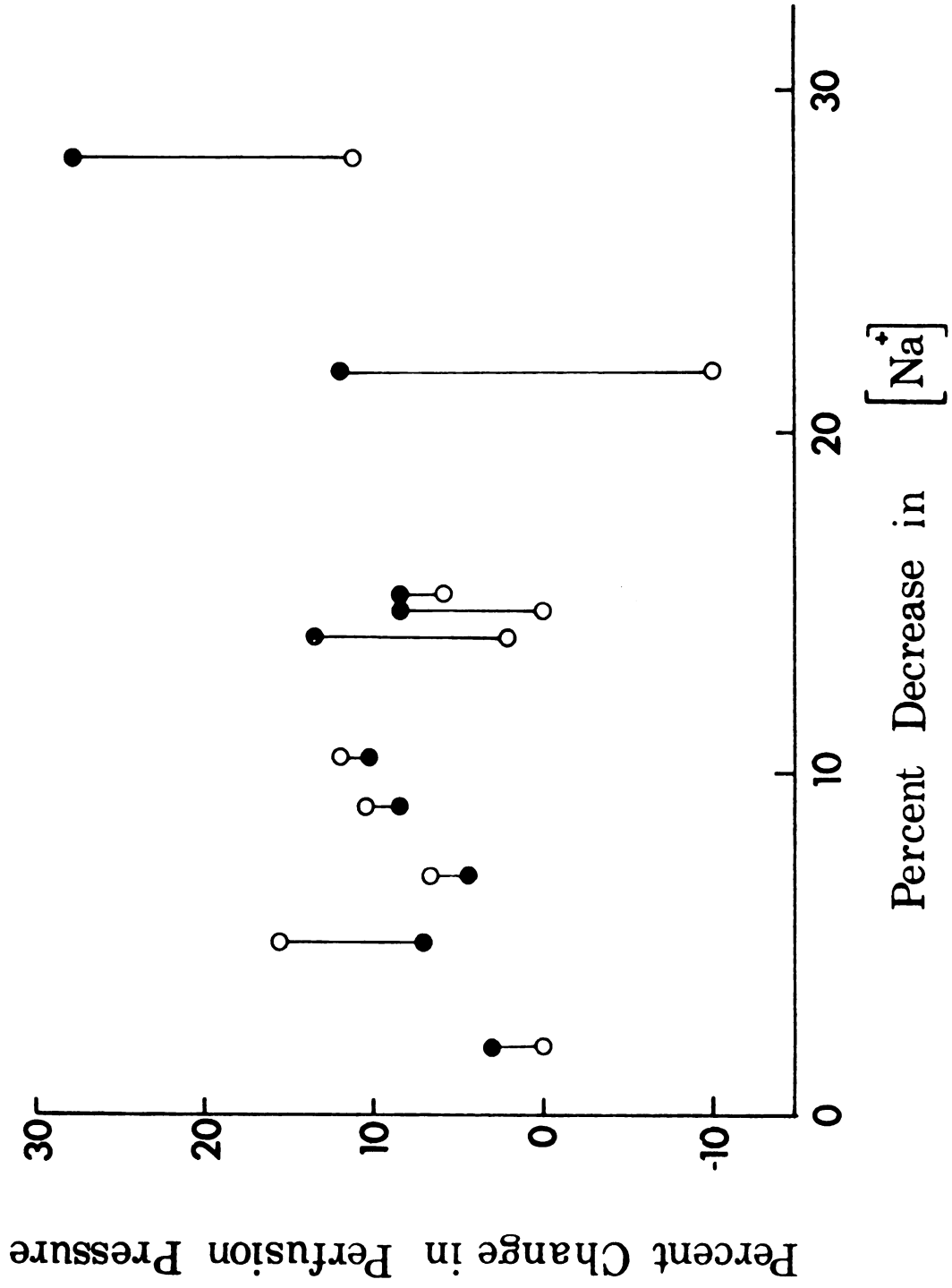


Figure 38. Effects of hyponatremia on gracilis perfusion pressure.

plasma  $[Na^+]$  is reduced. The data obtained by switching from the low sodium dialysate to normal sodium are platted in Fig. 38 as open circles. Note that while the muscle vasculature always responded to a lowering of plasma  $[Na^+]$  with an increase in resistance, the responses were inconsistent when the  $[Na^+]$  was returned to normal. Lithium chloride and choline chloride were also tested as NaCl substitutes, but these agents were found to be extremely vasoactive in the concentrations necessary to replace significant amounts of sodium.

## Ouabain

### 1. Gracilis Muscle

The average effects (n=12) of a continuous infusion of ouabain (2.5 ug/min) into the gracilis artery are shown in Figure 39. Ouabain produced a gradual rise in gracilis artery perfusion pressure ( $P_{PGA}$ ) which reached a maximum in an average of 8 minutes. Pressure then gradually fell (ouabain infusion continuing), reaching a steady state in an average of 20 minutes which was not significantly different from the control period. Figure 39 also shows that the ouabain infusion was without effect on systemic arterial pressure ( $P_s$ ).

The data indicate that the effects of ouabain are concentration dependent. In the experiments, the infusion rate was the same in each animal and thus the ouabain concentration in the perfusing blood varied inversely with

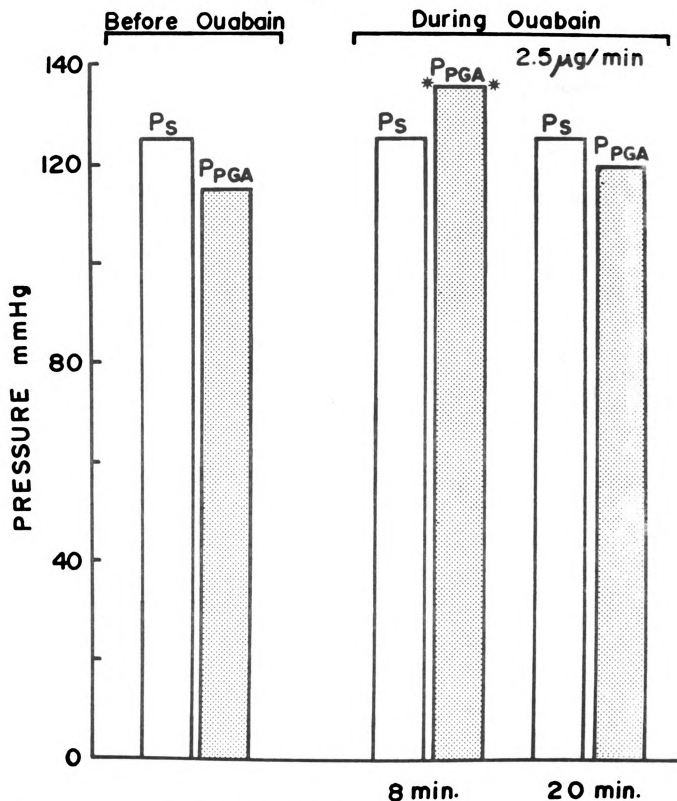


Figure 39. Average effects of a continuous ouabain infusion on gracilis perfusion pressure.

blood flow rate. Figure 40 shows that the maximum increase in resistance occurred earlier with the lower flow rates. Furthermore, the time at which the maximum pressure occurred correlates well with flow rate ( $r=0.838$ ).

## 2. Heart

The average effects of a continuous infusion of ouabain (12 ug/min for 15 min) into the left common coronary artery while maintaining flow constant are shown in Figure 41. Contractile force increased linearly throughout the infusion period. Perfusion pressure initially rose, reached a maximum (30% increase) and declined slowly, still being 20% above control at the end of the infusion period. Systemic pressure did not change significantly during ouabain infusion.



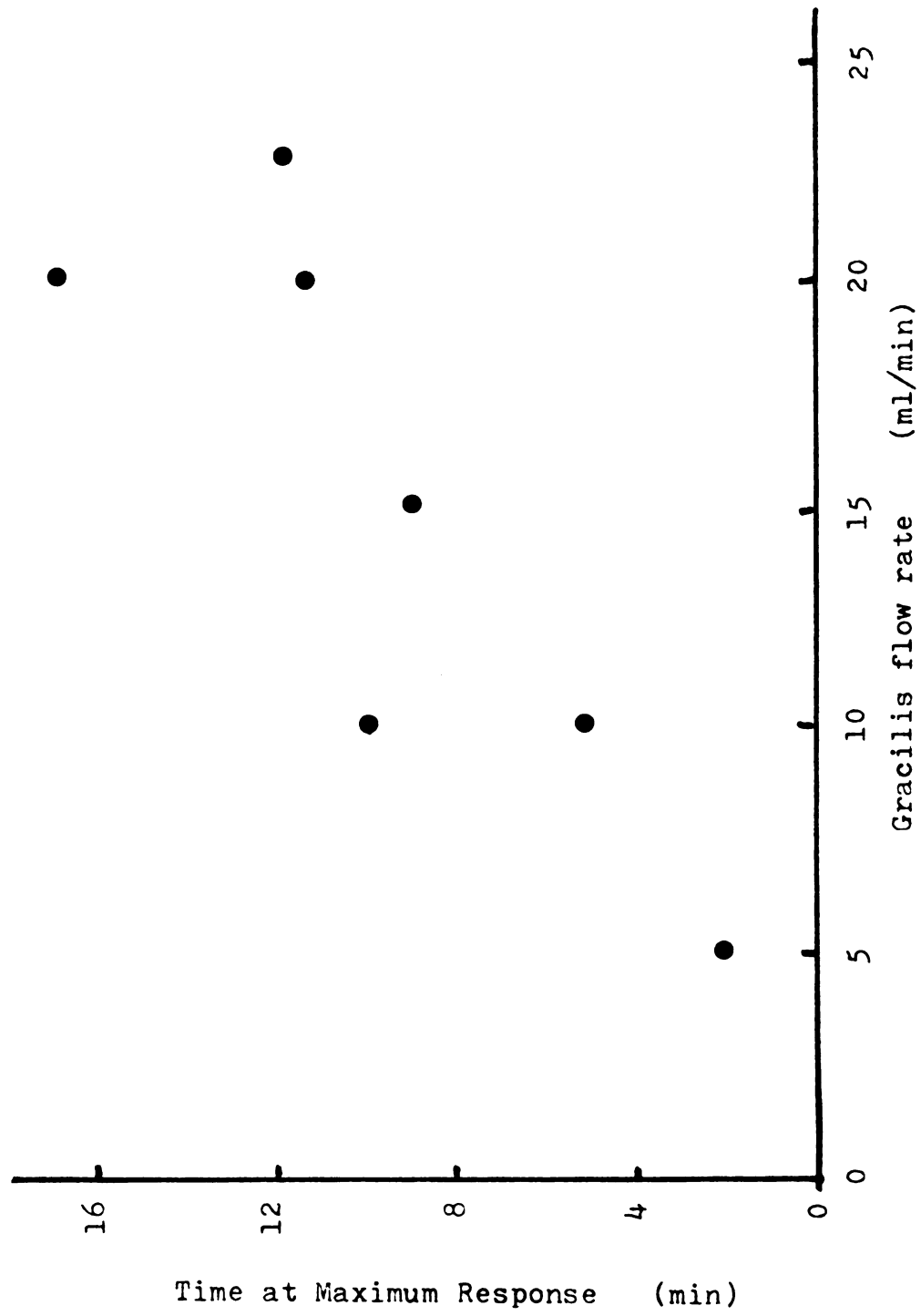


Figure 40. Effect of flow rate on time of maximum response during ouabain infusion.



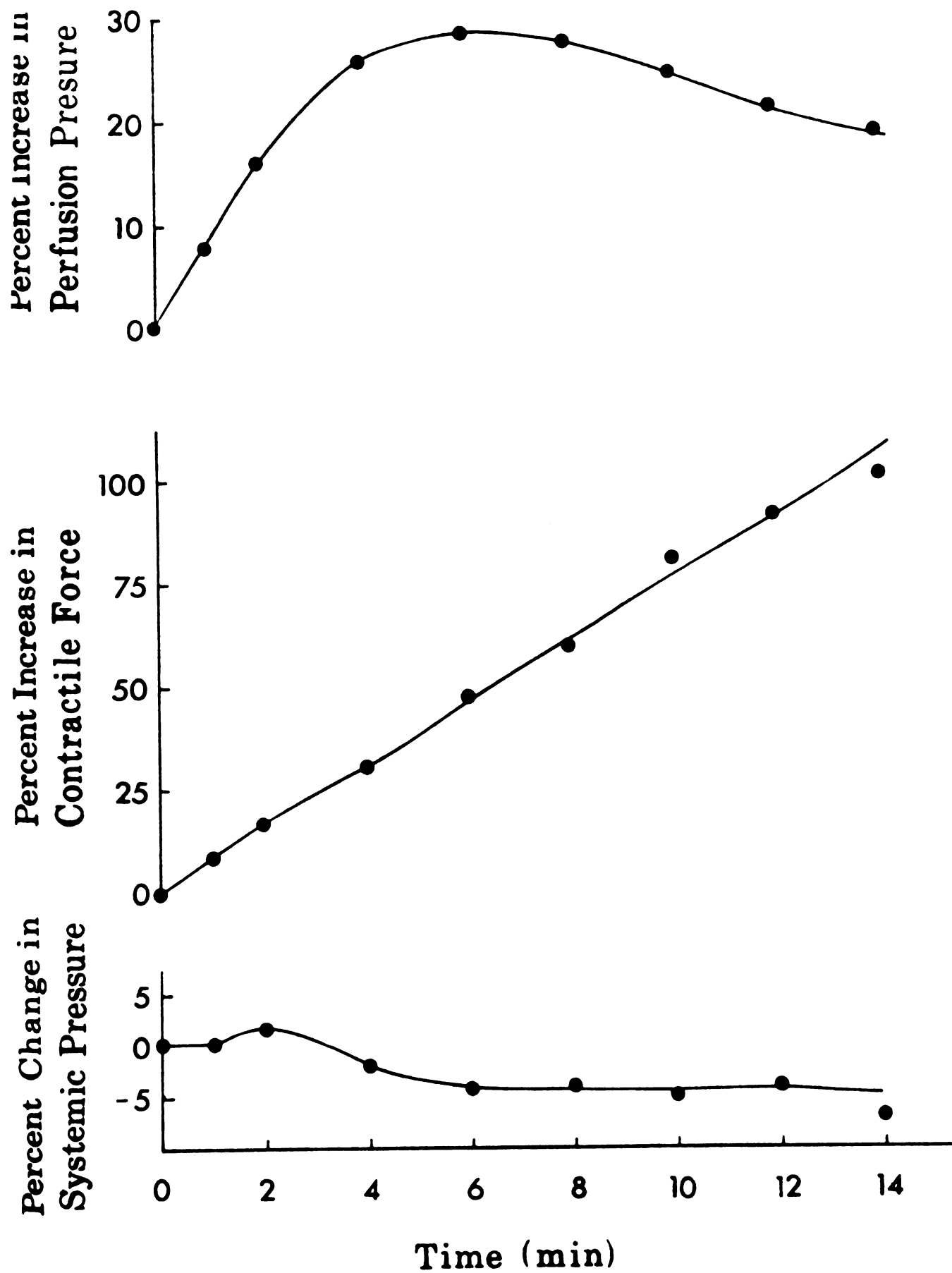


Figure 41. Average effects (n=6) of ouabain administration on myocardial contractile force, coronary perfusion pressure, and systemic arterial pressure during perfusion of the coronary bed at constant flow.

## DISCUSSION OF EXPERIMENTAL RESULTS

### Potassium

These studies are in agreement with the previous studies which showed that local acute hypokalemia increases skeletal muscle vascular resistance to blood flow and myocardial contractile force(44,46). The new findings include the following:

- 1) The change in skeletal muscle vascular resistance to blood flow produced by altering the arterial plasma  $[K^+]$  appears to be linearly related to plasma  $[K^+]$  over the range of 0 to 8 mEq/liter.
- 2) Low plasma  $[K^+]$  significantly increases coronary vascular resistance. However, this increase in resistance wanes with time and after approximately 10 minutes resistance becomes less than during normokalemic perfusion.

In the gracilis muscle, the increase in resistance is due to a reduction in the blood vessel diameter elicited by the changes in plasma  $[K^+]$ . The details of the mechanism which produce this increased resistance are discussed in PART III of this thesis. The same mechanism is involved in the increased coronary vascular resistance. However, coronary resistance may also passively increase due to the mechanical effect of an increased contractile force.

The changes in coronary vascular resistance produced by hypokalemia differed when the coronary artery was perfused at constant flow and constant pressure. For example, the maximal changes in coronary resistance for approximately equal changes in  $[K^+]$  were a 39% increase during the constant flow experiments, but only a 13% increase during the constant pressure experiments. This could be related to 1) difference in transmural pressures, i.e., during the constant flow experiments, the increase in transmural pressure may have elicited an active myogenic response and 2) reduction of flow during constant pressure perfusion may cause greater accumulation of vasodilator metabolites.

During prolonged constant pressure perfusion of the coronary artery, resistance initially rose sharply when exposed to hypokalemia and then gradually declined. This transient change in resistance may be due to 1) vasodilator metabolite buildup and 2) predictable effects of the electrogenic Na-K pump, i.e., the slowed extrusion of  $Na^+$  allows the intracellular  $[Na^+]$  to increase, stimulating the electrogenic pump with a resulting gradual repolarization of the vascular smooth muscle cells. Clearly, this latter effect should also occur in the constant flow experiments. However, since we did not study hypokalemia for a comparable length of time, it is difficult to access whether the increase in resistance during the constant flow studies also waned with time.

The present finding that hypokalemia increases contractile force in vivo is consistent with in vitro observations on isolated hearts and cardiac tissues(67,69,82). A decrease in  $[K^+]_e$  almost immediately increases contractile force in isolated rabbit hearts(82). Reiter et al(69) reported that in papillary muscles of guinea-pig ventricle "a half maximal inotropic effect is reached about 2 minutes after  $[K^+]_e$  has been reduced." (For a discussion of the mechanisms involved see 13,56,82).

#### Magnesium

The absence of a resistance change when  $[Mg^{++}]$  was lowered agrees with the previous studies using the dilution techniques(44). One might have expected an increase in resistance since increasing the plasma  $[Mg^{++}]$  reduces resistance(26,61,73,83). Furthermore, it has been previously reported that exposure of rabbit aortic strips to  $Mg^{++}$ -free Krebs-Ringer solution for 60 minutes increased the tension from 10 to 50% in some of the strips(3). In the present work, the smooth muscle cells were never exposed to  $Mg^{++}$ -free blood and exposure times were much shorter. Hence, the lack of response is not necessarily inconsistent.

#### Hypoosmolality

Past studies(35,36,61,81) have shown that local plasma hypoosmolality increases vascular resistance in skeletal

muscle, forelimb and kidney. In those studies, the dilutional technique used to reduce osmolality produced other blood changes such as hypokalemia, hypocalcemia, reduced hematocrit, etc. Thus it was difficult, if not impossible, to separate the effects of hypoosmolality from the effects of the secondary abnormalities. In the present studies, hemodialysis was used to reduce osmolality by selective removal of NaCl and consequently produced fewer secondary changes in the perfusing blood. Thus the observed changes in resistance are more directly attributable to the effects of hypoosmolality per se.

The present studies show that acute local decreases in plasma osmolality, produced by partial removal of NaCl from blood, increase skeletal muscle and coronary vascular resistance to blood flow and increase myocardial contractile force. Furthermore, in the gracilis muscle, vascular resistance increased linearly as plasma tonicity decreased.

Stainsby and Fregly(81) also found that skeletal muscle vascular resistance was linearly related to osmolality over the range of approximately 200-450 mOsm/kg. The slope of the line relating resistance to osmolality in this study is slightly greater than that reported by Stainsby and Fregly (0.67 compared to 0.60). It is difficult to compare the data since they perfused with cell-free plasma and produced hypoosmolality by addition of water to the normal plasma. However, it appears that the secondary blood changes produced with the dilution technique are of little consequence in

comparison with the effects of the change in plasma osmolality. There are no previous in vivo studies on the effects of hypoosmolality on myocardial contractile force and coronary vascular resistance to compare with the present study.

The increase in coronary and skeletal muscle vascular resistance which occurred during the hypoosmolal perfusion most likely resulted from both passive and active decreases in vessel caliber and because of an increased blood viscosity subsequent to red cell swelling. These passive effects have been considered in previous communications(35,36). In brief, passive changes in vessel caliber may result from 1) endothelial cell swelling reducing lumenal diameter and 2) in the case of the coronary vascular bed, a decreased transmural pressure due to the effect of an increased contractile force. Active vasoconstriction also contributes to the increase in resistance. Gazitua, et al.(35) concluded that, in the kidney, the increase in vascular resistance produced by hypoosmotic perfusion resulted, to a large extent, from active vasoconstriction subsequent to osmotic shift of water into the vascular smooth muscle cells. Conversely, these authors also reported that the decrease in resistance with hyperosmolality in the forelimb and skeletal muscle may result in a large part from active vasodilation(36).

It is evident that changes in plasma osmolality produce active vasomotion by altering the intracellular ion concentrations(15). Studies in isolated tissues showed that, with hypoosmolality, the intracellular concentrations of



$\text{Na}^+$  and  $\text{K}^+$  decreased(15) and partial depolarization resulted(18) as the cells gain water. It has been suggested that depolarization most likely results from the reduced  $[\text{K}^+]_i$  decreasing the passive  $\text{K}^+$  efflux(36). In addition, the decreased  $[\text{Na}^+]_i$  would slow the electrogenic pump. Thus both intracellular  $\text{Na}^+$  and  $\text{K}^+$  appear to be important in the change in membrane potential and muscle activity. In this regard, calculation with "the model" indicates that hypoosmolality does indeed reduce resting potential for the above reasons. For a more complete discussion of this point, see page 148, PART III, of this thesis.

Acute local decreases in plasma osmolality increase coronary vascular resistance and myocardial contractile force during both constant flow and constant pressure perfusion of the coronary vasculature bed. However, the effects of hypoosmolality were greater when the left common coronary artery was perfused at constant flow compared with perfusion at constant pressure. For approximately equal changes in plasma osmolality, coronary vascular resistance increased by about 33% and myocardial contractile force increased by 20% with constant flow perfusion, whereas the corresponding changes during constant pressure perfusion were approximately a 15% increase in resistance and a 10% increase in contractile force. These differences could be related to 1) reduction of flow during constant pressure perfusion and thus accumulation of vasodilator metabolites and myocardial depressors as well as decreased oxygen

tension, and 2) differences in transmural pressure, i.e., during the constant flow experiments, the increase in perfusion pressure may have elicited an active myogenic response in the coronary blood vessels.

During constant pressure perfusion of the left common coronary artery, the initial increase in contractile force waned with time eventhough coronary sinus oxygen tension remained constant (Fig. 36). This suggests that the transient decrease in contractile force is not due to the effects of metabolite buildup. It may be due to loss of Na from the myocardial cells.

Clearly, local hypoosmolality produces significant increases in contractile force. The mechanisms involved in the increased contractile force are discussed in reference 14.

### Sodium

The data on hyponatremia suggest that the Na ion may have a specific effect on smooth muscle activity. The gracilis muscle always responded to a decrease in plasma  $[Na^+]$  and  $[Cl^-]$  with an increase in vascular resistance eventhough plasma osmolality,  $[K^+]$ ,  $[Ca^{++}]$ , hematocrit and pH did not change. From Figure 32, it is seen that a 20% decrease in osmolality increased resistance by 40%, whereas, as seen in Figure 38, a 20% reduction in  $[Na^+]$  increased resistance by only 10%. While it is difficult to evaluate the effects of the change in  $[Cl^-]$  on resistance, it has

been reported that altering the  $[Cl^-]$  had no affect on resistance(61). Thus it appears that the Na ion has a small but specific affect on smooth muscle activity.

In contrast with this conslusion, a previous study(61) in which the dilutional technique was used, failed to show any apparent effect of the Na ion on vascular smooth muscle. This discrepancy may be due to the difficulty in quantitating small differences in resistance when using the dilutional technique. The effect of the Na ion is further complicated by the fact that resistance did not always return to control when the normal  $[Na^+]$  was reinstituted. However, in vitro data suggest that the Na ion should be vasoactive since altering the  $[Na^+]$  produces changes in cell membrane potential (15,18,55).

### Ouabain

These studies show that the effects of ouabain are biphasic in skeletal muscle and coronary vascular beds. Initially ouabain increases resistance and this is followed by a gradual fall in resistance eventhough the ouabain infusion continues. In the gracilis muscle, the change in resistance is due to an active change in blood vessel diameter. However, the increases in coronary vascular resistance may also have a passive component since the increased contractile force might passively reduce vessel caliber. The active increases in resistance are due to

the direct effects of ouabain and the mechanism of this effect is discussed in PART III of this thesis.

The increase in contractile force during ouabain administration is in agreement with many previous studies (c.f., 71).

PART III:

MECHANISMS OF THE EFFECTS OF  $K^+$ , OUABAIN AND  
OSMOLALITY ON VASCULAR RESISTANCE TO BLOOD FLOW

Thus far, the experimental effects of  $K^+$ ,  $Mg^{++}$ ,  $Na^+$ , and osmolality on vascular resistance to blood flow have been presented and it has been shown that the effects of ions ( $Na^+$ ,  $K^+$ , and  $Cl^-$ ) on resting membrane potential can be predicted theoretically.

It appears that the ions affect vascular resistance to flow through their ability to alter the transmembrane electrical potential difference of vascular smooth muscle cells in precapillary blood vessels (primarily arterioles). Variations in membrane potential normally produce subsequent changes in the tension developed by the vascular smooth muscle, thereby altering blood vessel diameter and thus resistance to flow.

In order to examine the mechanisms of the effects of ions on resistance to blood flow, it is useful to establish the relationship between resting membrane potential and vascular resistance. Then the experimental quantitative and transient effects of ions on vascular resistance may be compared with the theoretically predicted effects.

## RELATIONSHIP BETWEEN RESTING MEMBRANE POTENTIAL AND VASCULAR RESISTANCE TO BLOOD FLOW

The relationship between membrane potential of vascular smooth muscle cells in the walls of the arterioles and resistance to blood flow is not simple(79,80). Altering extracellular ion concentrations produces changes in the membrane potentials of the vascular smooth muscle cell, including changes in resting membrane potential as well as changes in frequency, duration, slope and height of the action potentials. It is well established that a change in cell potential is normally associated with a change in the contractile state of vascular smooth muscle, i.e., hyperpolarization is associated with relaxation and hypopolarization with constriction.

This relationship is illustrated in Figure 42, which is a graph of simultaneously recorded tension in grams (g) and membrane potential of intestinal smooth muscle made by Bulbring(17). Note that even though action potentials were occurring, tension changed almost exactly as resting membrane potential changed. Figure 43 is another graph made by Bulbring(17) which shows that tension is approximately linearly related to resting potential. Bulbring (and others) also showed that tension correlated well with frequency of

Membrane Potential

mV 30

50

g 5—

4—

Tension

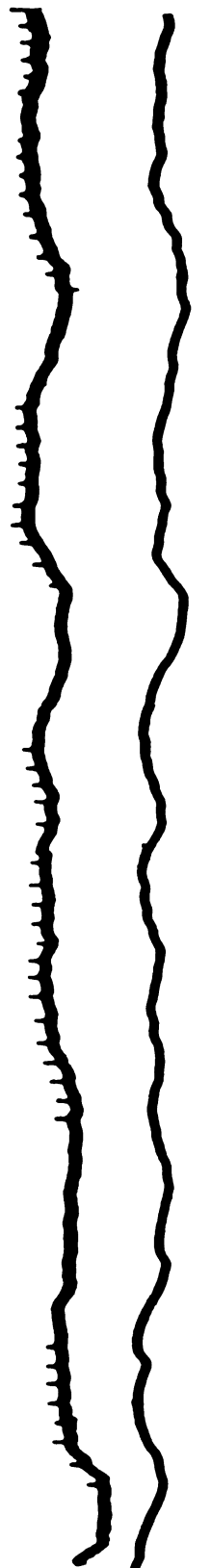


Figure 42. Changes in smooth muscle tension as a function of membrane potential.



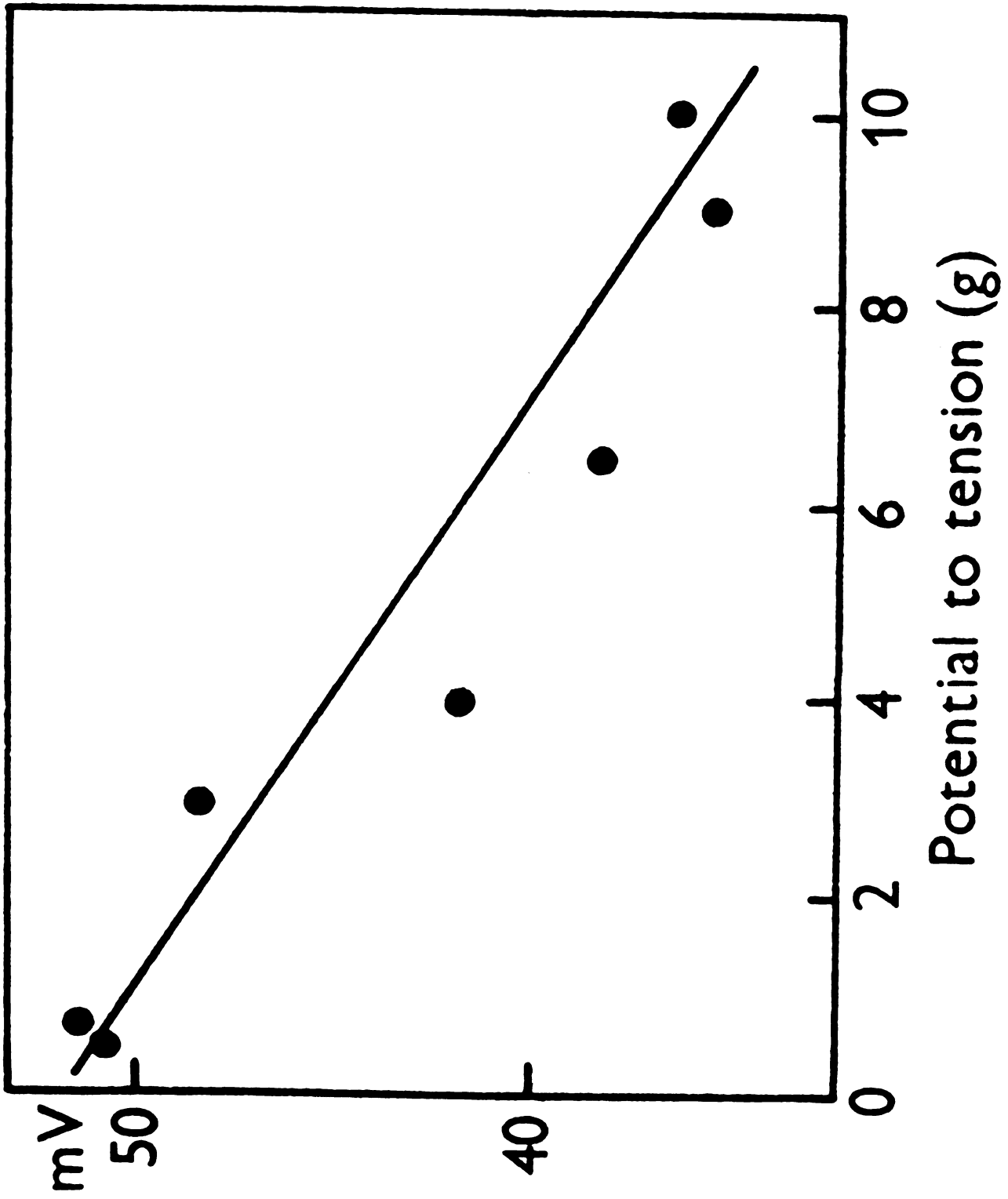


Figure 43. Changes in resting membrane potential as a function of tension.

action potentials. However, since action potential frequency is often a function of resting potential, a very simplified approach is to assume that muscle tension is linearly related to resting membrane potential. Since blood vessels are compliant, any change in tension alters luminal diameter of the vessel and thus alters resistance. However, it is also possible that tension changes will open or close some of the vessels in a vascular bed(19). Because of this complication, it will be assumed that vascular resistance is linearly related to resting membrane potential. With this assumption, the experimental changes in resistance will now be compared with the changes in resting membrane potential predicted through use of the model developed in PART I of this thesis.

## MECHANISM OF THE EFFECTS OF $K^+$ ON VASCULAR RESISTANCE

An elevation of potassium ion concentration over the range of 4 to 10 mEq/liter in the blood perfusing a vascular bed produces a decrease in vascular resistance(25,26,32,45, 46,53,61,62,72,73,75,77,83) due to relaxation of vascular smooth muscle. Reduction of the plasma potassium ion concentration produces an increase in resistance(4,5,11,13, 44,45,61,70,75) attributable to smooth muscle contraction. Thus over the range of 0 to 10 mEq/liter, the potassium ion is a vasodilator. These changes in resistance are opposite to those predicted from either the Nernst or the Goldman equation and thus the mechanism of the vasodilation has been unknown. However, we recently proposed that this dilation is due to the effects of  $K^+$  on the electrogenic Na-K pump located in the membrane of the vascular smooth muscle cells(5,11,13,25).

In order to test this hypothesis, we examined the resistance response of the canine gracilis muscle to hypokalemic and hyperkalemic perfusion before and after administration of ouabain, a well known inhibitor of the Na-K ATPase which supplies energy to the Na-K pump(34,92). If changing the  $[K^+]_e$  does indeed alter resistance through

its effect on the electrogenic Na-K pump, then after blockage of the active transport of  $\text{Na}^+$  and  $\text{K}^+$ , the changes in  $[\text{K}^+]$  would be expected to have little effect on vascular resistance or even have an effect opposite to that observed before inhibition of the Na-K pump (i.e., resistance changes should be predictable with the Goldman equation).

Figure 44 shows that ouabain completely inhibited the vascular response to hypokalemia. Indeed, in 4 of 12 animals the response to hypokalemia was actually reversed when compared to the preouabain response.

Figure 45 shows that the fall in perfusion pressure produced by hyperkalemia was greatly attenuated after ouabain. In 5 of 12 animals the fall in perfusion pressure produced by hyperkalemia was converted to a rise after ouabain.

Plasma osmolality and hematocrit were not altered by the dialyzer and were constant throughout the experiment. In these experiments, the vasculature was not dead since it still responded normally to norepinephrine, acetylcholine and adenosine.

Similar experiments were performed on four isolated canine forelimbs also at constant flow. The preparation used permitted separation of skin and muscle outflow(74). Hypokalemia increased resistance proportionately in both vascular beds. Ouabain blocked the response to hypokalemia and greatly attenuated the response to hyperkalemia.

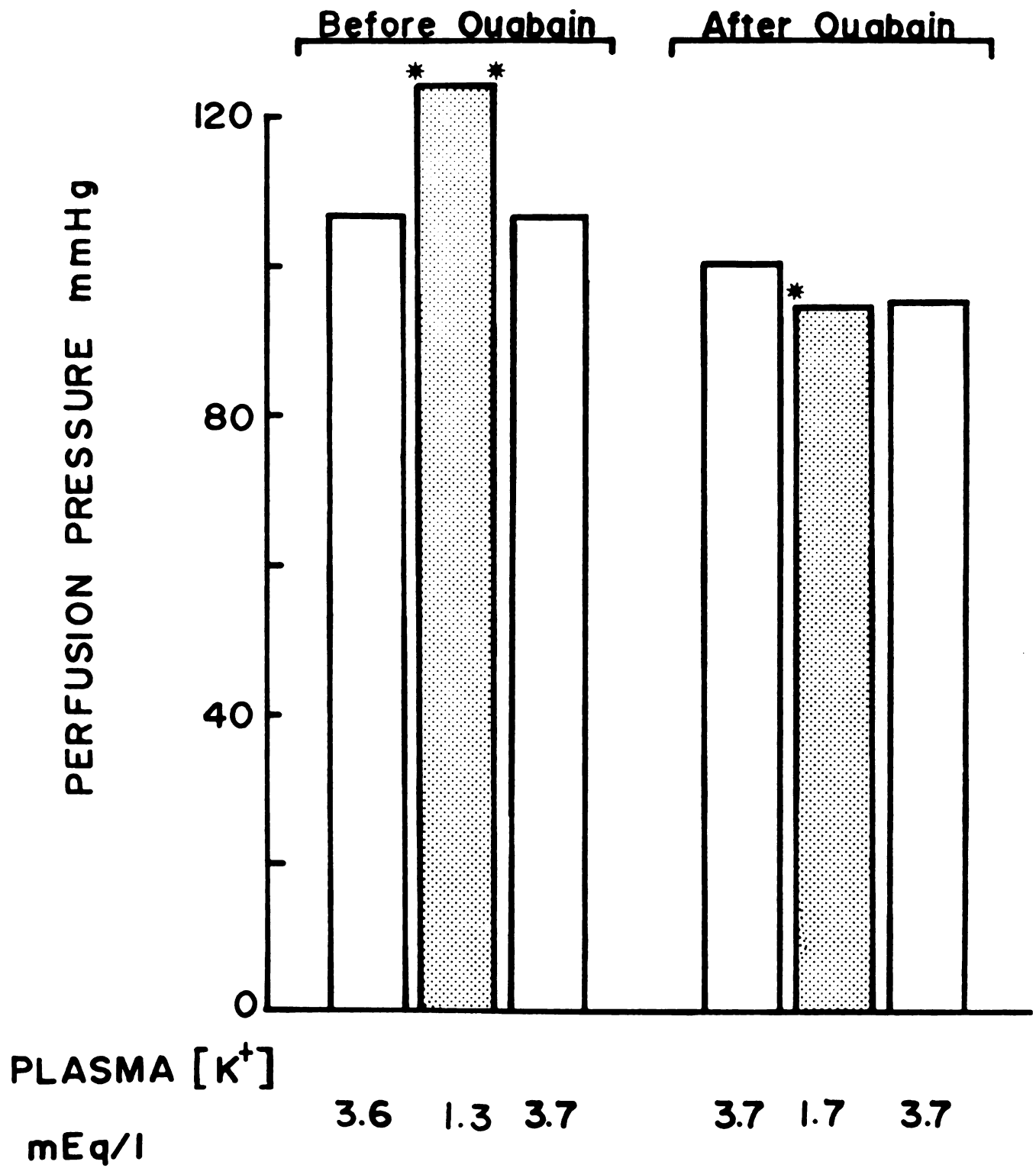


Figure 44. Average effects ( $n=12$ ) of ouabain on skeletal muscle vascular response to hypokalemia.

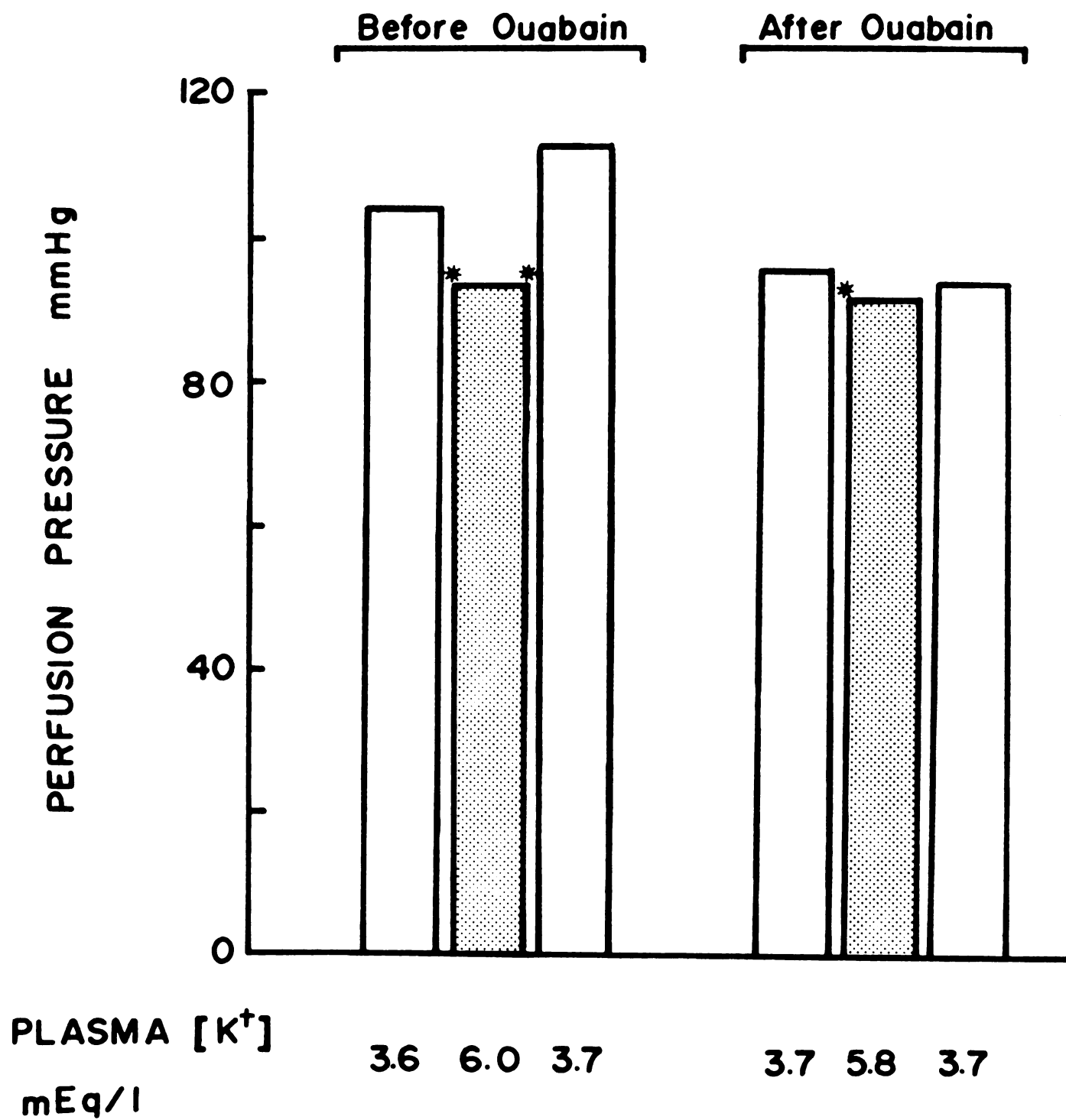


Figure 45. Average effects ( $n=12$ ) of ouabain on skeletal muscle vascular response to hyperkalemia.

Analysis of these in vivo data in view of the data presented in PART I of this thesis leads to the conclusion that deviations in the plasma  $[K^+]$  either below or moderately above normal do indeed alter resistance to flow through their effect on the electrogenic Na-K pump.

Figure 46 is a graph of the experimental effects of varying  $[K^+]$  on gracilis muscle vascular resistance (Fig. 23). The graph includes the resting membrane potential calculated through use of the model for the cell represented in Table 1, assuming a pump exchange ratio of 1.7 Na ions per K ion. The line represents the calculated potentials a few seconds after step changes in the  $K_e^+$  concentrations have been made. Note that there is excellent agreement between the calculated resting potentials and observed changes in resistance.

The transient effects on vascular resistance of altering the arterial plasma  $[K^+]$  should also be predictable. Figure 47 shows the calculated transient effects of a 2 mEq/l increase and decrease in the  $[K^+]_e$  on resting membrane potential. Initially increasing the  $[K^+]$  produces a hyperpolarization followed by a gradual depolarization as the increased rate of  $Na^+$  extrusion lowers the  $[Na^+]_i$  and thus slows the electrogenic pump. The opposite changes in potential are predicted when the  $[K^+]_e$  is reduced. However, note that with an increased  $[K^+]$ , the initial hyperpolarization is gradually replaced with a depolarization whereas with a reduced  $[K^+]$  the membrane potential does not completely return to its initial value. After 10 minutes,

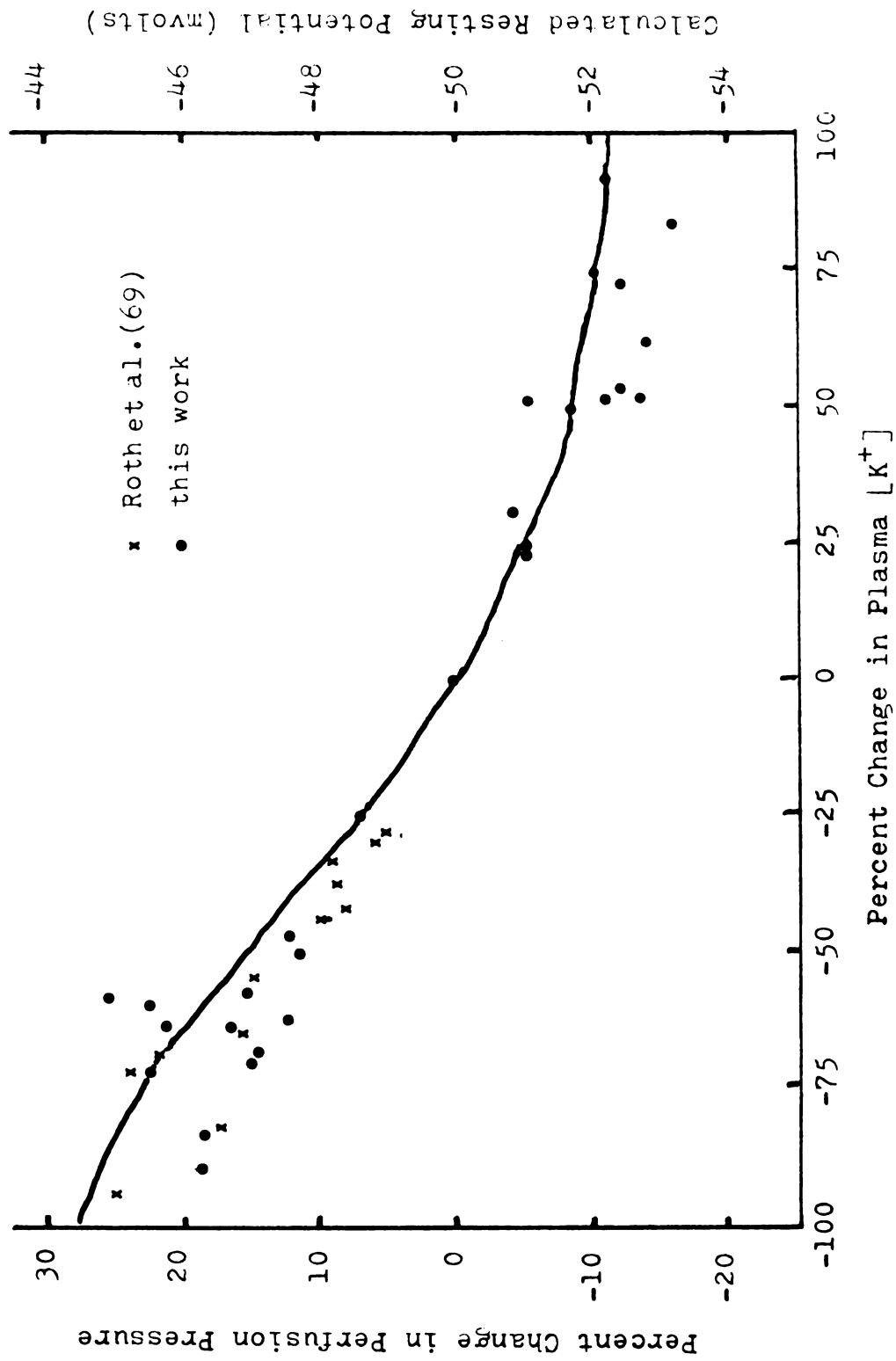


Figure 46. Predicted and experimental changes in resistance produced by altered plasma potassium ion concentration.



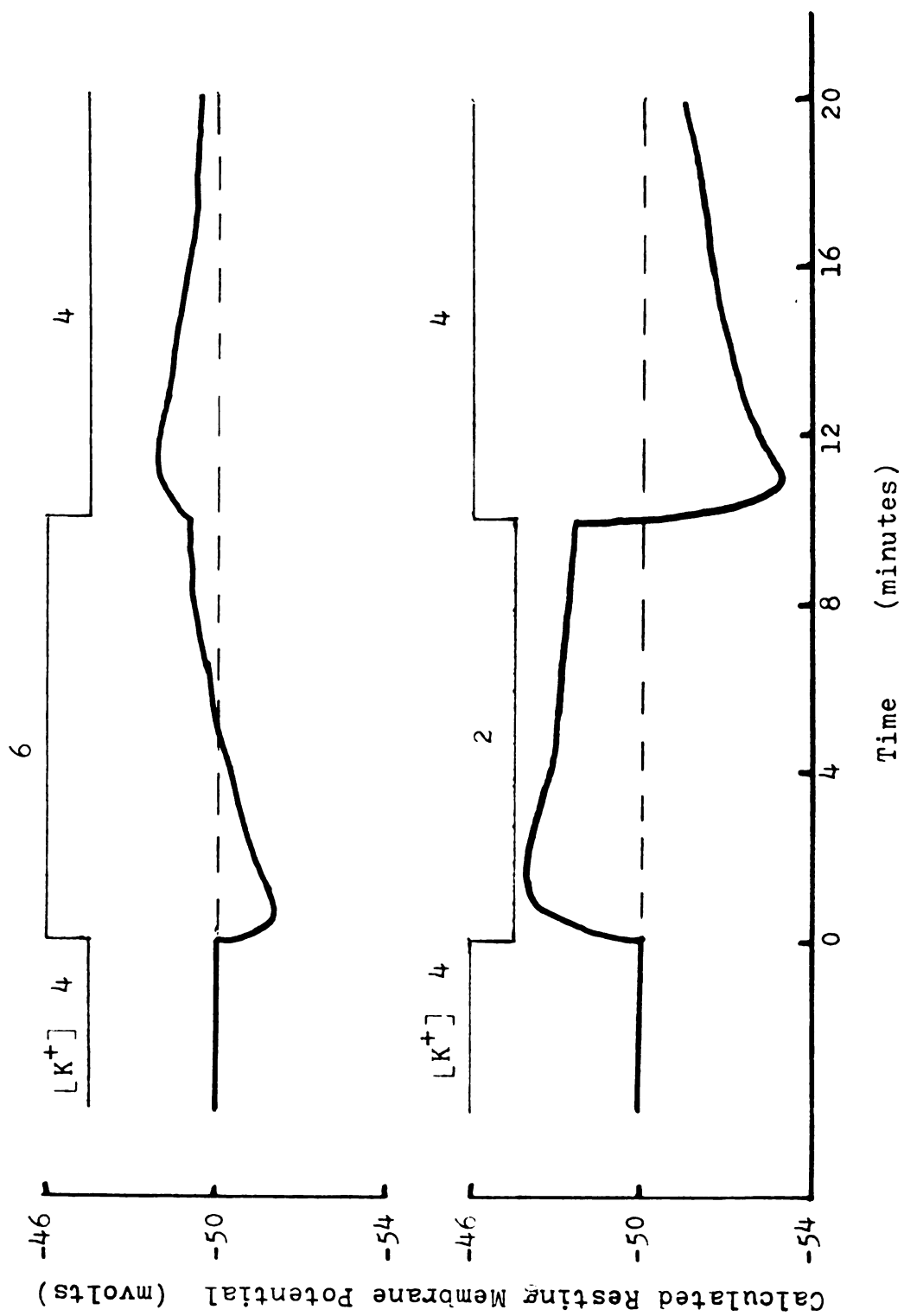


Figure 47. Calculated transient changes in resting potential with increased and decreased potassium ion concentration.

the  $K^+$  concentrations were returned to the initial 4 mEq/l and the opposite changes in calculated potential occurred.

Compare these calculated effects with the average (n=2) experimental changes in perfusion pressure in the canine forelimb produced by raising and lowering the  $[K^+]$  of the perfusing blood (Figure 48). Also see Figure 22. With hyperkalemia, resistance initially decreased as expected and then gradually increased until resistance was above control. Upon returning the  $[K^+]$  to normal, resistance increased further before declining. With hypokalemia, the opposite changes in resistance occurred. Resistance initially increased and then waned slightly with time. Upon returning to the control dialysate, resistance fell to a value slightly less than the control value and then slowly increased. Note that the experimental resistance does follow the predicted patterns and there is good general agreement. Some of the disagreement may be due to the fact that simulated step changes in concentration at the cell surfaces do not adequately represent the experimental changes in  $[K^+]$  at the surface of the vascular smooth muscle cells. In addition, resistance is above control after hypokalemia and this is not predicted.

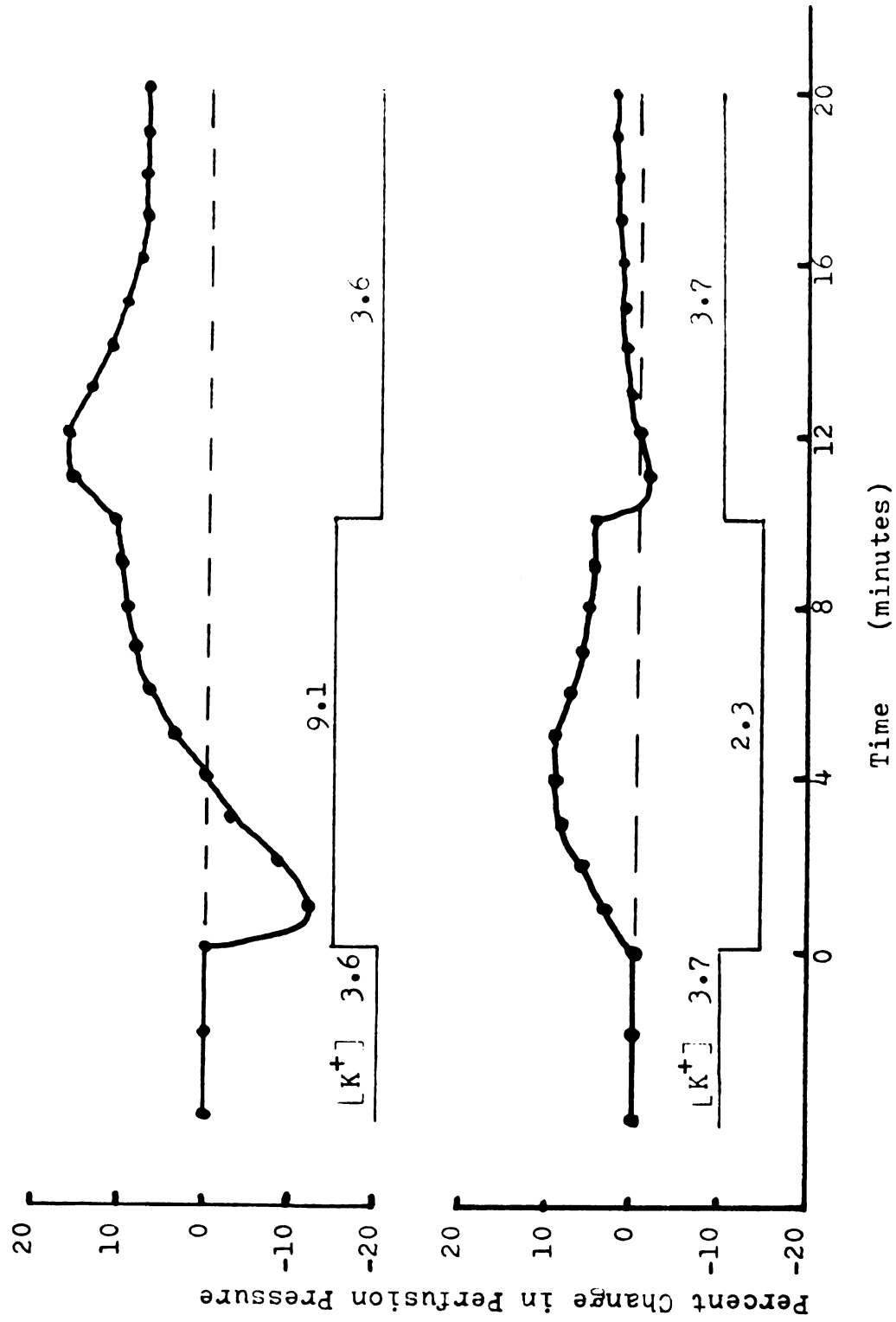


Figure 48. Transient changes in forelimb perfusion pressure produced by hypo- and hyperkalemic perfusion during constant flow.

## MECHANISM OF THE EFFECT OF OUABAIN ON VASCULAR RESISTANCE

Ouabain is a cardiac glycoside which is well known for its ability to inhibit the active transport of the Na-K pump. Since the Na-K pump in vascular smooth muscle cells appears to be electrogenic, any slowing of it should partially depolarize the cell membrane and lead to an increase in resistance to blood flow. These studies show that this is indeed the case in skeletal muscle(25), forelimb(25), and coronary(13) vascular beds. This adds further support to the hypothesis that the Na-K pump in vascular smooth muscle is electrogenic. In addition, we found the effects of ouabain to be biphasic. Initially, ouabain administration produced an increase in resistance which reached a maximum in an average of 6 to 8 minutes and then resistance slowly decreased with time even though the ouabain infusion continued at a constant rate.

The filled circles in Figure 49 represent the average response ( $n=6$ ) of the coronary vascular bed to a continuous infusion of ouabain (12  $\mu\text{g}/\text{min}$ ). Resistance increased by 30% in 6 minutes and then decreased to a 20% increase by the end of 14 minutes. The solid line represents the calculated resting potential during ouabain infusion.

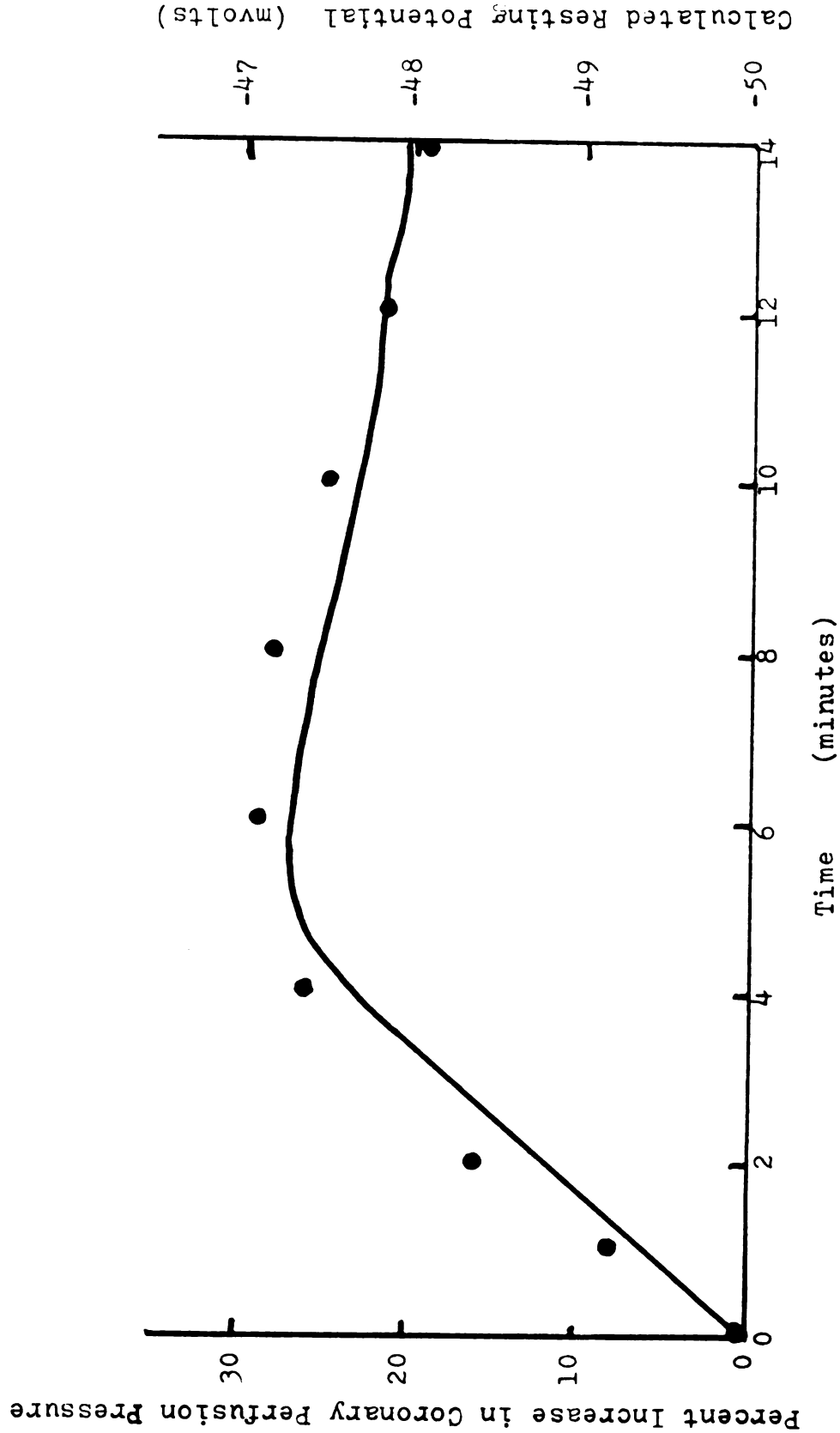


Figure 49. Calculated and Experimental Effects of Ouabain on Coronary Vascular Resistance during Constant Flow Perfusion of Left Common Coronary Artery.

It is well established that ouabain is only partially effective in blocking active transport by the Na-K pump, depending on ouabain concentration(92). In order to calculate changes in cell potential, it was assumed that the ouabain concentration used in the experiments was 50% effective in blocking the Na-K pump and the inhibition proceeded linearly with maximal ouabain binding at 5 minutes. The calculation shows that the initial resistance increase with ouabain administration is due directly to slowing of the electrogenic pump. When the pump is slowed, the rate of  $\text{Na}^+$  extrusion from the cell is reduced, with a resultant gradual increase in the  $[\text{Na}^+]_i$  because of passive diffusion of  $\text{Na}^+$  into the cell. The decrease in resistance after 6 minutes appears to be due to the stimulating effect which the slowly increasing  $[\text{Na}^+]_i$  has on the electrogenic pump. As the  $[\text{Na}^+]_i$  increases, the electrogenic pump operates at a faster rate and causes the cell membrane to gradually repolarize with a resultant decrease in vascular resistnace.

With this explanation of the secondary fall in resistance during ouabain infusion, it is assumed that the ouabain concentration used in the experiments was sufficiently low so that the Na-K pump was not completely inhibited and thus the increase in  $[\text{Na}^+]_i$  was effective in stimulating the pump. There are several points which indicate that this may be the case: 1) The vascular response to hypokalemia and hyperkalemia was gradually reduced during the infusion.

If the ouabain had completely inhibited the pump, the vascular responses to  $[K^+]$  changes would have been rapidly blocked. 2) In several experiments, the response to hypokalemia and hyperkalemia was not completely blocked. 3) Toward the end of the ouabain infusions, the vasculature appeared more responsive to increases in  $[K^+]$  than to decreases in  $[K^+]$ , indicating that the ouabain concentration was low enough so that  $K^+$  could still compete for the binding sites. 4) Upon terminating the ouabain infusion, the vasculature appeared to regain its sensitivity to changes in the plasma  $[K^+]$ . Thus the above explanation of the secondary fall in resistance during ouabain infusion appears to represent the actual processes which alter resistance.

## MECHANISM OF THE EFFECT OF OSMOLALITY ON VASCULAR RESISTANCE

Vascular resistance to blood flow varies inversely with osmolality as the plasma osmolality is raised or lowered(14,61,76,81). With increased osmolality, it was suggested that the observed change in resistance does not depend on the agent since NaCl,  $\text{Na}_2\text{SO}_4$ , or dextrose each produce essentially the same change in resistance(61). However, a more recent study by Radawski(68) suggests that arterial infusion of hyperosmotic glucose produced a greater decrease in resistance than infusion of hyperosmotic NaCl. During either constant flow or constant pressure perfusion of the gracilis muscle, the decrease in resistance was greater in 4 of 5 animals during hyperosmotic glucose (900 mOsm/kg) infusion than during hyperosmotic NaCl infusion at infusion rates of 0.38 ml/min and 0.76 ml/min. (See Table 12.)

There are two main factors contributing to the changes in resistance which occur when the plasma osmolality of the blood perfusing an organ is altered: 1) change in blood vessel geometry, and 2) change in blood viscosity. Cell-free perfusion studies indicate that most of the change in resistance is not produced by changes in blood viscosity(81).



Thus the changes in resistance are primarily due to changes in geometry.

With a change in plasma osmolality, there are passive and active changes in blood vessel diameter (for a detailed discussion see Gazitua et al.(35,36)). With reduced osmolality, swelling of endothelial and vascular smooth muscle cells into the blood vessel lumen passively decreases vessel caliber and hence raises resistance. Also, resistance may increase due to active vasoconstriction subsequent to the shift of water. During hyperosmolal perfusion, the opposite effects reduce resistance to flow.

Calculations with the "model" show that hypoosmolality is expected to actively increase vascular resistance and hyperosmolality expected to actively decrease resistance. With hypoosmolality, the gain in cell water reduces the  $[K^+]_i$  and  $[Na^+]_i$ , reducing the passive  $K^+$  efflux and slowing the electrogenic pump. Both of these effects tend to depolarize the cell membrane and thus produce active vasoconstriction.

Figure 50 shows that calculated resting membrane potential (for the cell of Table 1) decreases approximately linearly as osmolality is lowered from 300 to 200 mOsm/kg by NaCl removal from the bathing fluid. This prediction agrees with the experimental changes in resistance as was seen in Figure 32. In addition, the calculated cell volume increased linearly as osmolality was reduced.

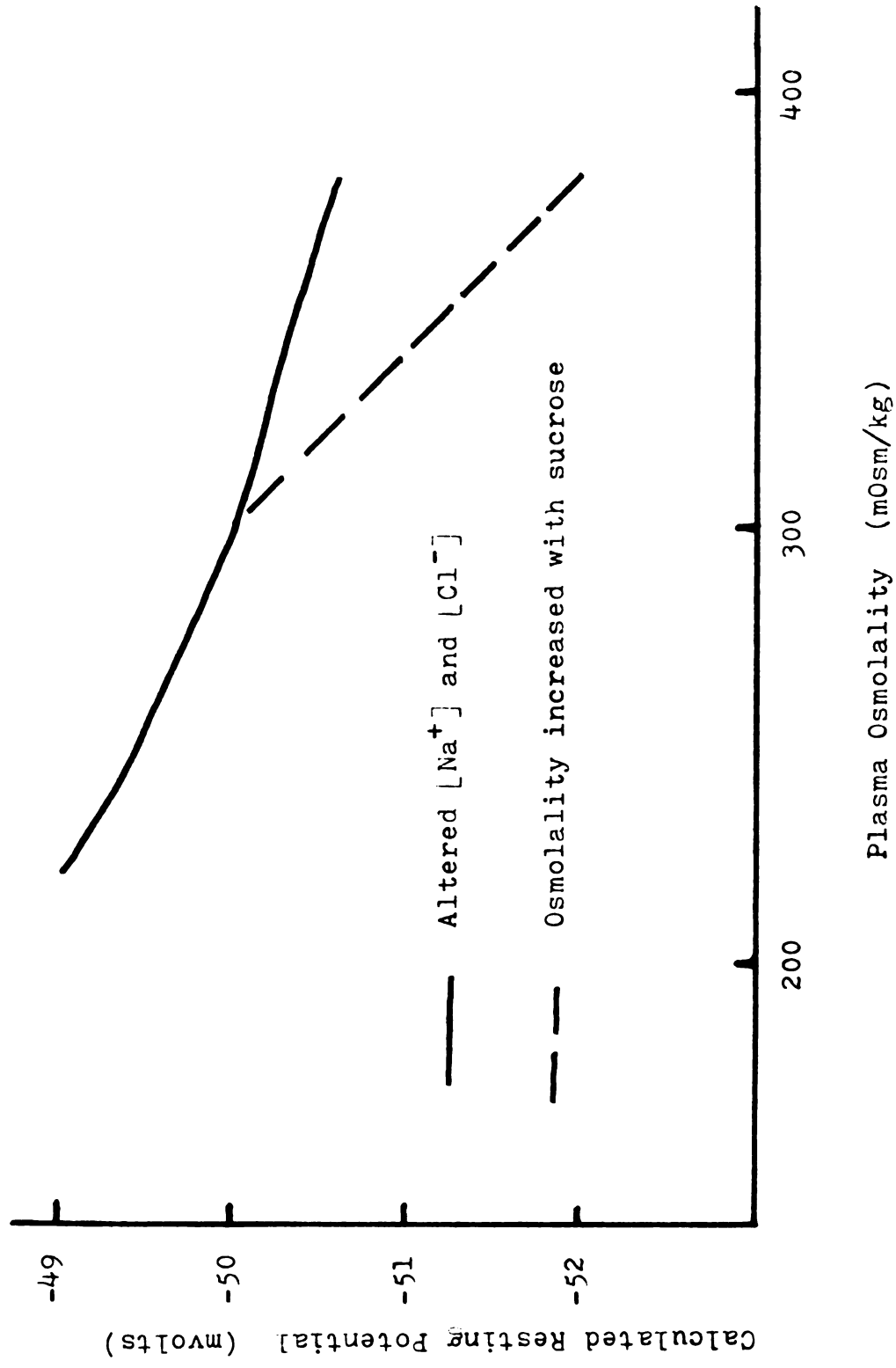


Figure 50. Calculated effects of osmolality on vascular smooth muscle resting membrane potential.



Figure 50 also shows the calculated resting potential when osmolality is increased with NaCl (solid line) or with a nonpermeating molecule such as sucrose (dashed line). This suggests that the active decrease in resistance during hyperosmolality should be agent dependent as seen by the fact that the calculated hyperpolarization was greater when osmolality was increased with sucrose than with NaCl. (The differences in calculated potentials are due to the effects of  $[Na^+]_e$  and  $[Cl^-]_e$  on passive  $Na^+$  and  $Cl^-$  fluxes.) This prediction is in agreement with Radawski's data (Table 12) where infusion of hyperosmotic glucose produced approximately a 12% greater decrease in resistance during constant flow perfusion of the gracilis muscle than during infusion of the same amount of hyperosmotic NaCl. Eventhough this data suggest that the changes in resistance during hyperosmotic perfusion of a vascular bed is agent dependent, the data are not conclusive since the differences in resistance were significant only during the constant perfusion pressure experiments (Table 12).

It is difficult to separate the contribution of the passive and active changes in resistance which occur when plasma osmolality is altered. However, the calculated potential changes are relatively small, suggesting that passive changes in resistance may be the major contribution to total resistance changes. This may not be true in the kidney since the kidney response to hypoosmolal perfusion is much greater than that of skeletal muscle(35) and Gazitua

et al.(35,36) concluded that most of the increase in renal resistance was due to active vasoconstriction. Perhaps some other mechanisms are involved in the kidney.

## DISCUSSION OF MECHANISMS WHICH ALTER VASCULAR RESISTANCE

The mechanisms of the effects of potassium, ouabain and osmolality on vascular resistance to blood flow can be explained by the changes in resting membrane potential which are produced by each agent. When the plasma  $[K^+]_e$  of the blood perfusing an organ is altered from the normal 4 mEq/l over the range of 0 to 10 mEq/l, the initial change in resistance is due to the effects of  $[K^+]_e$  on the electrogenic Na-K pump. Increasing the  $[K^+]_e$  stimulates the Na-K pump, causing the vascular smooth muscle cells to hyperpolarize and thus produces vasodilation. Lowering  $[K^+]_e$  does the opposite. Furthermore, the transient changes in vascular resistance are explainable in terms of the effects produced by changes in the  $[Na^+]_i$ . The initial fall in resistance with hyperkalemia is followed by a gradual increase in resistance. This is caused by the decreasing  $[Na^+]_i$  slowing the electrogenic pump which gradually depolarizes the cell membrane. ( $[Na^+]_i$  decreases since the high  $[K^+]_e$  stimulates the rate of  $Na^+$  extrusion by the Na-K pump.)

The effects of altered plasma  $[K^+]_e$  on resistance is explained only in terms of the electrogenic pump. Other suggested mechanisms are not consistent with all observed

changes in vascular resistance. For example, it has been suggested that with an electroneutral Na-K pump, a moderate elevation in  $[K^+]$  would cause vascular smooth muscle cells to hyperpolarize and thus produce vasodilation since the increased rate of  $Na^+$  extrusion by the pump lowers the  $[Na^+]_i$  and produces hyperpolarization as suggested by the Goldman equation. Similarly, hypokalemia would increase resistance since the slowed  $Na^+$  extrusion caused  $[Na^+]_i$  to increase and depolarization results as suggested by the Goldman equation. It can be seen this this proposed mechanism is not adequate since intracellular ion concentrations do not change as rapidly as resistance is observed to change. Furthermore, hyperkalemia would be expected to produce a continual decrease in vascular resistance as the  $[Na^+]_i$  declined, whereas resistance acutally increases after the initial decrease.

The initial increase in vascular resistance observed during ouabain administration is expected since the electrogenic Na-K pump is slowed by ouabain, causing the vascular smooth muscle cells to depolarize. However, the mechanisms which produce the secondary fall in resistance after 5-10 minutes of ouabain infusion are not well understood. This change was explained by assuming that the increase in  $[Na^+]_i$  caused by reduced extrusion was effective in stimulating the electrogenic Na-K pump. It can be questioned whether the Na-K pump can still be stimulated in the presence of

ouabain. With the infusion rates used in the experiments, the blood ouabain concentration (approximately  $2 \times 10^{-7}$  molar) would cause only partial inhibition of the Na-K pump. The uninhibited fraction would respond to an increased  $[\text{Na}^+]_i$  by increasing the pumping rate. Furthermore, J.F. Hoffmann (private discussion) showed that high  $[\text{Na}^+]_i$  reduces the rate of ouabain inhibition. Depending on the mechanism of ouabain inhibition, it is possible that an increasing  $[\text{Na}^+]_i$  may be effective in reversing some of the ouabain inhibition at low ouabain concentrations. Thus it appears that the secondary fall in vascular resistance during ouabain infusion is due to a stimulation of the electrogenic pump by the elevated  $[\text{Na}^+]_i$ . This results in hyperpolarization of the vascular smooth muscle cells and reduces resistance to blood flow.

The mechanisms which alter resistance when plasma osmolality is varied are somewhat more complicated since both passive and active changes in resistance occur(35,36). Swelling or shrinking of smooth muscle and endothelial cells passively alters blood vessel diameter. Active changes in resistance appear to be produced by changes in intracellular ion concentrations. With hypoosmolality, the gain in cell water reduces the  $[\text{Na}^+]_i$  and  $[\text{K}^+]_i$ . Depolarization of the vascular smooth muscle cells and hence increased resistance results since the electrogenic pump is slowed by the reduced  $[\text{Na}^+]_i$  and the passive  $\text{K}^+$  efflux is reduced



by the low  $[K^+]_i$ . Both of these effects contribute to the depolarization.

Calculations with the computer model and Radawski's data (Table 12) suggests that the changes in vascular resistance during hyperosmotic perfusion of a vascular bed are agent dependent. Further experiments are necessary in order to determine whether this is indeed the case.

## SUMMARY AND CONCLUSIONS

The purposes of this study were to 1) develop a general method of calculation that would accurately predict the appropriate directional and transient changes in resting membrane potential as functions of extracellular ion concentrations, 2) determine quantitatively the effects of changes in plasma ionic composition on vascular resistance to blood flow, and 3) use the method of predicting resting potentials to predict, and thus offer an explanation of, the mechanisms involved in observed change in resistance to blood flow when the concentration of an ion in the blood plasma is acutely varied.

The effects on resting membrane potential of varying  $[K^+]_e$ ,  $[Na^+]_e$ ,  $[Cl^-]_e$  or extracellular osmolality are predicted for several cell types with a computer model that was developed for this study. It was concluded that the model accurately represented the passive and active fluxes of ions across the cell membrane. Furthermore, the mechanisms which produce the changes in cell membrane potential were investigated with the computer model. It was concluded that the electrogenic Na-K pump plays a very important role in determining membrane potential and that the

transient changes in resting potential could be calculated only when the electrogenic character of the Na-K pump was introduced.

The quantitative and transient effects of altering arterial plasma  $[K^+]$  and osmolality on vascular resistance to blood flow were examined in the coronary and skeletal muscle vascular beds of the dog. Hypokalemic perfusion of the left common coronary artery caused large, rapid increases in left ventricular contractile force and coronary vascular resistance. The increases in resistance to blood flow caused by hypokalemia and decreases in resistance caused by hyperkalemia are abolished after ouabain administration in the gracilis muscle and coronary vascular beds. Ouabain infusion produced an increase in resistance which reached a maximum in approximately 5-10 minutes and then resistance decreased even though the infusion continued. In addition, vascular resistance increased linearly as plasma osmolality was reduced in the gracilis muscle vascular bed. A 10% decrease in osmolality produced a 20% increase in resistance. Hypoosmotic perfusion of the coronary artery caused an increase in coronary vascular resistance and myocardial contractile force, and decreased the QT interval.

It was concluded that the changes in resistance produced by altered arterial plasma  $[K^+]$  over the range of 0-10 mEq/l are opposite to those predicted from the Nernst and Goldman equations because of the effects of  $[K^+]_e$  on the electrogenic Na-K pump. Lowering the  $[K^+]_e$  slows the

electrogenic Na-K pump and depolarizes the vascular smooth muscle cells, thus increasing resistance to flow. Elevating the  $[K^+]_e$  up to 10 mEq/l reduces vascular resistance since the increase in  $[K^+]_e$  stimulates the electrogenic pump and hyperpolarizes the cells. The transient changes in resistance produced by hypokalemia and hyperkalemia are predictable and were shown to be produced by changes in the  $[Na^+]_i$ . In addition, the transient effects of ouabain on resistance are predicted. Initially, ouabain administration increases resistance by partially inhibiting the electrogenic pump and depolarizing the cell membrane. The decrease in resistance after 5-10 minutes of ouabain infusion appears to be produced by an increasing  $[Na^+]_i$  stimulating the pump. Furthermore, altering plasma osmolality produces active and passive changes in resistance. With low osmolality, vascular smooth muscle and endothelial cells swell due to an osmotic shift of water and thus passively increase resistance. It was concluded that the active increase in resistance results from a depolarization of the vascular smooth muscle cells caused by reduced intracellular ion concentrations, i.e., the lowered  $[Na^+]_i$  slows the electrogenic pump and the reduced  $[K^+]_i$  reduces the passive  $K^+$  efflux. With increased osmolality, calculations indicate that the active changes in resistance should be agent dependent. Increasing osmolality with sucrose produces a greater hyperpolarization than when osmolality is increased with NaCl. This predicted affect of osmotic agent

may indeed occur since it appears that infusion of hyperosmotic glucose produces a greater decrease in resistance than infusion of hyperosmotic NaCl at the same rate.

## RECOMMENDATIONS

It appears that several experimentally observed phenomena may be explained in terms of the electrogenic Na-K pump. This study showed that the transient effects of hypokalemia and hyperkalemia on vascular resistance are predictable. It is recommended that these transient changes in resistance be further examined and the results published since this is new and important information. Furthermore such phenomena as autoregulatory escape and the Bayliss response might be explainable in terms of the effects of the electrogenic pump and permeability changes on resting membrane potential.

It is also recommended that the suggested mechanism of the transient effects of ouabain on resistance be further investigated. If the secondary fall in resistance is due to an increasing  $[Na^+]_i$  stimulating the electrogenic pump, then higher ouabain concentrations should prevent the secondary fall in resistance if the concentration is high enough to completely inhibit the Na-K pump.

The quantitative and transient effects of hyperosmolality on resistance should be further investigated both experimentally and with the model to determine if the changes in resistance during hyperosmotic perfusion are indeed agent

dependent as suggested. A simple experiment would be to compare the transient effects of 5 minute hyperosmotic infusion in the gracilis muscle or forelimb vasculature during constant flow perfusion.

## BIBLIOGRAPHY



## BIBLIOGRAPHY

1. Abe, Y., and T. Tomita. Cable properties of smooth muscle. *J. Physiol.* 196:87-100, 1968.
2. Akiyama, T., and H. Grundfest. The hyperpolarization of frog skeletal muscle fibers induced by removing potassium from bathing medium. *J. Physiol.* 217: 33-60, 1971.
3. Altura, B.M., and B.T. Altura. Influence of magnesium on drug induced contractures and ion content in rabbit aorta. *Am. J. Physiol.* 220:938-944, 1971.
4. Anderson, D.K., R.A. Brace, S.A. Roth, D.P. Radawski, J.B. Scott and F.J. Haddy. Local vascular effects of potassium and magnesium depletion and the role of potassium in active hyperemia. *Vascular smooth muscle*. Ed. E. Betz, Sprivger-Verlag, New York, 1972.
5. Anderson, D.K., S.A. Roth, R.A. Brace, D. Radawski, F.J. Haddy and J.B. Scott. Effect of hypokalemia and hypomagnesemia produced by hemodialysis on skeletal muscle vascular resistance; role of potassium in active hyperemia. *Cir. Res.* 31: 165-173, 1972.
6. Arvill, A., B. Johansson and O. Jonsson. Effects of hyperosmolarity on the volume of vascular smooth muscle cells and the relation between cell volume and muscle activity. *Acta Physiol. Scand.* 75: 484-495, 1969.
7. Babb, A.L., and L. Grimsrud. A new concept in hemodialyzer membrane support. *Trans. Am. Soc. Artificial Organs.* 10:31, 1964.
8. Baetjer, A.B. Relation of potassium to the contraction of mammalian skeletal muscle and its similarity to the effect of sympathetic stimulation. *Am. J. Physiol.* 109:3-4, 1934.

9. Baetjer, A.M. The diffusion of potassium from resting skeletal muscle following a reduction in blood supply. *Am. J. Physiol.* 112:139-151, 1935.
10. Bloor, C.M., D.E. Walker, and R.R. Pensinger. Ouabain induced primary coronary vasoconstriction. *Proc. Soc. Exp. Bio. Med.* 140:1409-1413, 1972.
11. Brace, R.A., J. Scott, W. Chen, D. Anderson, and F. Haddy. Effects of local hypokalemia on myocardial contractile force and coronary resistance. *Proc. 5th Ann. Mtg. Intl. Study Group for Research in Cardiac Metabolism.* Winnipeg, 1972.
12. Brace, R.A., and D.K. Anderson. Predicting transient and steady state changes in resting membrane potential. *J. Appl. Physiol.* In press.
13. Brace, R.A., D.K. Anderson, W.T. Chen, J.B. Scott and F.J. Haddy. Local effects of acute hypokalemia on canine myocardial contractile force and coronary vascular resistance. In preparation.
14. Brace, R.A., J.B. Scott, W.T. Chen, D.K. Anderson, and F.J. Haddy. Local effects of plasma hypoosmolality on canine vascular resistance and myocardium. In preparation.
15. Brading, A.F., and J. Setekleiv. The effect of hypo- and hypertonic solutions on volume and ion distribution of smooth muscle of guinea-pig taenia coli. *J. Physiol.* 195:107-118, 1968.
16. Brennan, F.J., J.L. McCans, M.A. Chiong, and J.O. Parker. Effects of ouabain on myocardial potassium and sodium balances in man. *Cir. Res.* 45:107-113, 1972.
17. Bulbring, E. Correlation between membrane potential, spike discharge and tension in smooth muscle. *J. Physiol.* 128:200-221, 1955.
18. Bulbring, E., and H. Kuriyama. Effects of external sodium and calcium concentrations on spontaneous electrical activity in smooth muscle of guinea-pig taenia coli. *J. Physiol.* 166:29-58, 1963.
19. Burton, A.C. Physiology and biophysics of circulation. Yearbook Medical Publishers, Chicago, 1968.
20. Carpenter, D.O., and B.O. Alving. A contribution of an electrogenic  $\text{Na}^+$  pump to membrane potential in *Aplysia neurone*. *J. Gen. Physiol.* 52:1-21, 1968.

21. Casteels, R. Calculation of the membrane potential in smooth muscle cells of the guinea-pig's taenia coli by the Goldman equation. *J. Physiol.* 205: 193-208, 1969.
22. Casteels, R., G. Droogmans and H. Hendrickx. Electrogenic sodium pump in smooth muscle cells of the guinea-pig's taenia coli. *J. Physiol.* 217:297-313, 1971.
23. Casteels, R. The distribution of chloride ions in smooth muscle cells of the guinea-pig taenia coli. *J. Physiol.* 214:225-243, 1971.
24. Casteels, R., G. Droogmans and H. Hendrickx. Membrane potential of smooth muscle cells in K-free solution. *J. Physiol.* 217:281-295, 1971.
25. Chen, W.T., R. A. Brace, J.B. Scott, D.K. Anderson and F.J. Haddy. The mechanism of the vasodilator action of potassium. *Proc. Soc. Exp. Bio. Med.* 140:820-824, 1972.
26. Chou, C.C., and T.E. Emerson, Jr. Local effects of  $\text{Na}^+$ ,  $\text{K}^+$ ,  $\text{Mg}^{++}$ , and  $\text{Ca}^{++}$  on vascular resistances in dog liver.
27. Claret, M., and J.L. Mazet. Ionic fluxes and permeabilities of cell membrane in rat liver. *J. Physiol.* 223:279-295, 1972.
28. Cole, K.S. Electrodifusion models for the membrane of squid giant axon. *Physiol. Rev.* 45:340-379, 1965.
29. Delahayes, J.F., and E. Bolzer. Effects of drugs on  $^{45}\text{Ca}$  movement in frog ventricle. *Proc. Soc. Exp. Bio. Med.* 141:423-430, 1972.
30. Devi, S.K., R. Moore, N. Davids, A.F. Findeis and R.L. Berger. Simulation of water movement across the cell membrane in a hypertonic medium. *Comput. Biol. Med.* 1:141-153, 1970.
31. Dunham, E.T., and I.M. Glynn. Adenosinetriphosphatase activity and the active movements of alkali metal ions. *J. Physiol.* 156:275-293, 1961.
32. Emanuel, D.A., J.B. Scott and F.J. Haddy. Effect of potassium on small and large blood vessels of the dog forelimb. *Am. J. Physiol.* 197:637-642, 1959.
33. Freund, J.E. Mathematical statistics. Prentice Hall, New York, 1962.

34. Ganong, W.F. Medical physiology. Lange Medical Publications, Los Altos, Calif., 1969.
35. Gazitua, S., J.B. Scott, C.C. Chou and F.J. Haddy. Effect of osmolality on canine renal vascular resistance. Am. J. Physiol. 217:1216-1223, 1969.
36. Gazitua, S., J.B. Scott, B. Swindall and F.J. Haddy. Resistance responses to local changes in plasma osmolality in three vascular beds. Am. J. Physiol. 220:384-391, 1971.
37. Glitsch, H.G., H. Reuter and H. Scholz. The effect of internal sodium concentration on calcium fluxes in guinea-pig auricles. J. Physiol. 209:25-43, 1970.
38. Goldman, D.E. Potential, impedance and rectification in membranes. J. Gen. Physiol. 27:37-60, 1943.
39. Gorman, A.L.G., and M.F. Marmor. Contributions of the sodium pump and ionic gradients to membrane potential of a molluscan neurone. J. Physiol. 210:896-917, 1970.
40. Gorman, A.L.F., and M.F. Marmor. Temperature dependence of the sodium-potassium permeability ratio of a molluscan neurone. J. Physiol. 210:919-931, 1970.
41. Grimsrud, L., and A.L. Babb. Optimization of dialyzer design for the hemodialysis system. Trans. Am. Soc. Artificial Int. Organs. 10:101, 1964.
42. Grimsrud, L. A theoretical and experimental investigation of a parallel-palte dialyzer in the laminar flow regime with applications to hemodialyzer design. Ph.D. Thesis, University of Wash., 1965.
43. Grimsrud, L., and A.L. Babb. Biomechanical and human factors symposium, ASME, New York, 1967.
44. Haddy, F.J., J.B. Scott, M.A. Florio, R.M. Daugherty, Jr., and J.N. Huizenga. Local vascular effects of hypokalemia, alkalosis, hypercalcemia and hypomagnesemia. Am. J. Physiol. 204:202-212, 1963.
45. Haddy, F.J., and J.B. Scott. Effects of electrolytes and water upon resistance to blood flow through intact vascular beds. Electrolytes and cardiovascular diseases. Ed. by E. Bajusz. pp. 383-400, S. Karger, Basel, New York, 1965.

46. Haddy, F.J., and J.B. Scott. Metabolically linked vasoactive chemicals in local regulation of blood flow. *Physiol. Rev.* 48:688-707, 1968.
47. Haddy, F.J., J.B. Scott, D.K. Anderson, R.A. Erace and D.P. Radawski. Effects of hypoosmolality on resistance to blood flow and upon blood pressure. *Vascular smooth muscle*. Ed. E. Betz, Sprivger-Verlag, New York, 1972.
48. Hodgkin, A.L., and B. Katz. The effect of sodium ions on the electrical activity of the giant axon of the squid. *J. Physiol.* 198:37-77, 1949.
49. Hodgkin, A.L., and A.F. Huxley. A quantitative description of membrane current and its application to conduction and excitation in nerve. *J. Physiol.* 117:500-544, 1952.
50. Hodgkin, A.L., and Horowicz. The influence of potassium and chloride ions on the membrane potential of single muscle fibers. *J. Physiol.* 148:127-160, 1959.
51. Johansson, B., and O. Jonsson. Cell volume as a factor influencing electrical and mechanical activity of vascular smooth muscle. *Acta Physiol. Scand.* 72:456-468, 1968.
52. Kerkut, G.A., and R.W. Meech. The effect of ions on the membrane potential of snail neurones. *Comp. Biochem. Physiol.* 20:411-429, 1967.
53. Kjellmer, I., and H. Odelram. The effect of some physiological vasodilators on the vascular bed of skeletal muscle. *Acta Physiol. Scand.* 63:94-102, 1965.
54. Koch-weser, J. Influence of osmolality of perfusate on contractility of mammalian myocardium. *Am. J. Physiol.* 204:957-962, 1963.
55. Kuriyama, H., K. Oshima, and Y. Sakamoto. The membrane properties of the smooth muscle of the guinea-pig portal vein in isotonic and hypertonic solutions. *J. Physiol.* 217:179-199, 1971.
56. Langer, G.A. Effects of digitalis on myocardial ionic exchange. *Circ.* 46:180-186, 1972.
57. Mellander, S., B. Johansson, S. Gray, O. Jonsson, J. Lundavall and B. Ljung. The effects of hyperosmolality on intact and isolated vascular smooth muscle, possible role in exercise hyperemia. *Angiologica* 4:310-322, 1967.

58. Moreton, R.B. An application of the constant-field theory to the behavior of giant neurones of the snail, *Helix Aspersa*. *J. Exp. Biol.* 48:611-623, 1968.
59. Moreton, R.B. An investigation of the electrogenic sodium pump in snail neurone, using the constant-field theory. *J. Exp. Biol.* 51:181-201, 1969.
60. Nagle, F.J., J.B. Scott, B.T. Swindall, and F.J. Haddy. Venous resistances in skeletal muscle and skin during local blood flow regulation. *Am. J. Physiol.* 214:885-891, 1968.
61. Overbeck, H.W., J.I. Molnar, and F.J. Haddy. Resistance to blood flow through the vascular bed of the dog forelimb. *Am. J. Cardiol.* 8:533-541, 1961.
62. Overbeck, H.W. Vascular responses to cations, osmolality and angiotensin in renal hypertensive dogs. *Am. J. Physiol.* 223:1358-1364, 1972.
63. Overbeck, H. W., R.M. Daugherty and F.J. Haddy. Response of the human upper extremity vascular bed to intrabrachial arterial infusions of magnesium sulfate and hypotonic sodium chloride. *Physiologist.* 9:258, 1966.
64. Perry, M.C., and C.N. Hales. Rates of efflux and intracellular concentrations of potassium, sodium and chloride in isolated fat cells from the rat. *Biochem. J.* 115:865-871, 1969.
65. Plonsey, R. Bioelectric phenomena. McGraw-Hill, New York, 1969.
66. Ponder, E. Hemolysis and related phenomena. Green and Stratton, New York, 1948.
67. Prasad, K., and J.C. Callaghan. Effect of replacement of potassium by rubidium on the transmembrane action potential and contractility of human papillary muscle. *Circ. Res.* 24:157-166, 1969.
68. Radawski, D.P. Role of cations and osmolality in local blood flow regulation and in hemorrhage. Ph.D. Thesis. Mich. State U., 1971.
69. Reiter, M., K. Seibel and F.J. Stickel. Sodium dependence of the inotropic effect of reduction in extracellular potassium concentration. *Naunyn-Schmiedebergs Arch. Pharmacol.* 268:361-378, 1971.

70. Roth, S.A., J.B. Scott, F.J. Haddy, D.P Radawski and D.K. Anderson. The use of hemodialysis in the study of the local vascular effects of potassium depletion. Chem. Engr. Symp. Ser. Vol. 67, No. 114, 1971.
71. Ross, J., J.A. Waldhausen and E. Braunwald. Studies on digitalis. J. Clin. Invest. 39:930-942, 1960.
72. Scott, J.B., D. Emanuel and F.J. Haddy. Effect of potassium on renal vascular resistance and urine flow rate. Am. J. Physiol. 193:305-308, 1959.
73. Scott, J.B., E.D. Frohlich, R.A. Hardin and F.J. Haddy.  $\text{Na}^+$ ,  $\text{K}^+$ ,  $\text{Ca}^{++}$ , and  $\text{Mg}^{++}$  action on coronary vascular resistance in the dog heart. Am. J. Physiol. 210:1095-1100, 1961.
74. Scott, J.B., R.M. Daugherty, Jr., and F.J. Haddy. Effects of severe local hypoxia on transcapillary water movement in dog forelimb. Am. J. Physiol. 212: 847-851, 1967.
75. Scott, J.B., R.M. Daugherty, Jr., H.W. Overbeck and F.J. Haddy. Vascular effects of ions. Fed. Proc. 27:1403-1407, 1968.
76. Scott, J.B., R.A. Brace, D.K. Anderson and F.J. Haddy. Effects of hypoosmolality and hyponatremia on resistance to flow through skeletal muscle. Physiologist. Vol. 14, No. 3, 1971.
77. Skinner, N.S., and W.J. Powell, Jr. Action of oxygen and potassium on vascular resistance of dog skeletal muscle. Am. J. Physiol. 212:533-540, 1967.
78. Somlyo, A.P., and A.V. Somlyo. Vascular smooth muscle. Pharm. Rev. 20:197-272, 1968.
79. Somlyo, A.V., and A.P. Somlyo. Electromechanical and mechanoelectrical coupling in vascular smooth muscle. J. Pharm. Exptl. Ther. 159, 1968.
80. Somlyo, A.V., and A.P. Somlyo. Electromechanical and pharmomechanical coupling in vascular smooth muscle. J. Pharm. Exptl. Ther. 159:129-145, 1968.
81. Stainsby, W.N., and M.J. Fregly. Effect of osmolality on resistance to blood flow through skeletal muscle. Proc. Soc. Exp. Bio. Med. 128:284-287, 1968.
82. Surawicz, B., E. Lepeschkin, H.C. Herrlich and B.F. Hoffman. Effect of potassium and calcium deficiency on the monophasic action potential, electrocardiogram and contractility of isolated rabbit hearts. Am. J. Physiol. 196:1302-1307, 1959.

83. Textor, E.C., Jr., H.C. Laureta, E.D. Frohlich and C.C. Chou. Effects of major cations on gastric and mesenteric vascular resistances. *Am. J. Physiol.* 212:569-573, 1967.
84. Thomas, R.C. Membrane current and intracellular sodium changes in snail neurone during extrusion of injected sodium. *J. Physiol.* 201:495-514, 1969.
85. Thomas, R.C. Intracellular sodium activity and the sodium pump in snail neurone. *J. Physiol.* 220:55-71, 1972.
86. Thomas, R.C. Electrogenic sodium pump in nerve and muscle cells. *Physiol. Rev.* 52:563-594, 1972.
87. Tomita, T. Electrical responses of smooth muscle to external stimulation in hypertonic solution. *J. Physiol.* 183:450-468, 1966.
88. Tomita, T., and T. Yamamoto. Effects of removing the external potassium of the smooth muscle of guinea-pig taenia coli. *J. Physiol.* 212: 851-868, 1971.
89. Waddel, W.J., and R.G. Bates. Intracellular pH. *Physiol. Rev.* 49:285-329, 1969.
90. Weidmann, S. *Elektrophysiologie der herzmuskelfaser.* Bern, Huber, 1956.
91. Whittam, R., and M.E. Ager. The connexion between active cation transport and metabolism in erythrocytes. *Biochem. J.* 97:214-227, 1965.
92. Whittam, R., and K.P. Wheeler. Transport across cell membranes. *Ann. Rev. Physiol.* 32:21-60, 1970.
93. Zelman, A., and H.H. Shih. The constant field approximation: numerical evaluation for monovalent ions migrating across a homogeneous membrane. *Biophys. Soc. Absts.* p. 264, 1972.



APPENDIX: TABULATED DATA

Table 4. Effects of altering plasma  $[K^+]$  on gracilis muscle perfusion pressure.

Exp. No.	% $\Delta[K^+]$	% $\Delta P$	% $\Delta[K^+]$	% $\Delta P$
1	-58	15.2		
2	-64	15		
3	-63	21	53	-12
6			51	-11
8	-60	22.6	51	-13.7
9	-61	12.2	31	- 4.5
10	-46	12	51	- 5.2
11	-64	16.2	62	-14.3
12			24	- 5
13	-70	15	91	-11.3
14	-58	25.5		
15			84	-16
16	-69	14.4	72	-12.1
17	-83	18.2		
18	-72	22.6		
*	-44	10.3		
*	-64	15.8		
*	-68	21.8		
*	-31	5.9		
*	-34	9.35		
*	-37.5	8.9		
*	-39.6	7.9		
*	-29	5.2		
*	-55	15.2		
*	-72	24.2		
*	-81.6	17.6		
*	-96	25.1		
*	-89	18.4		
*	-82.8	18.2		
*	-72.2	22.6		

\* Roth et al.(70)

Table 5. Effects of reduced plasma  $[K^+]$  on coronary perfusion pressure and heart.\*

Exp. No.	% $\Delta [K^+]$	pre ouabain		post ouabain		pre ouabain		post ouabain		pre ouabain		post ouabain	
		% $\Delta$ PP		% $\Delta$ SP		% $\Delta$ CF		% $\Delta$ QT		% $\Delta$ R			
1	-78	30.4		6.0		65		21.4		0			
3	-21.6 -40.5	10.0 11.3		6.2 2.6		9 18		- 8.3 1.4		-6.5 -4.5			
5	-30.6 -72.2	34.5 77.7		4.7 9.3		45 149							
6	-16.7 -73.3	33.2 75.2	6.2	2.4 -1.3	-11.1	51 220	13.3	0 24.5		2.1 -3.4			
7	-26.5 -67.6	26.3 50.1	-2.5	0 6.6	15.5	35 179	40.9	10.0 20.0		-2.2 -1.7			
8	-41 -71.8	11.0 51.2	4.5 14.5	-1.8 -5.0	- 2.6 - 5.5	52 215	10.5 24.4	16.1 26.7		1.2 -3.0			
9	-44.1 -85.3	16 45.7		2.2 -0.4		34 75		8.5 14.4		3.7 -2.3			
10	-30.2 -68.3	27.1 69.0	2.1	6.1 10.8	10.7	13.5 56.5	10.7	6.5		-1.2			
11	- 4.4 -53.7	26.9 58.5	5.4	1.0 1.3	0	20.6 48	11.3	0		-0.6			

\* PP=coronary perfusion pressure, SP=systemic pressure, CF=contractile force, QT=QT interval, R= heart rate.

Table 6. Average effects of 5 minute hypokalemic perfusion on coronary artery and heart during constant pressure perfusion.

	% K <sup>+</sup> removal*	Time (minutes)										
		0	1	2	3	4	5	6	7	8	9	10
		hypokalemic perfusion										
coronary flow (ml/min)	69	109	96	95	94	94	93	113	109	112	110	108
	35	99	94	91	94	92	94	100	98	96	96	95
coronary sinus P <sub>O</sub> 2 (mm Hg)	69	17.7	15.8	14.8	15.2	15.3	15.5	17.5	20	19.7	19.7	19.3
	35	17.1	16	15.3	15.2	15.2	15.2	15.4	16.4	16.3	16.1	15.9
contractile force (arbitrary units)	69	88	98	111	118	122	125	96	90	88	87	87
	35	81	87	89	89	90	91	85	86	89	89	90
systemic pressure (mm Hg)	69	108	108	108	108	109	108	107	107	106	106	106
	35	112	110	109	109	109	109	109	109	108	108	108

\* 69% K<sup>+</sup> removal, n=10; 35% K<sup>+</sup> removal, n=4.

Table 7. Average effects (n=8) of prolonged hypokalemia on the myocardium and coronary vessels produced while maintaining coronary perfusion pressure constant.

		Time (minutes)															
		0	2	4	6	8	10	12	14	16	18	20	21	22	23	24	25
		68% K <sup>+</sup> removal															
coronary flow (ml/min)																	
88	79	82	85	88	92	94	97	99	101	106	118	124	122	117	115		
coronary sinus P <sub>O</sub> (mm Hg)																	
16.3	14	14.6 <sup>2</sup>	15.4	15.9	16.4	16.7	17.4	17.9	18.3	18.8	21.1	23.1	23.2	23	22.6	174	
contractile force (arbitrary units)																	
103	119	130	134	138	140	141	140	141	141	141	140	140	120	109	102	100	102
systemic pressure (mm Hg)																	
80	78	77	79	79	78	76	75	72	71	70	67	65	64	65	65		



Table 8. Effects of hypoosmolality on gracilis muscle perfusion pressure during constant flow perfusion.

Exp. No.	% $\Delta$ in osmolality	% $\Delta$ in pressure
3	13.3	34.8
4	16.3	38.9
13	8.0	11.4
13	12.7	23.9
14	10.7	19.9
14	22.9	47.6
15	10.9	22.7
15	5.2	8.2
17	5.3	10.3
17	1.3	3.5

Table 9. Effects of hypoosmotic perfusion of coronary \* artery on myocardium and coronary resistance.

Exp. No.	% $\Delta$ osm	% $\Delta$ PP	% $\Delta$ SP	% $\Delta$ CF	% $\Delta$ QT	% $\Delta$ Rate
1	10.2	80.1	0	6.2	-8.3	-1.1
	4.6	48.8	0	16.1	-16.7	7.5
3	4.0	10.0	1.2	5.1	0	-1.0
	1.7	5.5	1.1	7.2	0	0
5	4.0	40.2	1.8	14.1		
	11.3	138.4	10.5	22.3		
6	5.7	34.0	-5.3	22.5		
	12.4	50.1	0	75.2	-29.4	5.7
7	5.0	15.0	-1.0	34.8	-10.0	1.8
	10.7	38.0	-2.6	23.0		1.8
8	4.2	23.2	2.9	7.0	-5.3	0.6
	9.0	35.4	0	7.6	-11.1	-4.8
9	5.3	9.6	2.3	16.5		
	10.7	7.2	5.2	32.6	-16.7	2.4
10	3.0	29.4	-0.8	1.2	-15.0	0
	7.7	39.1	-4.4	5.1	-17.5	0.6
11	6.6	2.5	-3.8	26.9		
	15.2	10.6	-3.6	19.8	-11.8	1.1

\* osm=osmolality; PP=perfusion pressure; SP=systemic pressure; CF=contractile force; QT=QT interval; Rate= heart rate.



Table 10. Average effects (n=11) of hypoosmotic perfusion of the coronary artery on myocardium and coronary vessels during constant pressure perfusion.

	Time (minutes)										
	0	1	2	3	4	5	6	7	8	9	10
	7% osmolality reduction										
coronary flow (ml/min)	88.4	84.8	81.3	80.7	78.2	75.5	75.4	79.8	79.8	80.9	77.3
coronary sinus P <sub>O</sub> <sub>2</sub> (mm Hg)	15.9	15.7	14.8	14.9	14.8	14.9	14.8	16.5	16.8	16.5	16.5
contractile force (arbitrary units)	98.2	108.3	108.5	105.4	103.3	101.8	93.4	94.3	98.3	102.2	103.9
systemic pressure (mm Hg)	83.3	82.3	79.4	77.6	76.0	75.2	74.4	74.9	75.1	75.4	74.7

Table 11. Effect of isoosmotic replacement of plasma NaCl with mannitol on gracilis artery perfusion pressure.

Exp. no.	% in plasma [ $\text{Na}^+$ ]	% in perfusion pressure	
		on response	off response
3	14.8	8.5	-8.5
6	14.0	13.6	-11.8
7	28.0	27.7	-16.5
9	14.8	8.6	-2.6
10	21.7	12.0	-22.0
13	7.0	4.5	2.1
15	10.5	10.0	1.7
15	5.3	7.4	8.1
18	2.0	3.0	-1.5
19	9.0	8.8	1.5

Table 12. Effects of hyperosmotic NaCl and glucose (900 mOsm/l) infusions on gracilis muscle vascular resistance.\*

infusion rate (ml/min)	0.38	0.38	0.76	0.76
agent	NaCl	glucose	NaCl	glucose
<hr/>				
Date of Exp.	Resistance (Percent of Control)			
Constant flow data				
10-14-68	80.8	64.8	75.5	40.2
10-15-68	77.4	95.2	66.8	88.3
10-24-68	95.8	89.8	87.2	76.5
10-31-68	95.0	77.7	81.3	73.0
11-04-68	97.0	62.5	68.7	41.3
	P < 0.4		P < 0.4	
Constant perfusion pressure data				
09-17-68	98.4	92.4	91.3	87.5
09-23-68	76.4	88.0	65.5	65.5
09-26-68	73.5	71.5	62.3	55.0
10-02-68	91.6	85.5	85.8	76.5
10-03-68	85.5	75.0	61.4	60.8
	P < 0.4		P < .05	

\* Data supplied by Daniel P. Radawski.

MICHIGAN STATE UNIVERSITY LIBRARIES



3 1293 03196 3485